A STUDY OF THE SPARK SPECTRA OF SELENIUM

by

SIMON GEORGE

B.Sc. The University of Travancore, India, 1951
M.Sc. The University of Saugar, India, 1954

A THESIS SUBMITTED IN PARTIAL FULFILMENT OF THE REQUIREMENTS FOR THE DEGREE OF

DOCTOR OF PHILOSOPHY

in the Department

of

PHYSICS

We accept this thesis as conforming to the required standard

THE UNIVERSITY OF BRITISH COLUMBIA

September, 1962

In presenting this thesis in partial fulfilment of the requirements for an advanced degree at the University of British Columbia, I agree that the Library shall make it freely available for reference and study. I further agree that permission for extensive copying of this thesis for scholarly purposes may be granted by the Head of my Department or by his representatives. It is understood that copying or publication of this thesis for financial gain shall not be allowed without my written permission.

Department of Physics

The University of British Columbia,
Vancouver 8, Canada.

Date Sep 20, 1962

The University of British Columbia

FACULTY OF GRADUATE STUDIES

PROGRAMME OF THE

FINAL ORAL EXAMINATION

FOR THE DEGREE OF

DOCTOR OF PHILOSOPHY

of

SIMON GEORGE

B.Sc. University of Travancore, India, 1951
M.Sc. University of Saugar, India, 1954

THURSDAY, SEPTEMBER 20th, 1962, AT 1:30 P.M.
IN ROOM 303, PHYSICS BUILDING

COMMITTEE IN CHARGE

Chairman. F. H. Soward

A. M. CROOKER — R. A. NODWELL
F. W. DALBY — C. REID
K. C. MANN — C. A. SWANSON

External Examiner: B. EDLÉN
Lunds Universitet, Sweden

A STUDY OF THE SPARK SPECTRA OF SELENIUM

ABSTRACT

The spark spectra of selenium have been photographed from the infra-red to the vacuum ultra-violet on a variety of spectrographs including a two metre vacuum spectrograph, a twenty-one foot concave grating, a Hilger constant deviation, a Hilger medium quartz and a Hilger large automatic glass-quartz prism spectrograph. Two light sources have been used: An electrodeless spark discharge and a spark in helium. About 2200 selenium lines have been measured in the region 10450 to 345 Ångstroms. Approximately 800 of these lines had not been previously observed.

Using the present observations, a complete revision of the term structure of Se II, Se III, Se IV, Se V and Se VI has been made. Most of the term values have been revised and the previous analyses in Se III, Se IV, and Se V have been extented considerably.

In Se III, the deepest excited term $4s4p^3\ ^5S^\circ_2$ has been established. Also the levels $4p5d\ ^3Po$, $4p7s\ ^3Po, 1, 2, ^1P1$ and $4s4p^3\ ^1So$ have been found. A new limit is calculated from the 4pns series $(4p^2\ ^3Po = 248583\ cm^{-1})$ I.P. = 30.8 volts.

In Se IV, the deepest excited term $4s4p^2\ ^4P$ has been found. In addition, the levels $4s^26p\ ^2P\frac{1}{2}, 1\frac{1}{2}$, $4s^27p\ ^2P\frac{1}{2}, 1\frac{1}{2}$ and $4p^3\ ^4S1\frac{1}{2}$ have also been established. The level $4s^2\ 7s\ ^2S\frac{1}{2}$ suggested by Rao has been rejected and a new value has been found for this. The $4s^2ng$ series has been extended up to $n = 9$. For the first time, the $4s^2nh$ series has been established in this type of spectra and extended up to $n = 8$. A new ionization potential, (I.P.) has been calculated using this series $4p\ ^2P^\circ_{\frac{1}{2}} = 346,375 \pm 100\ cm^{-1}$, I.P. = 42.94 ± 0.01 volts.

In Se V, a comparison of the n* values with those of As IV showed a discrepancy regarding the I.P. =73.1 volts, given by Rao. By an extrapolation along the isoelectronic sequence the I.P. is estimated to be 68.4 volts which is in close agreement with the value 68.3 ± 0.1 volts calculated from screening constants given by Finkelnburg and Humbach (1955).

In this spectrum the levels $4s5p\ ^3Po, 1, 2, ^1P1$, $4s4f\ ^3F2, 3, 4, ^1F3$ and $4s5s\ ^1So$ have been established. The levels $4s5d\ ^3D1, 2, 3$, are tentatively suggested.

Intermediate coupling theory has been compared with observed levels wherever possible. In most cases the agreement is good.

Using an electrodeless discharge tube excited by a high frequency generator, wave lenths of 38 lines in the arc spectrum of potassium have been determined interferometrically. A water cooled Hg^{198} electrodeless tube (Meggers lamp) was used for the standard line $\lambda_{air} = 5460.7532$ Å. Most of these lines have been measured interferometrically for the first time. The wave lenths of the four satellites in the diffuse series agree well with the calculated values. The only previous measurements, by Masaki and Kobayakawa are probably in error due to an incorrectly assumed integral order in the interference pattern.

GRADUATE STUDIES

Field of Study: Optical Spectroscopy

Quantum Mechanics	W. Opechowski
Nuclear Physics	J. B. Warren
Spectroscopy	A. M. Crooker

Related Studies.

Modern Geometry II	M. Benedicty

ABSTRACT

The spark spectra of selenium have been photographed from the infra-red to the vacuum ultra-violet on a variety of spectrographs including a two meter vacuum grating spectrograph, a twenty-one foot concave grating, a Hilger Constant Deviation, a Hilger medium quartz and a Hilger large automatic glass-quartz prism spectrograph. Two light sources have been used: An electrodeless spark discharge and a spark in helium. About 2200 selenium lines have been measured in the region 10450 to 345 Angstroms. On the basis of these measurements, new levels have been found in Se III, Se IV, and Se V.

The most important achievement was the discovery of the deepest excited terms $4s4p^3\ {}^5S_2^o$ in Se III and $4s4p^2\ {}^4p$ in Se IV. The chief extension of the analysis has been in Se IV.

A few interferometric measurements were made in Se II and Se III. Using an electrodeless discharge tube excited by a high frequency generator wavelengths of 38 lines in the arc spectrum of potassium have been determined interferometrically.

ACKNOWLEDGMENTS

I wish to express my deepest gratitude to Professor A.M. Crooker for suggesting this problem and for his invaluable help and stimulating discussions throughout the course of this investigation.

The technical assistance given by Mr. J. Lees, Mr. A. Fraser and Mr. W. Morrison is also acknowledged. Thanks are also due to Mr. Y. N. Joshi for his help in some calculations.

TABLE OF CONTENTS

TABLES

FIGURES

Following Page

A STUDY OF THE SPARK SPECTRA OF SELENIUM

INTRODUCTION

With the advent of quantum mechanics in 1927 the theory of spectra was given a very firm foundation. The semi-classical rules of the old quantum and Bohr theories became a natural consequence of the new quantum mechanics. Slater (47), Goudsmit and Bacher (23), Condon and Shortley (7), and others developed the theory which was capable of explaining the major details of spectra. Subsequently interest in the field declined rapidly, particularly from the experimental point of view. The opinion, that further study would not lead to profitable results, became common among physicists. However, a glance at the "Atomic Energy Levels" compiled by Mrs. Sitterly (33) reveals the gaps which occur in our knowledge of many spectra. Harrison (14) estimated that approximately one million lines must be ascribed to their parent ions in order to meet the needs of astronomers, physicists, and chemists, whereas at that time only about 280,000 were known. A large number of fairly complete analyses must be available to make a comprehensive test of the theory of complex spectra in terms of intermediate coupling parameters, Slater coefficients, interconfiguration perturbations, etc.

The problem facing the modern spectroscopist is as follows. He must carry out the measurements of the existing wavelengths with the maximum accuracy obtainable with modern laboratory equipment. Then he must examine the earlier analyses in the light of the new data, correcting any errors in the accuracy or in identification of levels which may arise, and extend the analysis to include other lines which are not accounted for. Finally, this experimental data must be used to make a quantitative test of modern atomic theory, the most elegant form of which is probably that of Racah and his coworkers. The task is not an easy one. In the words of Shenstone (45) "to complete an already partially analysed spectrum is much more difficult than to begin a new one because it is always the easy part that is already done."

The following chapters will describe the application of the foregoing discussion to the spectra of selenium.

The various investigations of the arc and spark spectra of selenium done prior to 1930 are summarized in Kayser's Handbuch der Spectroscopie, Volume 6 (19). None of the workers made any attempt in classifying the lines. The first attempts at analysing the arc spectrum were made independently by Ruedy and Gibbs (42a,b) and Meissner (29,30) in 1934; but the two lists disagree in many instances. Recently an analysis has been carried out by Shenstone in the arc spectrum of selenium who states that the analysis of Ruedy and Gibbs, as presented by Mrs. Sitterly, is basically correct.

The singly ionized selenium atom has its ground state a $4s^2 4p^3$ configuration and hence gives rise to a complex spectrum.

In 1935, Martin (24) made an excellent analysis of this spectrum. Other workers in selenium II spectrum are Bartelt (5a,b), Krishnamurthy and Rao (21) and Van den Bosch (49).

Se III was first studied by Badami and Rao (4) and Rao and Murthi (39) who classified 218 lines between 517 Å and 6613 Å. Goudet (12) gives a list of selenium spark lines in the vacuum ultraviolet region from 1294 Å to 360 Å. Se IV has been analysed by Rao and Badami (37) who have published 35 classified lines between 635 Å and 3059 Å. In Se V Sawyer and Humphreys (44) have classified 16 lines between 505 and 837 Å. In 1931 Rao and Badami (38) slightly extended the analysis of Se V by adding 6 more lines to the classification. In Se VI by extrapolation along the isoelectronic sequence Sawyer and Humphreys (44) have classified 7 lines between 452 Å and 886 Å.

THEORY

1. General Theory of Atomic Spectra

The general theory of atomic spectra and its interpretation in terms of the vector model is well known. Here we summarize briefly those results which are necessary to understand the spectroscopic notation and the procedures used in identifying unknown levels. For detailed derivations and discussions the reader is referred to one of the many texts on the subject (7,22,35,50).

Terms and Energy Levels

The first step in the interpretation of spectra consists in finding a set of energy levels which gives the observed spectral lines as combinations by means of equation

$$\nu = \frac{W_1 - W_2}{h} \tag{1.1}$$

where W_1 and W_2 are the energy values for 2 levels

h is the Planck's constant

and ν is the frequency of the spectral line.

This equation gives the frequency, in sec^{-1}. To obtain the wave number used customarily in spectroscopy it is necessary to divide this by c, the velocity of light Thus energies divided by hc have the dimension cm^{-1}. The energy states expressed in these units are generally called terms and their values term values.

Relative and Absolute Term Values

In many spectra which have been analyzed quite completely, it is possible to calculate with great precision the energy necessary to remove one electron from the lowest energy level to an infinite distance, i.e. the ionization energy. In these spectra it is customary to put the energy at which the electron is removed completely, equal to zero. The other term values will therefore be negative, the normal state being the state with the largest negative energy, but one always omits the negative sign and denotes the term values by positive numbers Term values in which the ionization limit is put equal to zero are called absolute term values.

In other spectra,for which the ionization energy is not known, it is customary to set the state with the lowest energy equal to zero. In this case the term values are referred to as relative term values.

When the term values decrease, one knows that they are absolute, and when they increase that they are relative term values. In the former case n increases and in the latter n decreases.

Odd and Even Terms

The analysis of spectra shows that the levels of each spectrum can be divided into two groups called odd and even terms. When the arithmetical sum of all l's of the electrons is even, one obtains even energy levels; and, in the other case odd ones. Usually the symbols for odd levels are distinguished by the sign ° at the upper right side and the term value printed in italics. Transitions occur only between odd and even states and not between states belonging to the same group.

However, transitions between two odd or two even terms may occur under the influence of disturbing electric fields Even in the absence of such disturbing fields, such 'forbidden' transitions may occur, due to quadrupole radiation; but they are then very much weaker than allowed transitions involving the same terms.

Rydberg Series

The absolute value of a term may be written as

$$T_n = \frac{RZ_o{}^2}{n^{*2}} = \frac{RZ_o{}^2}{(n - \delta n)^2} \qquad (1.2)$$

where R is the Rydberg Constant

Z_o = effective nuclear charge (1,2,--for arc, 1st spark,-- spectra)

n = principal quantum number

n^* = effective quantum number

δn = quantum defect

A series of terms with the same L , J and n increasing by integers constitute a Rydberg series or an n^* sequence. The usual method of setting up absolute term values is to assume that δn approaches a constant as n increases, and hence that n^* increases by integral steps for high n. Hence from the observed difference (Tn - Tn+1), and using the Rydberg conversion tables one may calculate Tn+1 and Tn. Having thus established absolute term values using two terms; one may predict unknown members of the same or other series by an inverse process. The absolute term value is then computed from the above equation, the simplest method of doing this computation is to look it up in the tables mentioned above. For large n, and especially when L is also large, the procedure is quite accurate. For smaller n the accuracy is reduced because δn has not approached a constant and also because intercombination perturbations are likely to perturb the series.

Shenstone and Russell (46) have studied the case when a series is perturbed by a level from another electron configuration. The formula 1.2 may be written in the form

$$T_n = \frac{RZ_o^2}{n^{*2}} = \frac{RZ_o^2}{(n + \mu + \alpha T_n)^2} \qquad (1.3)$$

where μ, α are negative constants and $|\alpha| << |\mu|$. The behavior of a series may then be examined by plotting $(n^* - n)$ Vs T_n. A Rydberg series ($\alpha = o$) gives a straight line parallel to the T_n axis, while a Ritz series gives a straight line of slope α and intercept μ on the ordinate axis. For a perturbed series Shenstone and Russell write (1.3) in the form

$$T_n = \frac{RZ_o^2}{(n + \mu + \alpha T_n + \frac{\beta}{T_n - T_o})^2} \qquad (1.4)$$

where T_o is the value of the perturbing term. The plot of (1.4) as before gives a hyperbola with vertical asymptote $T_n - T_o$ and horizontal asymptote $n^* - n = \mu + \alpha T_n$. They found that many series which did not fit (1.3) could be made to fit (1.4) quite well, once the perturbing term had been identified. In some cases they found that the perturbing term had been included as a member of the series, and hence all the higher quantum numbers were wrong and ionization potential incorrect. A more accurate method for the determination of term values is given by Edlén and Risberg (11).

Isoelectronic Sequences and Moseley Diagrams

The term isoelectronic sequence refers to a sequence of atoms having the same number of extranuclear electrons. In general such a sequence starts with any element in the periodic table and is followed by other elements in the order of their atomic number. Since each neutral element contains one more electron than the one just preceding it in the periodic table, each atom must be stripped, i.e. ionized, of just the right number of electrons to leave it isoelectronic with the first element in the sequence. Suppose, for example, that a sequence starts with germanium Z = 32. The following elements, arsenic, Z = 33, selenium, Z = 34, bromine, Z = 35, etc. are all made isoelectronic with neutral germanium (Ge I) by removing one electron from arsenic, yielding As II; two electrons from selenium; yielding Se III; three electrons from bromine yielding Br IV, etc. Because each atom in such a sequence contains the same number of extranuclear electrons the energy levels and the spectrum lines arising from each atom will show remarkable similarities from element to element.

Term values are given by the formula

$$T_n = \frac{R(Z - \sigma)^2}{n^2} \tag{1.5}$$

where Z = atomic number

σ = screening constant.

From the theory of penetrating orbits they may be represented by

$$T_n = \frac{RZ_o^{\,2}}{(n - \delta n)^2} \tag{1.6}$$

Equation (1.5) can be written as

$$\sqrt{\frac{T_n}{R}} = \frac{1}{n}\,(Z - \sigma) \tag{1.7}$$

from which we see that $\sqrt{\frac{T_n}{R}}$ in an isoelectronic sequence is a linear function of Z with slope $\frac{1}{n}$ and intercept $-\frac{\sigma}{n}$ on the ordinate axis.

Plots of (1.7) are called Moseley diagrams. They are extremely useful for predicting terms in an unknown spectrum by extrapolation from terms already established in the isoelectronic sequence.

Irregular Doublet Law

The irregular doublet law, extended from X-ray to isoelectronic sequences in optical spectra by Millikan and Bowen, may be stated in terms of the energy levels as follows: the difference between the square roots of the term values of the levels having the same principal quantum number n is independent of the atomic number Z. In other words such levels on a Moseley diagram run parallel to each other.

The irregular doublet law is a mathematical expression of the fact that the difference between the square roots of the term values having the same principal quantum number n is independent of Z. From (1.7) for two terms T_{n_1} and T_{n_2} with the same n we get

$$\sqrt{\frac{T_{n_1}}{R}} - \sqrt{\frac{T_{n_2}}{R}} = \frac{1}{n}(Z - \sigma_1) - \frac{1}{n}(Z - \sigma_2)$$

$$= \frac{\sigma_2 - \sigma_1}{n} \qquad (1.8)$$

A more useful form of the law is found by studying the term values themselves rather than their square roots. We find using (1.5)

$$T_{n_1} - T_{n_2} = \frac{R}{n^2} \left\{ (Z - \sigma_1)^2 - (Z - \sigma_2)^2 \right\}$$

$$= \frac{R}{n^2} \left\{ 2Z(\sigma_2 - \sigma_1) - (\sigma_2^2 - \sigma_1^2) \right\}$$

$$= c_1 Z + c_2 \qquad (1.9)$$

where c_1, c_2 are constants.

Thus the difference $(T_{n_1} - T_{n_2})$ is a linear function of Z in an isoelectronic sequence. For the many electron case we replace the condition that the two terms have the same principal quantum number by the condition that the total quantum numbers of the electrons in the two states be the same. Rigorously the law would be expected to hold between neighboring states of the same J value, i.e. between $^{2s+1}L_J$ and $^{2s+1}(L+1)_J$. Empirically however it is found that the law holds approximately even for different J's so long only as the individual electron total quantum numbers are the same.

Regular Doublet Law

The regular doublet law is a direct consequence of the fine structure splitting caused by the spin-orbit interaction. For a one electron spectrum the energy due to this interaction is given by

$$W = a\,\vec{l}.\vec{s} \tag{1.10}$$

where a is a constant

$\vec{l}, \vec{s}$ = orbital and spin angular momenta of the electron.

Using the vector model to evaluate $\vec{l}.\vec{s}$ and the value of 'a' from quantum mechanics (1.10) becomes

$$W = \frac{Rhc\alpha^2 Z^4}{n^3 l(l+1)(l+\frac{1}{2})} \cdot \frac{J(J+1) - L(L+1) - S(s+1)}{2} \tag{1.11}$$

For a one electron spectrum $J = l \pm \frac{1}{2}$ and (1.11) becomes

$$T = \frac{W}{hc} = \frac{R\alpha^2 Z^4}{n^3 l(l+1)(l+\frac{1}{2})} \cdot (l+\tfrac{1}{2})$$

$$= a(l+\tfrac{1}{2}) \tag{1.12}$$

where $a = \dfrac{R\alpha^2 Z^4}{n^3 l(l+1)(l+\frac{1}{2})}$

For non-hydrogenic systems we write

$$a = \frac{R\alpha^2}{l(l+1)(l+\frac{1}{2})} \frac{(Z-s)^4}{n^3} \tag{1.13a}$$

for non-penetrating orbits, and

$$a = \frac{R\alpha^2}{\ell(\ell+1)(\ell+\frac{1}{2})} \frac{Z_i^{\,2}\, Z_o^{\,2}}{n^{*3}} \qquad (1.13b)$$

for penetrating orbits, where

s = screening constant

Z_i = effective nuclear charge on inner part of the orbit

Z_o = effective nuclear charge on outer part of the orbit.

Thus the doublet separation varies as Z^4 or $(Z - S)^4$ or $Z_i^{\,2}\, Z_o^{\,2}$. This is called the regular doublet law. We get a Z^2 divergence on the Moseley diagram. Note that as opposed to the irregular doublet law, we are dealing here with the term difference ${}^{2s+1}L_J - {}^{2s+1}L_{J+1}$.

Landé Interval Rule

We note from (1.12) that the fine structure splitting in a relativistic doublet is given by

$$\Delta T = a(\ell+\tfrac{1}{2})$$

and hence is proportional to the higher of the two J values. For Russell-Saunders coupling this Landé interval rule is also found to hold for multiplets in many electron spectra. In this case we can easily show that the splitting between two levels of a multiplet is given by

$$\Delta T = W(J'') - W(J')$$

$$W(J) = A\,\frac{J(J+1) - L(L+1) - S(S+1)}{2}$$

$$J'' = J + 1$$

$$J' = J \qquad (1.14)$$

$$\Delta T = A(J + 1)$$

Hence ΔT is proportional to the higher of the two J values. Humphreys and Goudsmit (35,pp.164) evaluate A by considering the addition of an electron to a configuration of known A'. They obtain

$$A = A'\,\frac{\ell(\ell+1)+\ell_1(\ell_1+1)-\ell_2(\ell_2+1)}{2\ell(\ell+1)}\cdot\frac{s(s+1)+s_1(s_1+1)-s_2(s_2+1)}{2s(s+1)}$$

$$+\; a_2\,\frac{\ell(\ell+1)+\ell_2(\ell_2+1)-\ell_1(\ell_1+1)}{2\ell(\ell+1)}\cdot\frac{s(s+1)+s_2(s_2+1)-s_1(s_1+1)}{2s(s+1)} \qquad (1.15)$$

where A' and a_2 are the interaction constants of atom core and added electron respectively,

ℓ_1, s_1 the orbital and spin quantum numbers of atom core

ℓ_2, s_2 those for added electron.

Equation (1.15) is useful in estimating A from a known A' in the next higher ion. With departures from L-S coupling (1.14) ceases to be true.

Selection Rules

The number of all possible differences between the terms of an atom is far greater than the number of transitions observed because of the operation of the selection rules. Considering only electric dipole radiation there are two chief rules which hold independently of the state of coupling. We may characterize all levels as either odd or even depending upon whether the sum of the individual electron quantum numbers in the configuration giving rise to levels is odd or even. "Laporte's rule" then states that transitions between two odd or two even terms are forbidden. The second rule of wide generality places restrictions on the change in J between two levels. We find

$$J = 0, \pm 1 \qquad (0 \longrightarrow 0 \text{ not allowed})$$

Many other rules may be formulated for special coupling cases as the following for L - S coupling

$\Delta S = 0$ (i.e. intercombination lines are forbidden)

$\Delta L = 0, \pm 1$

The appearance of forbidden lines in a spectrum usually indicates one of four possibilities, namely:

(i) departure from an assumed coupling case

(ii) occurrence of multipole radiation (other than electric dipole)

(iii) presence of external electric or magnetic fields (possibly produced by neighbouring atoms - in this case giving "enforced dipole radiation")

(iv) perturbations - causing a sharing of properties between two more states.

Intensity Sum Rule

The most widely applied and probably the most useful rule regarding intensities of observed lines is the Burger-Dorgelo-Ornstein sum rule. It states that the sum of the intensities of all the lines of a multiplet which belong to the same initial or final state is proportional to the statistical weight (2J + 1) of the initial or final state respectively. This rule by itself is insufficient to determine the relative intensities within a multiplet. Correct intensity formulas for L-S coupling have been derived both classically and quantum mechanically. Tables based on these formulas giving the expected relative intensities in most multiplets are available in White (50, pp.439) or Condon and Shortley(7, pp.241).

2. Theory of Complex Spectra

The quantum theory of many electron spectra assumes as a first approximation that the atomic electrons move in a central field and do not interact with one another. The Hamiltonian of a many electron atom may be written as

$$H = \sum_{i}^{N} \left(\frac{1}{2\mu} \vec{P}_i^{\,2} - \frac{Ze^2}{r_i} + aL_i \cdot S_i\right) + \sum_{i \neq j}^{N} \frac{e^2}{r_{ij}},$$

where $\vec{P}_i$ = the momentum of the i^{th} electron

$\frac{Ze^2}{r_i}$ = the Coulomb electrostatic energy between the nucleus and the i^{th} electron

$a\vec{L}_i \cdot \vec{S}_i$ = The magnetic interaction energy between the orbital and spin angular momenta of the i^{th} electron

$\frac{e^2}{r_{ij}}$ = the Coulomb electrostatic energy between the i^{th} and the j^{th} electron.

In this Hamiltonian, the terms are not separable due to the presence of the mutual repulsion of the electrons. In order to be able to treat the Hamiltonian mathematically we make the assumption that the outer electrons move in a central field potential due to the nucleus plus the electron core.

We then take as our approximate Hamiltonian

$$H_o = \sum_i^N \left[\frac{1}{2\mu} \vec{P}_i^2 + U(F_i)\right]$$

while the perturbation potential will be

$$H = \sum_i^N \left[a\vec{L}_i \cdot \vec{S}_i - \frac{Ze^2}{r_i} - U(r_i)\right] + \sum_{i \neq j}^N \frac{e^2}{r_{ij}}$$

Schrodinger's equation for the unperturbed case then becomes

$$\sum_i^N \left[-\frac{h^2}{2\mu} \nabla_i^2 + U(r_i)\right]\phi = E\phi$$

We now have the equation separable into coordinates for each electron, so that obviously ϕ may be written as

$$\phi = \prod_{i}^{N} U_i$$

$$\text{and} \quad E = \sum_{i}^{N} E_i$$

where U_i is the wave function for the i^{th} electron and designated by the four quantum numbers n, l, m_s, m_l . Because the electrons are indistinguishable, it matters not if the quantum numbers of the electrons are interchanged. There are N! ways of exchanging these parameters and any linear combination of these products will be an equally good solution. Thus we may write

$$\phi = \frac{1}{\sqrt{N!}} \begin{vmatrix} U_A(1) & U_B(1) & \cdots & U_N(1) \\ U_A(2) & U_B(2) & \cdots & U_N(2) \\ \vdots & & & \vdots \\ U_A(N) & U_B(N) & \cdots & U_N(N) \end{vmatrix}$$

where N! is a normalizing factor, and the number in brackets after each U represents the set of four quantum numbers.

This function satisfies the Pauli exclusion principle because interchange of any two electrons (i.e. interchange of any two rows) changes the sign of ϕ and therefore is antisymmetric as required.

Even though we have taken care of the degeneracy due to the N! possible distributions of electrons, there still remains another type of degeneracy because there may be other sets of U's differing from the first in that one or more of the quantum numbers m_s and m_l have been changed.

These quantum numbers do not affect the unperturbed energy, which, of course depend only on n and l. We must therefore set up a secular equation for all these possible functions in order to find the correct combinations and first approximation to the energy levels. Since there is only one possible set of quantum numbers for a completed shell, it is only necessary to consider electrons outside the completed shell.

Now first order perturbation theory shows that the secular equation is of the form

$$\begin{vmatrix} H_{11} - W & H_{12} & \cdots & H_{1k} \\ H_{21} & H_{21} - W & \cdots & H_{2k} \\ \vdots & & & \vdots \\ H_{k1} & \cdots & \cdots & H_{kk} - W \end{vmatrix}$$

where
$$H_{mn} = \int \phi_m H \phi_n d\tau = \langle \phi_m | H | \phi_n \rangle$$

and W is the perturbed energy level

H is the perturbed Hamiltonian

K is the number of allowed sets of functions.

This equation is of K^{th} degree; but may be simplified very considerably by means of a theorem which states that
$H_{mn} = 0$ unless

$$M_s = \sum m_s \quad \text{and} \quad M_L = \sum m_\ell$$

each have the same value for both ϕ_m and ϕ_n. (The proof of this theorem is given in Condon and Shortley p.169). Thus the secular equation is reduced to a number of lower order equations, each equation corresponding to fixed values of M_s and M_L. For example, an np^2 configuration has 15 possible combinations of quantum numbers, but only one combination gives $M_L = 2$ $M_s = 0$, so the equation for this ${}^1D_2$ term is a simple linear equation.

It is clear then that the energy of various levels can be calculated if the matrix elements can be evaluated. Unfortunately, the evaluation of these matrix elements is by no means simple. However, if one simplifies the perturbing Hamiltonian by assuming that only one of the factors is large, it is possible to reduce the integral to the product of a constant which depends on l and m_ℓ and an integral which involves only radial factors of the wave function. One method of proceeding would be to assume some form for the radial potential and use this to evaluate the integral. However a simpler method would be to evaluate the radial integral empirically by using determined energy levels, and then check on the theory from the fact that there are more known levels than integrals to be evaluated. In some cases of an incompletely known spectrum, unknown levels may be predicted from the integrals as an aid in finding these levels.

We proceed now to consider briefly the commonly used approximations.

L-S coupling

We consider first the case where the Coulomb interaction is very much greater than the magnetic spin orbit interaction. Our Hamiltonian then takes the form

$$H = \sum_{i=1}^{N} \left[-\frac{Ze^2}{r_i} - U(r_i) \right] + \sum_{i \neq j}^{N} \frac{e^2}{r_{ij}}$$

The first sum will contribute the same energy to all levels of a given configuration since it is purely radial. We are then left with the matrix element

$$\int \phi_n \frac{e^2}{r_{ij}} \phi_m \, d\tau$$

It can be shown (Condon and Shortley (7) p.174) that matrix elements of this type reduce to

$$H_{mn} = \sum_k \left[a^k F^k - b^k G^k\right]$$

where a^k and b^k are constants defined in terms of l and m_l for two of the electrons. These values have been computed for many configurations and may be obtained from tables (47).

F^k and G^k are integrals of radial functions and are usually treated as adjustable parameters. They are known as Slater integrals and are fundamental to a qualitative knowledge of atomic spectra. Having obtained the a^k's and b^k's for a given configuration, the secular equation mentioned above is used to determine the relative energies in terms of F^k's and G^k's as outlined above. Finally the spin orbit interaction is imposed as a second order perturbation. This gives rise to the splitting of each of the previously found levels into fine structure which follows the Landé interval rules described earlier in this chapter.

A serious objection to this method is that if a configuration gives rise to more than one term of a particular kind (e.g. $4d^9$ 5s6s ^2D ^2D ^4D) the method yields only the sum of their energies. Racah (36b) has developed a powerful tensor method to overcome this difficulty. For the particular case of ll's he has written explicitly a general form for the energies and applied it to the pds configuration.

j - j coupling

In this approximation we solve the secular determinant subject to the condition that the spin-orbit interaction is large and the Coulomb one small. The matrix elements then depend on H of the form

$$H' = \sum_{i=1}^{N} \left\{ - \frac{Ze^2}{r_i} - U(r_i) + a\vec{L_i}.\vec{S_i} \right\}$$

After solving the equations as before, the addition of a weak electrostatic energy is considered. The results of such calculations may be found in Condon and Shortley (7, p.259).

(j-s) and (j-l) coupling

In cases where one electron is firmly bound, the interaction with the second electron may appear as only a perturbation on the usual doublet splitting of the first electron.

i) Houston (16) has treated the case of intermediate coupling when one of the electrons is an s electron. The Houston formulas may be written in many ways. We usually calculate the Lande interval factor A, by dividing the difference $({}^3L_{\ell-1} - {}^3L_{\ell+1}$, independent of coupling) by $(2\ell + 1)$. Then if the position of the ${}^1L_\ell$ level and that of the ${}^3L_\ell$ level relative to the usual triplet (c.g)(namely ℓ.A deeper than ${}^3L_{\ell+1}$) are called ϵ_1 and ϵ_3 respectively then Houston's formulas give

$$(\epsilon_1+1)(\epsilon_3+1) = -\ell(\ell+1)$$

In strict (js) coupling this formula gives the levels as

$$\Delta\nu = (2\ell+1)A = (\ell+\tfrac{1}{2})a_{n\ell}$$

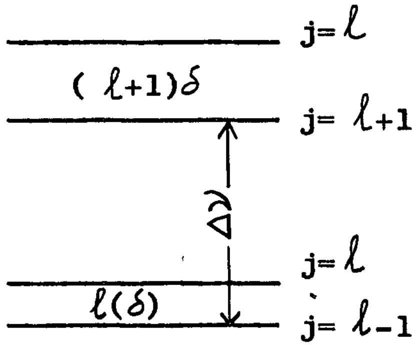

$$\delta = \frac{2G\ell}{(2\ell+1)}$$

ii) Racah (36) has carried through a suggestion of Shortley and Fried, for the case where the second electron is a weakly bound ℓ- electron, so that the spin-spin interaction is responsible only for a fine doubling of each (jl) state. Racah gives the formulas for (jl) coupling (f2 is the coefficient of F2 in energy level formula)

$$f_2(j\ell k) = -\frac{[6h^2 + 3h - 2j(j+1)\ell(\ell+1)]}{4j(j+1)(2\ell-1)(2\ell+3)}$$

where $$h = (\vec{j}.\vec{\ell}) = \frac{k(k+1) - j(j+1) - \ell(\ell+1)}{2}$$

and $$\vec{k} = (\vec{j} + \vec{\ell})$$

Pair coupling of electrons with high ℓ quantum numbers

The theory of intermediate coupling has been studied in the pair coupling approximation by Eriksson (11b) and applied to the $2s^2$ 2pnf configuration in NII. In this case there is a considerable electrostatic interaction between levels of different parentage, compared to the special case studied by Racah (36) where this interaction is small compared to the spin orbit interaction.

The Intermediate coupling formulas of Johnson (17a,b)

The matrices of the spin-orbit interaction may be used by adding the electrostatic energies to the diagonal terms and setting the determinant of the energy matrix = 0. In this operation a minor practical point is to properly include the change of datum from a multiplet (c.g) to a stated reference level. In order to make clear the procedure, we work through a simple example.

Example: the p^2 configuration in intermediate coupling

1) for J = 2 the magnetic energy matrix is (7 p.268)

$$\begin{array}{c|cc|c} & {}^1D_2 & {}^3P_2 & \\ {}^1D_2 & 0 & \sqrt{\tfrac{1}{2}} & a \\ {}^3P_2 & \sqrt{\tfrac{1}{2}} & \tfrac{1}{2} & \end{array}$$

We next add the electrostatic energies to the diagonal terms.

For $^1D_2$ this is (7 p.198)	$F_o - F_2$
" ^3P (c.g.)	$F_o - 5F_2$
" ^1S_o (although unnecessary)	$F_o + 10F_2$

If we transform now to energies relative to $^3P_1 = 0$, which relative to the centre of gravity of the ^3P lies at $-a/2$, by adding $-F_o + 5F_2 + a/2$ to these energies we obtain for

$^1D_2$	$6F_2 + a/2$
$^3P_1$	0
^1S_o	$15F_2 + a/2$

Our complete secular determinant for the determination of the energies relative to $^3P_1$, which is independent of coupling since this J only occurs once in our configuration we have for J = 2

$$\begin{vmatrix} W - (6F_2 + a/2) & \sqrt{1/2}\,a \\ \sqrt{1/2}\,a & W - a \end{vmatrix} = 0$$

i.e. $$W^2 - W(6F_2 + 3/2a) + 6aF_2 = 0$$

Similarly for J = 0 we get

$$\begin{vmatrix} W - (-a/2) & -\sqrt{2}a \\ -\sqrt{2}a & W - (15F_2 + a/2) \end{vmatrix} = 0$$

i.e. $$W^2 - W(15F_2) + \frac{15}{2}\, aF_2 - \frac{9}{4}\, a^2 = 0\ .$$

CHAPTER II

A. Light Sources.

1. The Electrodeless Discharge.

Electrodeless discharges are of two types depending largely on the nature of the radio frequency circuit used to excite the discharge. One may use continuous wave excitation or one may use highly damped radio frequency currents. In this work both these types of excitation were used, but in the major part of the work the discharge tube was excited by a highly disruptive radio frequency discharge. This type of electrodeless discharge has been used in this laboratory for many years since it is known to produce intense, sharp spectral lines even of highly excited ions. Several exposures were made using a Fabry Perot interferometer in order to establish excellent wavelength standards and also to check line profiles. It is possible that the line profiles could be useful in assessing to what ion a given line belongs. The higher excitation lines presumably are excited earliest in the discharge cycle, when electron and ion concentrations are high and produce high local fields. Certainly the more highly excited ions have greater width approaching $\nu = 0.2$ cm^{-1}. This electrodeless discharge probably produces narrower lines in the spectra excited by 200 volt electrons than are available in any other type of high excitation source.

To follow page 28

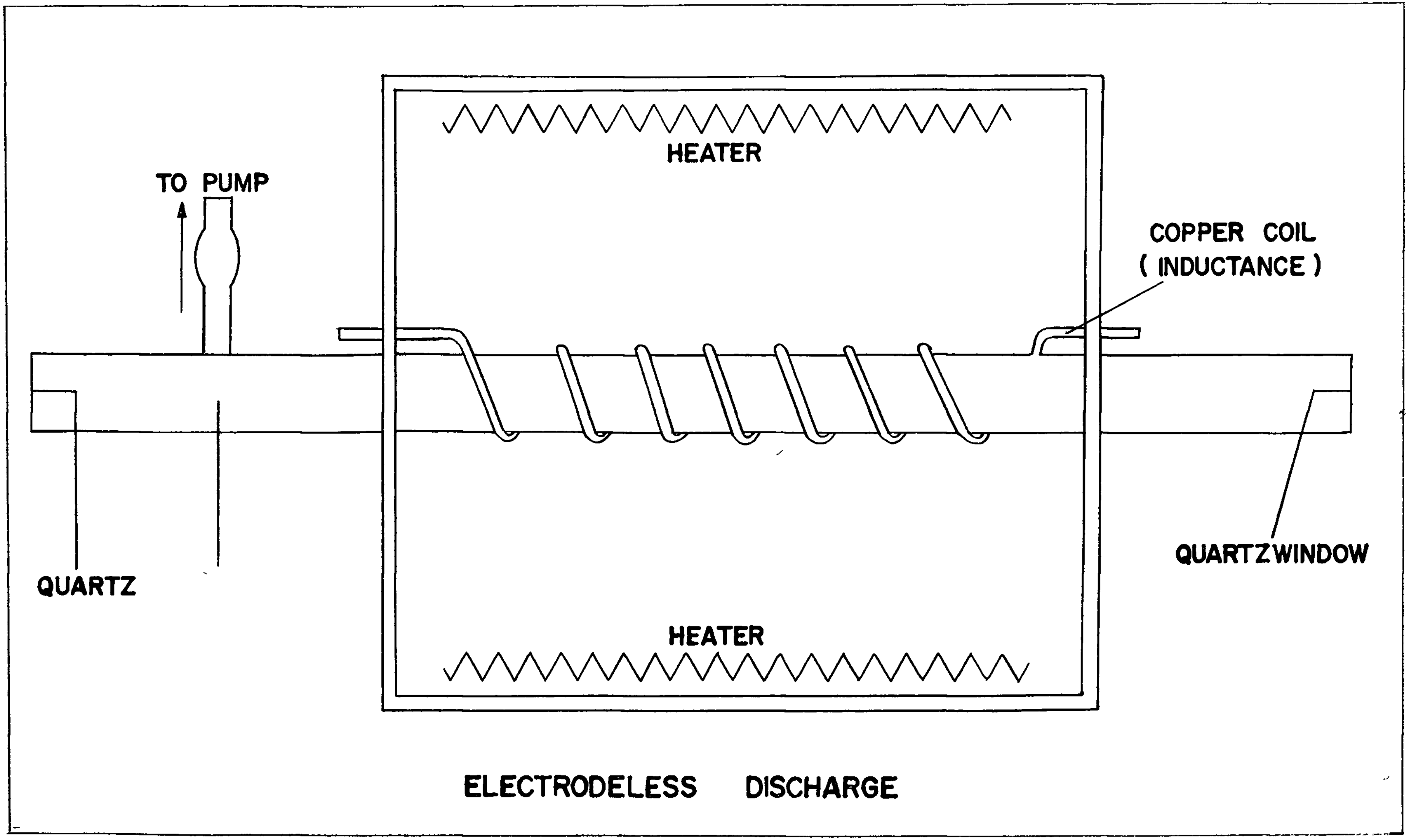

Fig. 1.

Description of Operation.

Approximately ten grams of pure selenium (99.998%), in the form of spherical pellets or "shot", manufactured by the Canadian Copper Refiners Ltd. of Toronto, were introduced into a translucent quartz tube about 20" long and 1/4" in diameter. This tube was wrapped with a thin mica sheet to improve the insulation, since the plasma inside the discharge tube is highly conducting, and this "screwed" inside a heavy copper coil consisting of 8 turns of number 6 gauge wire, diameter 0.162". This inductive coil, with interturn spacing of approximately 3 mm, was connected in series with a three centimeter spark gap and a Solar mica condenser bank to form the radio frequency tank circuit. The condenser bank consisted of 6 mica Solar condensers each of .0025 μf capacity, rated at 22 amperes and 25 kV at 3 Mc/sec, connected in 3 pairs, one on either side of earth as indicated in Figure 2. The coil had an inductance of about 2.6 μH and the condenser a capacitance of 0.0038 μf, thus making the circuit resonant at about 2 Mc/sec. The frequency and hence the inductance were calculated from the oscillogram showing the electric oscillations (Fig. 3). The oscillating circuit is shown in Figure 2 and is energized by a 5 kw, 50 kV x-ray transformer.

The tube was placed inside a transite furnace of dimensions 10½" x 9" x 9" which was heated by four electric heaters, each dissipating 500 watts at 12 amperes, supported

To follow page 29

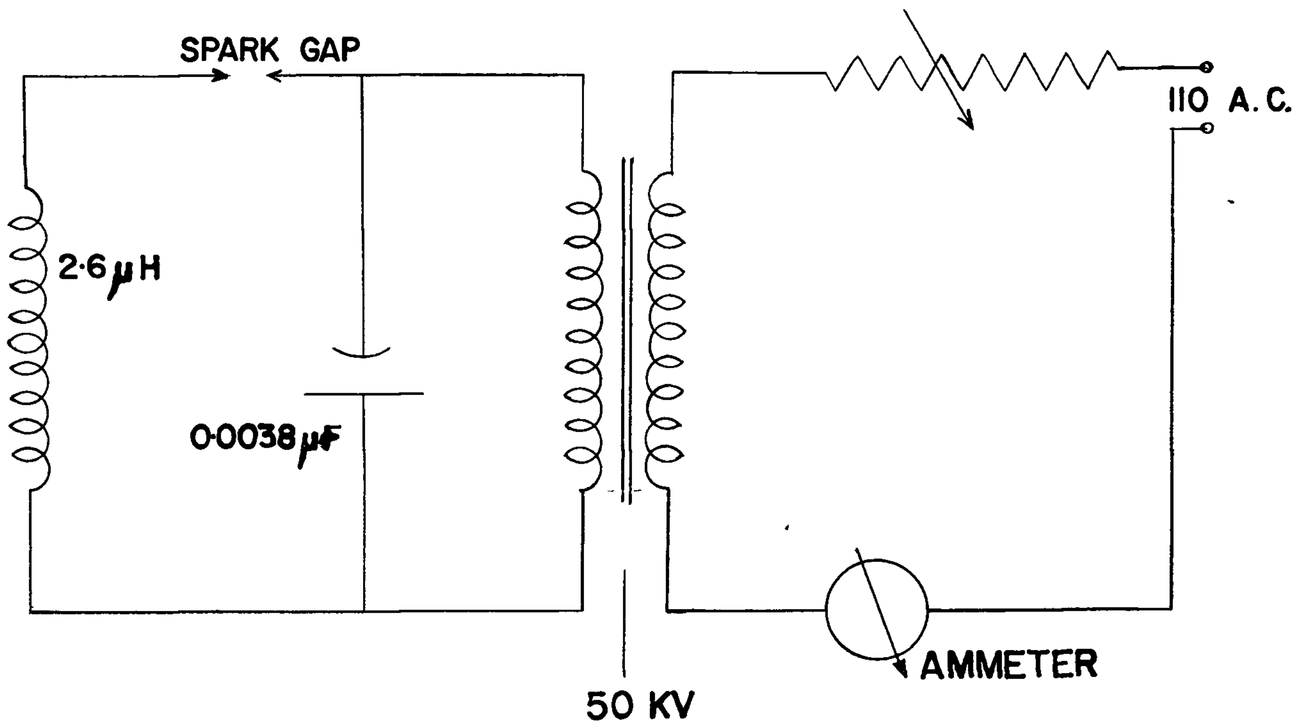

ELECTRODELESS DISCHARGE CIRCUIT DIAGRAM

Fig. 2.

inside the four long edges of the furnace. With this arrangement the 110 volt 60 cycle heating circuit was everywhere more than 3" from the high voltage exciting coil. The heating current was controlled by a Variac and measured by ammeter in order to control the selenium pressure within the tube. The tube ends were sealed with clear fused quartz windows and connected by a quartz side tube and a 4" length of rubber pressure tubing through the liquid nitrogen trap to a fore pump with ultimate vacuum 0.2 μHg. A pinch clamp on the rubber tubing served to control the operating pressure -- in general one operates at the lowest pressures consistent with good intensity for high excitation. One allows the pressure to build up and reduces the spark gap length to reduce the excitation. In order to avoid arcing across the spark gap, an electric fan was used to blow air across the spark gap and so to quench the discharge. After evacuating the tube the temperature was raised to about 600°K to produce the necessary vapour pressure.* After running the discharge for several minutes, and depending on the furnace temperature, it was found that selenium diffused out of the furnace into the cool part of the discharge tube, causing the windows to become coated with a thin film of selenium. This cut down the intensity of the emitted light. In order to overcome this undesirable situation the windows were cleaned as required by heating with a Bunsen flame. During every exposure, the changes in excitation, in other words

---

* The vapour pressure is given closely by the semi-empirical Clausius-Clapeyron relation $\log p = -AT^{-1}+B$ where for Se A = 5182°K and B = 8.30 in the operative range, when p is measured in mm of Hg.

To follow page 30

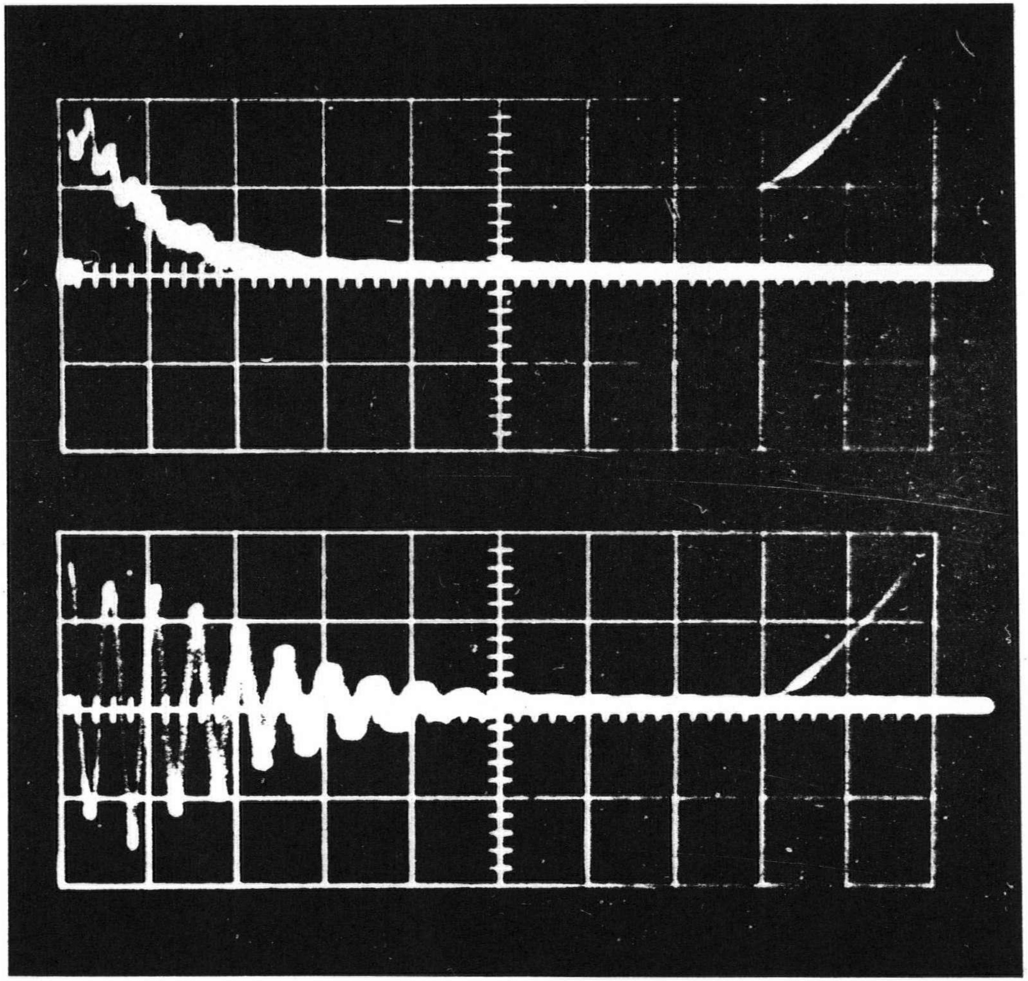

Oscillograms showing the Light Emission and the Electric Oscillations of the Electrodeless Spark Discharge. The total Length of each Oscillogram corresponds to 10 Microseconds.

the changes in intensity of known high excitation lines, were watched through a direct vision spectroscope. The excitation could be controlled by varying the operating temperature or the vapour pressure, or the spark gap. Exposure times varied from two to four hours on the 21 ft. grating and from 30 min. to one hour on the vacuum grating spectrograph.

2. Spark in Helium.

In order to obtain low excitation lines, a condensed spark in helium was used (Fig. 4a). This simple source consists of a glass bulb, with provisions for the windows, electrodes and the flow of helium. Copper rods with carbon cups at the ends served as electrodes. Small pieces of selenium were kept inside the carbon cups. The electrodes were held in position with the help of rubber stoppers. Helium, admitted into the bulb directly from the cylinder was allowed to flow continuously throughout the exposure, at a pressure of about one atmosphere. The helium gas on its way out was allowed to bubble through water in a beaker. When used with the vacuum spectrograph a brass taper with a lithium fluoride window was necessary. The power supply circuit for this source consisted of a 15,000 volt "Neon" transformer and a 0.0025 μf R.F. Solar mica transmitting condenser rated at 22 amperes at 3 Mc/sec. (Fig.4b). The standard Hilger de Gramont arc and spark stand was ideal for the source. If used with a stigmatic spectrograph this source can be very helpful in sorting out the high

Fig. 4(a)

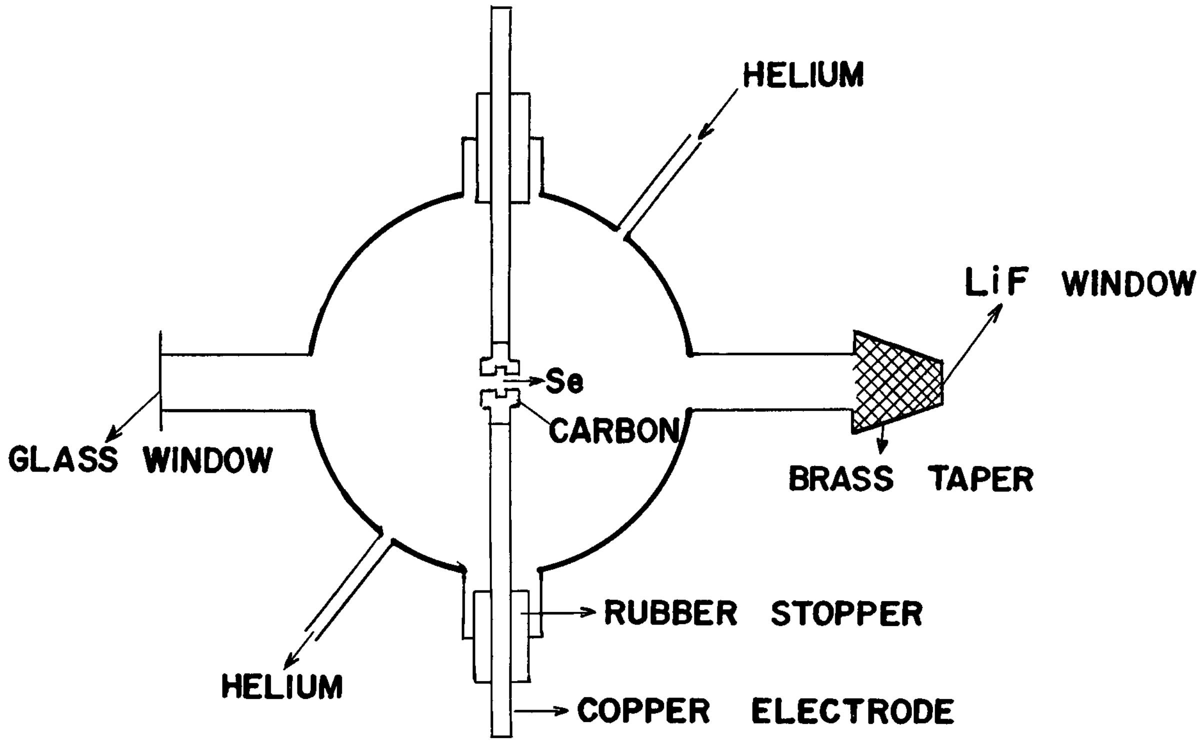

SPARK IN HELIUM

Fig. 4(b)

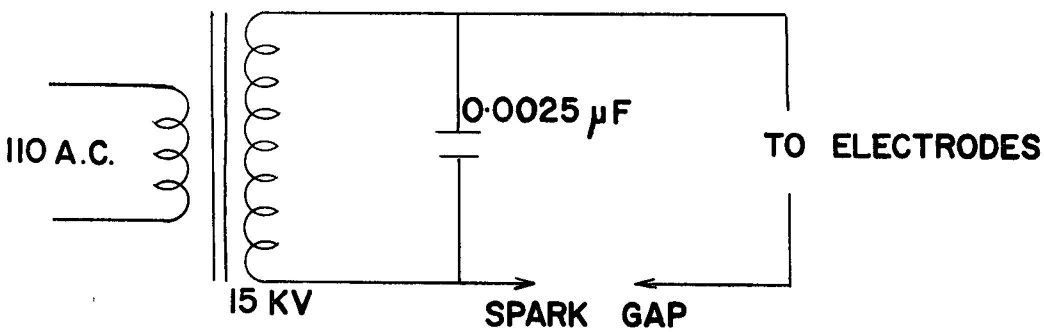

CIRCUIT DIAGRAM FOR SPARK IN HELIUM

excitation lines. The lines of different excitations then appear different due to pole effects. Another advantage of this source was the presence of accurately known carbon lines which served as standards.

B. Spectrographic Equipment.

Four different spectrographs were used in this work. The Lubzinski (22b) 2 meter vacuum spectrograph, a 21 foot grating, a Hilger medium quartz spectrograph, E 498, and a Hilger automatic Littrow spectrograph with interchangeable glass quartz prisms, E 478.

Reduction of Prism Spectrograms.

Computations of wavelengths on the prism plates were made using the well known Hartmann formula. Lines from copper arc, iron arc and in some cases neon lines from a geissler tube served as standard lines. The infrared spectrum was obtained with the large double prism spectrograph using Kodak N plates. For the region above 8500 Å hypersensitized Kodak M and Z plates were used. The plates were dipped in a bath of ammonium hydroxide (4 c.c.) and distilled water (100 c.c.) for about 3 minutes, and then in ethanol for the same length of time. Then it was dried by means of an electric fan. We succeeded in obtaining a few lines of both selenium and standard neon lines above 10000 Å. The wavelengths calculated were finally corrected using a correction curve plotted with the help of known neon lines superposed on the plate. Measurements on the 21 foot grating were made using iron standard lines. The dispersion was determined by the relation

$$\mathcal{D} = \frac{d(n\lambda)}{ds} = \frac{b}{R}\sqrt{1-\left(\frac{n\lambda}{b} - \sin 25°\right)^2} \; ,$$

with b = 16,933 Å; R = 6400 mm; i = 25°. The range and dispersion of this grating were

Max. nλ = 18,000 Å Dispersion = 2.0236 Å/mm.

Min. nλ = 9,500 Å Dispersion = 2.6111 Å/mm.

Rowland ghosts displayed by a grating can be an aid in identifying the order of lines since the ghost spacing at various nλ is a function of the order (Appendix). The grating is ruled with 15,000 lines per inch over an area 2 by 5½ inches. To distinguish the iron lines from the selenium lines, the iron arc was placed near Sirks focus. This gave shorter iron lines. To facilitate the identification of different orders the following method was used. A series of thin glass plates were arranged in front of the plateholder so as to cover the lower half of the plate. This acted as a filter for the lines below 3000 Å. Even though there was a small systematic shift of lines coming through the glass onto the plate, it was extremely useful in deciding the order of many lines. Ilford Q, Ilford H.P.3, Kodak II F and Kodak II N plates were used for this large grating.

Two Meter Vacuum Spectrograph.

The grating has a ruled surface of 2 by 3½ inches with 576 lines per mm. To increase the sharpness of the lines a portion of the ruled area is masked off. The masking is done with a "fore-mask" situated about 1/4" in front of the grating. In this way the masking is more pronounced at smaller wavelengths as should occur (23). Using a slit at grazing incidence (80°) the vacuum ultra violet spectrum was photographed. Maximum $n\lambda$ was found to be about 6000 Å. In order to photograph different exposures on the same plate a movable metal diaphragm was constructed and mounted in front of the plateholder. This was operated manually from outside the vacuum tank through a Wilson seal. In the ultra violet region carbon lines were used as standards. The final wavelengths were calculated using internal selenium standards either of known wavelength, or known frequency from the Ritz combination principle, or with wavelengths determined in a higher grating order. The presence of Lyman lines L_α and L_β on the plates was useful in the identification of some lines.

Reduction of Grating Spectrograms.

1. Classical Interpolation Procedure of Paschen and Runge.

The easiest method is the linear interpolation given by the formula:

$$\lambda = \lambda_1 + \frac{\lambda_2 - \lambda_1}{d_2 - d_1} (d - d_1) ,$$

where λ_1, λ_2 and d_1, d_2 are the wavelengths and comparator readings for the two reference lines, and λ and d the same values for the unknown. For small angles of diffraction, the correction curve will look smooth, since the correction is only due to non-linearity in the dispersion. However, in glancing-angle vacuum spectrographs, it may take quite an irregular shape due to non-systematic errors.

2. The Method of Shenstone and Boyce.

This method is of importance whenever one works with angles of diffraction nearly zero, as in the case of so called normal incidence vacuum spectrographs, with $i \approx 0$ say 10°, or in Rowland or Wadsworth mountings. Here at the center of the plate $\theta = 0$ and the dispersion $\vartheta = \frac{b}{R}$. As we proceed from this position the dispersion falls off to $\vartheta = \frac{b}{R} \cos\theta$, i.e. by an amount $d\vartheta = \frac{b}{R}(1 - \cos\theta)$. In a distance $ds = \frac{d\theta}{R}$ the error in wavelength is $\Delta\lambda$

$$= \frac{b}{R} \int_{\theta=0}^{\theta_2\lambda} (1-\cos\theta)ds = \frac{b}{R^2} \int_{\theta=0}^{\theta_1\lambda} (1-\cos\theta)d\theta.$$

$$= \frac{b}{R^2} \int_{\theta=0}^{\theta_1\lambda} \left(\frac{\theta^2}{2!} - \frac{\theta^4}{4!} + - - - -\right) d\theta \approx \frac{b}{R^2}\,\frac{\theta^3}{3!}$$

and $d(\Delta\lambda) = \frac{b}{2R^2}\,\theta^2 d\theta$ which relates the increment of θ to the

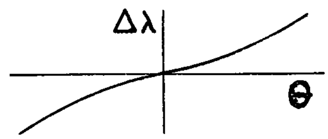

tabulated increments in $\Delta\lambda$.

$n\lambda = b(\sin i + \sin \theta)$

θ is positive when on same side of normal as is i.

θ is negative for $\lambda < \lambda_o$.

θ is positive for $\lambda > \lambda_o$.

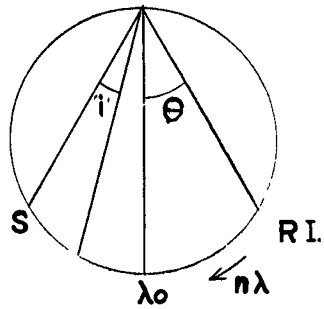

For $\lambda > \lambda_o$, when one calculates $\lambda - \lambda_o$ with $\mathcal{D} = \frac{b}{R}$, one gets too large a λ from which $\Delta\lambda$ should be subtracted. If $\lambda < \lambda_o$ this correction should be added. This change of the correction $\Delta\lambda$ at λ_o is already formally included by the θ^3 dependence. The correction $\Delta\lambda \approx \frac{b}{R^2} \frac{\theta^3}{3!}$ must be uniformly subtracted when due regard is taken of its sign, i.e. $\Delta\lambda$ positive for positive θ, negative for negative θ. In actual practice, in interpolating between λ_1 and λ_2 one first adds the approximate $\Delta\lambda$ to λ_1 and λ_2 with due regard to sign, before calculating the practical dispersion. One then uses this value instead of the theoretical dispersion $\mathcal{D} = \frac{b}{R}$ in interpolating wavelengths between λ_1 and λ_2*. The final correction curve will then be similar to that discussed under the method of set backs.

* This method is used by Shenstone and attributed by him to Boyce and the M.I.T. group.

3. Edlén's Method of Interpolation.

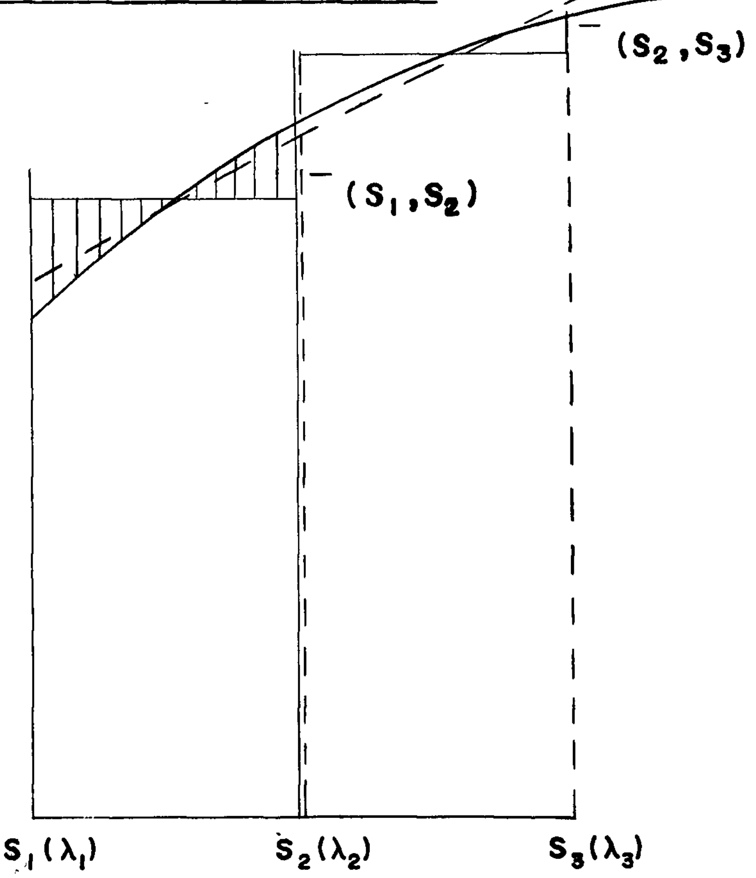

Edlen's method consists in calculating $\bar{\vartheta}(S_1,S_2) = \dfrac{\lambda_2-\lambda_1}{S_2-S_1}$ and $\bar{\vartheta}(S_2,S_3) = \dfrac{\lambda_3-\lambda_2}{S_3-S_2}$ with well spaced standards λ_1, λ_2, λ_3. Then these dispersions will be nearly "point" dispersions at $\dfrac{(S_1+S_2)}{2}$ and $\dfrac{S_2+S_3}{2}$ respectively. Next one constructs a line "point" dispersion formula as indicated by the "dotted" line passing through the points $\vartheta(S_1,S_2)$, $\dfrac{(S_1+S_2)}{2}$ and $\vartheta(S_2,S_3)$, $\dfrac{(S_2+S_3)}{2}$.

Obviously then as we calculate λ's from λ_1, we initially have too large a dispersion, then too small a dispersion and finally, again too large a dispersion. The correction curve should then appear as in the accompanying diagram.

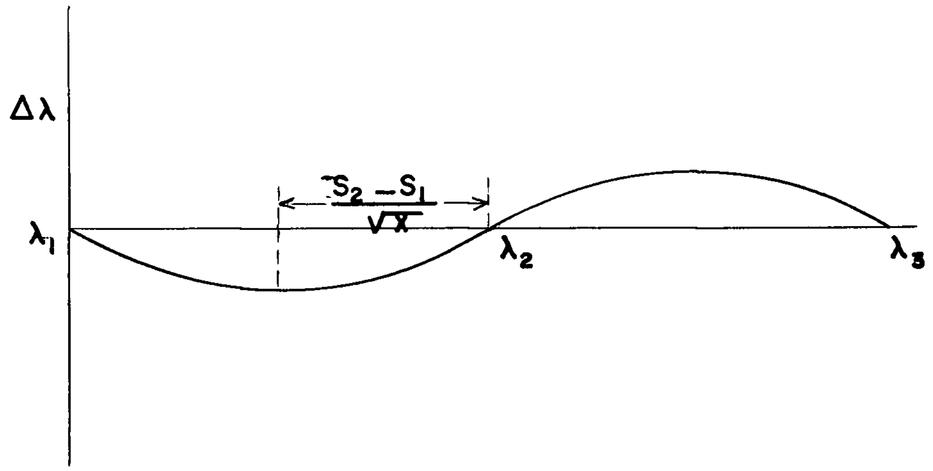

Now the question is -- can we specify the parameters of this correction curve in terms of grating parameters? Let us first return to the dispersion curve (page 37) which we shall assume to be the section of a circular arc, specified by the two parameters α and r. In due course these can be related to λ_2 and the grating radius r is obviously related to Δ .

$$r = \frac{d^2}{2(\text{sag})} = \frac{(S_3-S_2)^2}{\cos^2 \alpha} \quad \frac{1}{2\Delta\cos \alpha}$$

$$= \frac{(S_3-S_2)^2}{2\Delta\cos^3 \alpha} \quad .$$

Thus

$$\Delta = \frac{(S_3-S_2)^2}{2r \ \cos^3 \alpha} = \vartheta(\lambda_2) - \frac{1}{2} \left[\vartheta(\lambda_1) + \vartheta(\lambda_3)\right]$$

4. The Method of "Setbacks"

In this method one calculates for

$$\lambda_1 = b(\sin i - \sin \theta_1)$$

and

$$\lambda_2 = b(\sin i - \sin \theta_2).$$

The average dispersion

$$\bar{\vartheta} = \frac{\lambda_2 - \lambda_1}{S_2 - S_1}$$

where

$$(S_2 - S_1) = R(\theta_2 - \theta_1) .$$

This can then be compared with ϑ calculated at $\frac{\lambda_1 + \lambda_2}{2}$

from the point dispersion formula

$$\vartheta = \frac{b}{R} \cos \theta = \frac{b}{R} \sqrt{1 - (\sin i - \frac{\lambda}{b})^2} .$$

If the two dispersions do not correspond then one sets back the standard dispersion curve by the amount necessary to make the adjusted theoretical dispersion curve at $\frac{\lambda_1+\lambda_2}{2}$ agree with the observed average dispersion. Suppose for instance that the theoretical dispersion curve calculated from

$$\vartheta = \frac{b}{R} \cos \theta \quad \text{actually is smaller}$$

than the "observed" dispersion curve. Then two situations may arise.

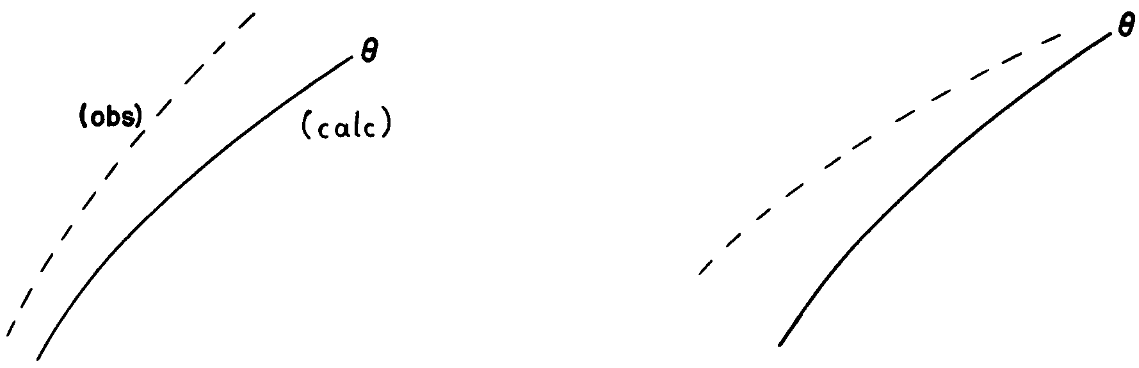

(a) (b)

In (a) the observed difference between the observed and the calculated differences is monotonically increasing and in (b) it is decreasing. After setting the dispersions back the situations are as in (a') and (b')

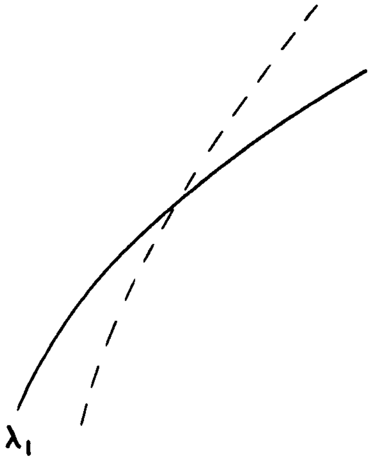

(a')

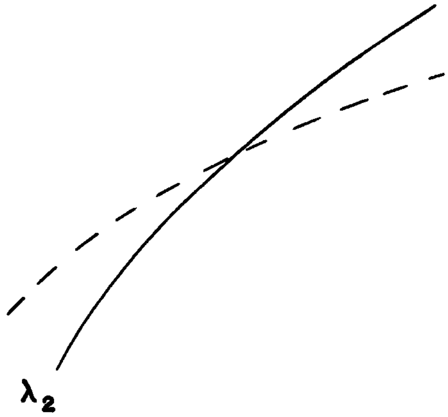

(b')

Obviously then we start with too large a dispersion from λ_1 in (a') and too small a dispersion in (b'). Consequently our correction curve in the two cases will have the respective forms shown below.

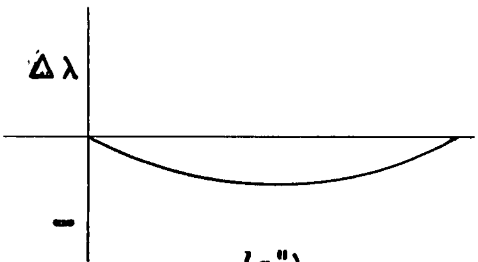

(a")

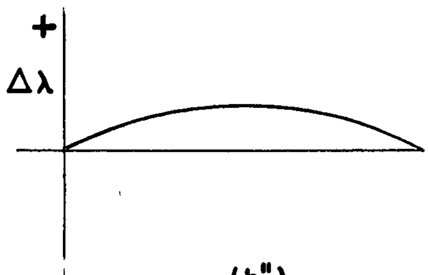

(b")

In this case, by definition, the correction vanishes at λ_2 and has its maximum value near $\frac{\lambda_1+\lambda_2}{2}$, so that the observed correction at $\frac{\lambda_1+\lambda_2}{2}$ will serve to give a good estimate of the actual correction curve. The case where the observed dispersion is less than theoretical can be handled similarly.

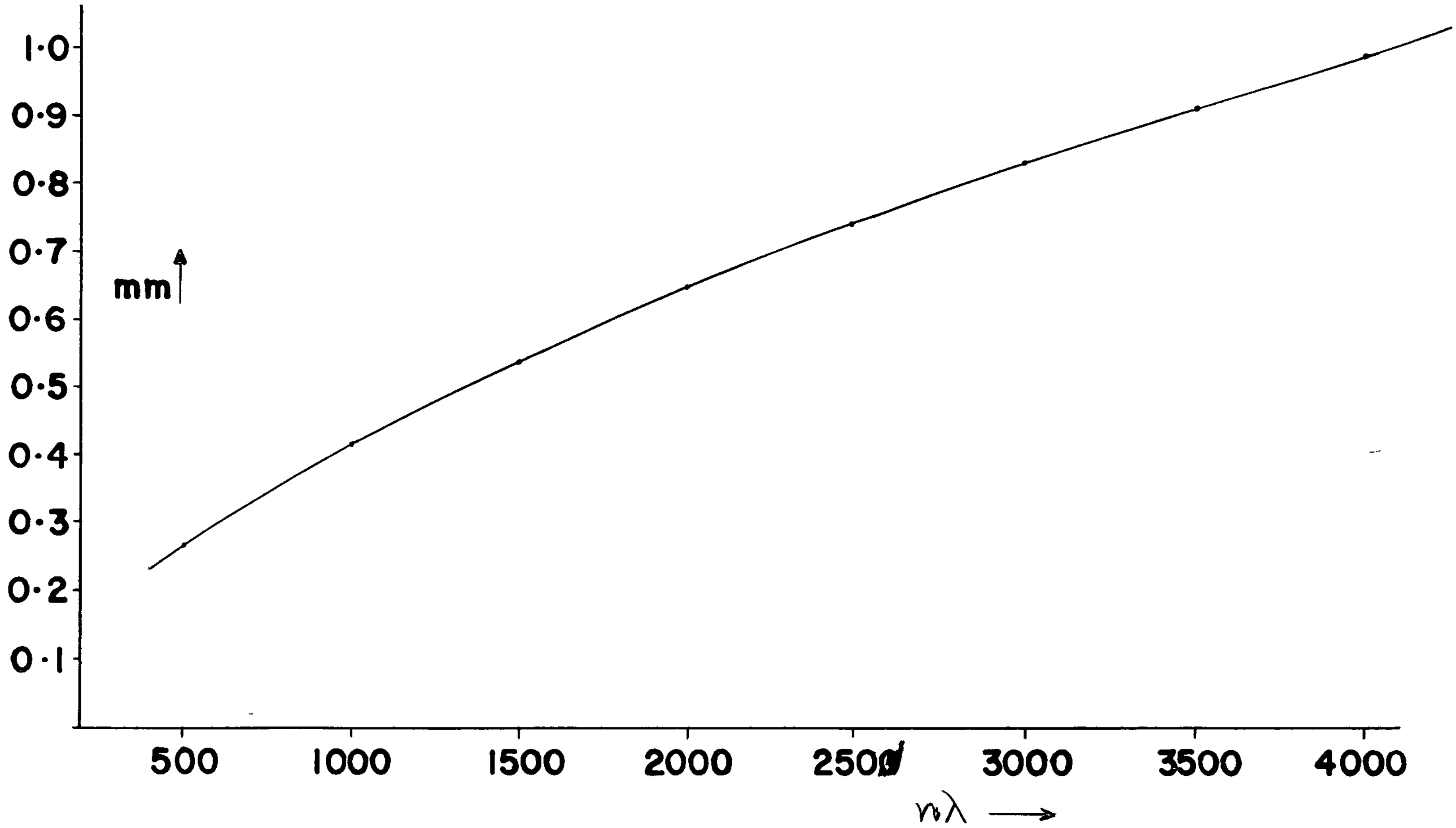

ROWLAND GHOSTS ON 2 METER VACUUM GRATING R = 2·0 m; b = 16,667A, B.&L.

Now, in general the theoretical curve is actually established from two or more standard lines in a region of the spectrum in superb focus. Then, if the slit and the plateholder were exactly located on the Rowland circle, there should be no departure from the theoretical dispersion . Since actual departures arise from cause, we can analyze these practical departures from the theoretical dispersion in order to improve the focus. The method does not require the calculation of the dispersions at each point along the plate, since these are furnished by the theoretical dispersion curve.

Interferometric Wavelength Measurements of Some Selenium Spark Lines.

A complete description of the Fabry Perot interferometer and its applications is given in Chapter IV. The spacer used for this purpose has a thickness 2t = 19.96953 mm. About thirty lines have been measured using neon standard lines and we estimate an accuracy of ± 0.005 Å. The large grating measurements agree with the interferometric measurements within the limits of error. The purpose of the interferometric measurements was not to obtain precision values but to support the ability of the electrodeless discharge source in producing sharp and intense lines. In this connection Chapter IV was included which describes all the details regarding reduction of interferograms using a Fabry Perot interferometer, in the case of the arc spectrum in potassium.

To follow page 42

INTERFEROGRAMS (10 mm etalon)

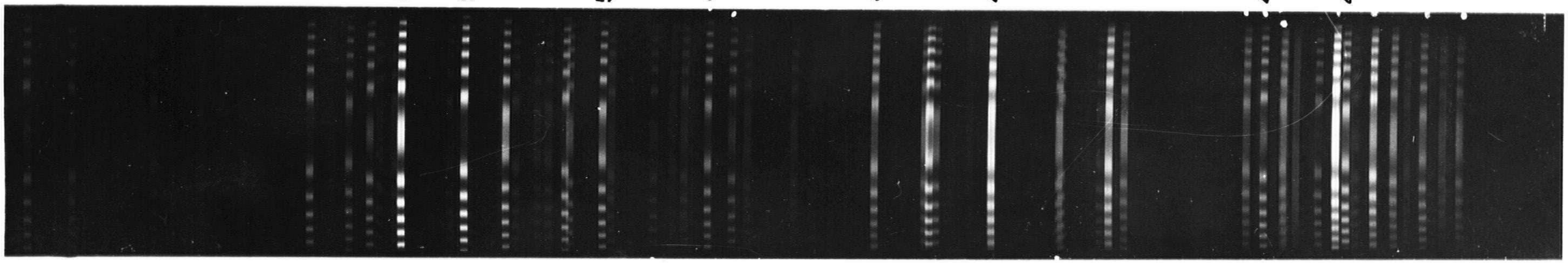

Selenium (Electrodeless discharge)

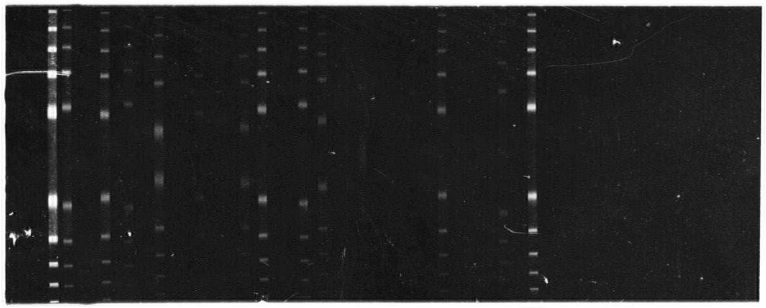

Neon (Geissler tube)

Vacuum Ultra Violet Standard Lines.

In order to obtain some useful standard lines in the vacuum ultra violet region, a few drops of benzene were introduced into the trap which was between the electrodeless tube and the fore pump. This enabled us to get some pure carbon and hydrogen lines which served as standards in some regions. In addition to this internal standards (known selenium lines) were also used, their values being determined from higher orders.

It is well known that the vacuum region standard lines are very rare and consequently the accuracy in wavelength measurements depends largely on the availability of reasonable standard lines in the desired region.

Probable Excitation.

Three sets of plates were taken on the 21 foot grating at different excitation conditions. The first set of plates was found to be of low excitation, while the second set of medium excitation and the third of high excitation. By comparing these plates using a Jarrell-Ash console comparator we could assign probable excitation for most of the lines. Figure 7 gives the different types of plates used, with the corresponding $n\lambda$ regions.

To follow page 43

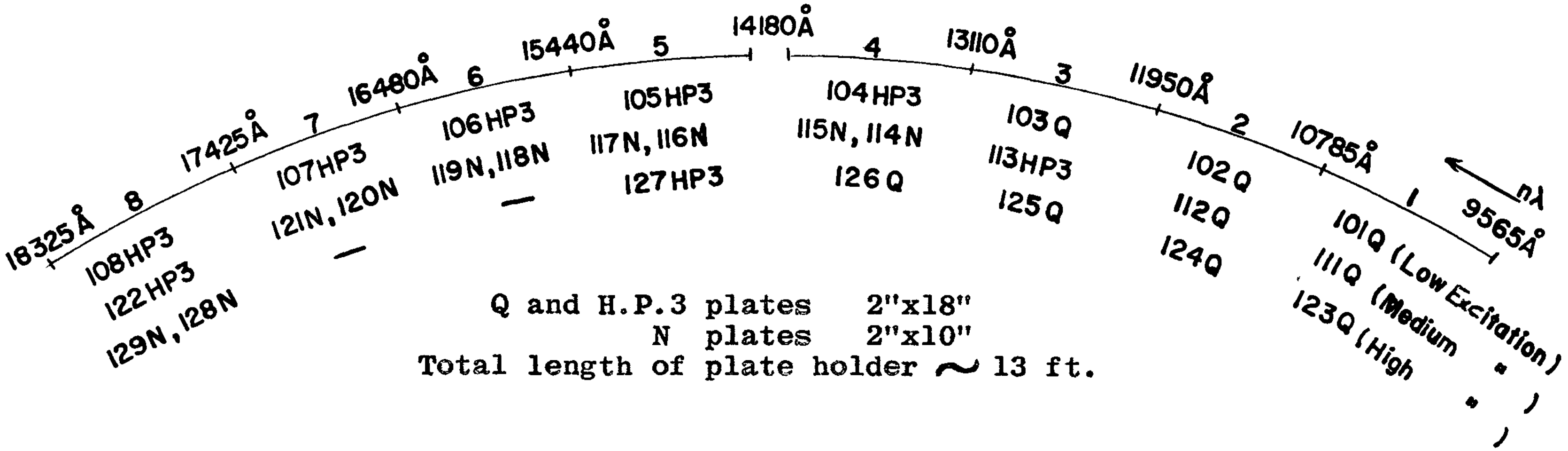

Fig. 6. 21 ' Grating plate holder showing the different plates with nλ regions.

Two Metre Vacuum Spectrograph Dispersion

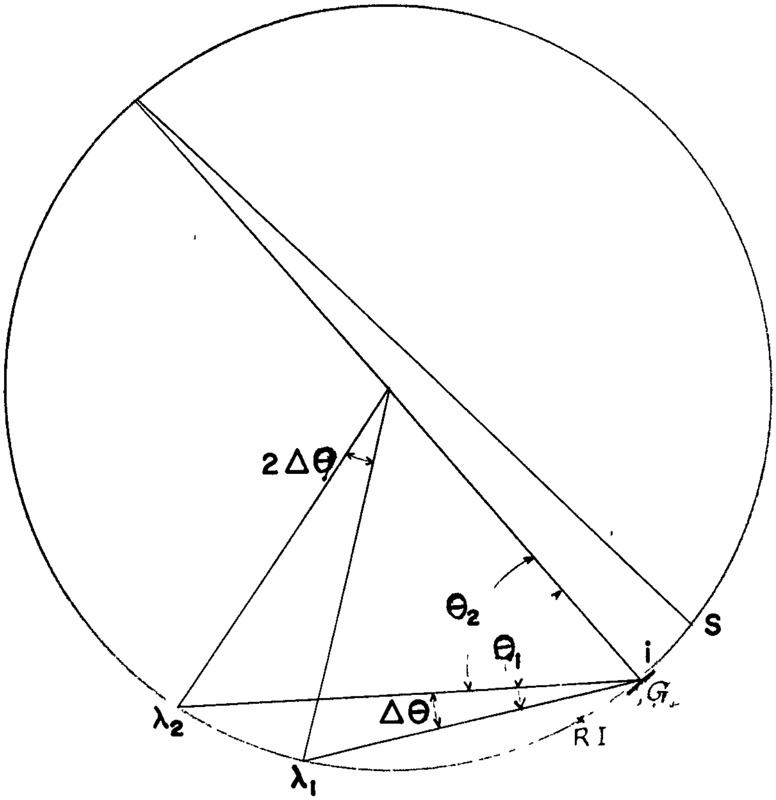

$\lambda_1 = b(\sin i - \sin \theta_1)$

$\lambda_2 = b(\sin i - \sin \theta_2)$

Measure s from R.I. (real image).

$$\bar{\vartheta} = \frac{\lambda_2 - \lambda_1}{S_2 - S_1} = \frac{b(\sin \theta_1 - \sin \theta_2)}{R(\theta_1 - \theta_2)} = \frac{b(\sin \theta_1 - \sin \theta_2)}{S_2 - S_1}$$

$$\vartheta = \frac{d\lambda}{ds} = \frac{b \cos \theta}{R} .$$

To obtain b and sin i.

Identify λ_1 and λ_2 and measure $(S_2 - S_1)$.

Calculate $\bar{\vartheta} = \dfrac{b(\sin \theta_1 - \sin \theta_2)}{R \ \Delta\theta}$.

Use for b and R their normal values, then find by trial and error θ_1 and θ_2.

We know $\Delta\theta(\text{rad}) = \frac{S_2 - S_1}{R} = 57.2958\ (\frac{S_2 - S_1}{R})$ degrees.

Find θ_1 and θ_2 from tables

Then λ_1 and λ_2 can be separately solved for i. If these agree, the whole procedure has some justification.

Further the distance of vertex from slit = $R\cos i$ is measurable.

$$\lambda_1(\text{vac}) = 2040.506\ \text{Å}$$

$$\lambda_2(\text{vac}) = 2838.062\ \text{Å}$$

$$S_2 - S_1 = 171.917\ \text{mm.}$$

$$\bar{\vartheta} = \frac{797.556}{171.917} = 4.639192\ \frac{\text{Å}}{\text{mm}}$$

$$= \frac{b(\sin\theta_1 - \sin\theta_2)}{171.917}$$

where

$$(\sin\theta_1 - \sin\theta_2) = \frac{797.556\ \text{Å}}{16{,}666.7\text{Å}} = 0.0478534$$

$$\theta_1 - \theta_2 = \frac{171.917}{2000}\ 57.2958$$

$$= 4.92506^\circ.$$

$$\sin\theta_1 = \sin 58.622270 = 0.8537572$$

$$\sin\theta_2 = \sin 53.69764 = 0.8059039$$

<u>Check</u>:

$$\bar{\vartheta} = \frac{797.557}{171.917} = 4.6391980.$$

$$\sin i = \frac{\lambda_1}{b} + \sin \theta_1 = \begin{array}{r} 0.1224303 \\ \underline{0.8537572} \\ 0.9761875 \end{array}$$

$$\sin i = \frac{\lambda_2}{b} + \sin \theta_2 = \begin{array}{r} 0.1702837 \\ \underline{0.8059039} \\ \underline{\underline{0.9761876}} \end{array}$$

$$\underline{\underline{i = 77.47135^\circ}}$$

TABLE I
Dispersion Table from nλ 300 — 4500 Å

Dispersion in Å/mm

2-Metre Vacuum Spectrograph

nλ (Å)	0	10	20	30	40	50	60	70	80	90
300	2.3845	2.4010	2.4175	2.4339	2.4502	2.4664	2.4825	2.4985	2.5144	2.5302
400	2.5459	2.5615	2.5769	2.5922	2.6074	2.6225	2.6375	2.6524	2.6673	2.6821
500	2.6968	2.7114	2.7259	2.7403	2.7546	2.7688	2.7830	2.7971	2.8111	2.8250
600	2.8388	2.8528	2.8665	2.8801	2.8936	2.9070	2.9204	2.9337	2.9469	2.9601
700	2.9732	2.9863	2.9993	3.0122	3.0250	3.0378	3.0505	3.0632	3.0758	3.0884
800	3.1009	3.1134	3.1258	3.1382	3.1505	3.1627	3.1749	3.1870	3.1990	3.2110
900	3.2229	3.2348	3.2467	3.2586	3.2704	3.2821	3.2937	3.3053	3.3168	3.3282
1000	3.3396	3.3510	3.3623	3.3736	3.3849	3.3961	3.4073	3.4185	3.4296	3.4406
1100	3.4516	3.4625	3.4734	3.4843	3.4951	3.5059	3.5167	3.5274	3.5381	3.5488
1200	3.5595	3.5701	3.5807	3.5912	3.6016	3.6120	3.6224	3.6327	3.6430	3.6532
1300	3.6634	3.6736	3.6837	3.6938	3.7039	3.7140	3.7240	3.7340	3.7440	3.7540
1400	3.7639	3.7738	3.7836	3.7934	3.8032	3.8129	3.8226	3.8323	3.8419	3.8515
1500	3.8611	3.8707	3.8802	3.8897	3.8991	3.9085	3.9179	3.9273	3.9366	3.9459
1600	3.9552	3.9645	3.9737	3.9829	3.9921	4.0013	4.0104	4.0195	4.0286	4.0376
1700	4.0466	4.0556	4.0646	4.0736	4.0825	4.0914	4.1002	4.1090	4.1178	4.1266
1800	4.1353	4.1440	4.1527	4.1614	4.1701	4.1787	4.1873	4.1959	4.2045	4.2131

Table I (continued)

nλ(Å)	0	10	20	30	40	50	60	70	80	90
1900	4.2216	4.2301	4.2386	4.2471	4.2555	4.2639	4.2723	4.2806	4.2889	4.2972
2000	4.3055	4.3138	4.3221	4.3303	4.3385	4.3467	4.3549	4.3630	4.3711	4.3792
2100	4.3873	4.3954	4.4035	4.4115	4.4195	4.4275	4.4355	4.4434	4.4513	4.4592
2200	4.4671	4.4750	4.4828	4.4906	4.4984	4.5062	4.5140	4.5217	4.5294	4.5371
2300	4.5448	4.5525	4.5601	4.5677	4.5753	4.5829	4.5905	4.5981	4.6057	4.6133
2400	4.6208	4.6283	4.6358	4.6432	4.6506	4.6580	4.6654	4.6728	4.6802	4.6876
2500	4.6950	4.7024	4.7097	4.7170	4.7243	4.7315	4.7387	4.7459	4.7531	4.7603
2600	4.7675	4.7746	4.7817	4.7888	4.7959	4.8030	4.8101	4.8172	4.8243	4.8313
2700	4.8383	4.8453	4.8523	4.8593	4.8663	4.8732	4.8801	4.8870	4.8939	4.9008
2800	4.9077	4.9145	4.9213	4.9281	4.9349	4.9417	4.9485	4.9553	4.9621	4.9689
2900	4.9756	4.9823	4.9890	4.9957	5.0024	5.0091	5.0156	5.0222	5.0288	5.0354
3000	5.0421	5.0487	5.0553	5.0618	5.0683	5.0748	5.0813	5.0878	5.0943	5.1008
3100	5.1072	5.1136	5.1200	5.1264	5.1328	5.1392	5.1456	5.1520	5.1584	5.1647
3200	5.1710	5.1773	5.1836	5.1899	5.1962	5.2025	5.2088	5.2150	5.2212	5.2274
3300	5.2336	5.2398	5.2460	5.2522	5.2584	5.2645	5.2706	5.2767	5.2828	5.2889
3400	5.2950	5.3011	5.3071	5.3131	5.3191	5.3250	5.3311	5.3371	5.3431	5.3491
3500	5.3551	5.3611	5.3670	5.3729	5.3788	5.3847	5.3906	5.3965	5.4024	5.4083
3600	5.4142	5.4201	5.4259	5.4317	5.4375	5.4433	5.4491	5.4549	5.4607	5.4665
3700	5.4722	5.4779	5.4836	5.4893	5.4950	5.5007	5.5064	5.5121	5.5178	5.5235

Table I (continued)

nλ(Å)	0	10	20	30	40	50	60	70	80	90
3800	5.5291	5.5347	5.5403	5.5459	5.5515	5.5571	5.5627	5.5683	5.5739	5.5794
3900	5.5849	5.5904	5.5959	5.6014	5.6069	5.6124	5.6179	5.6234	5.6289	5.6344
4000	5.6398	5.6453	5.6507	5.6561	5.6615	5.6669	5.6723	5.6777	5.6831	5.6884
4100	5.6937	5.6990	5.7043	5.7096	5.7149	5.7203	5.7255	5.7308	5.7361	5.7414
4200	5.7467	5.7519	5.7571	5.7623	5.7675	5.7727	5.7779	5.7831	5.7883	5.7935
4300	5.7987	5.8039	5.8091	5.8142	5.8193	5.8244	5.8295	5.8346	5.8397	5.8448
4400	5.8499	5.8550	5.8601	5.8652	5.8702	5.8752	5.8802	5.8852	5.8902	5.8952
4500	5.9002	5.9052	5.9102	5.9152	5.9202	5.9252	5.9302	5.9351	5.9400	5.9448

CHAPTER III

RESULTS AND ANALYSIS

Most of the lines have appeared on several plates and, in the case of exposures on the grating, in several different orders. For the 21 foot grating the weighted means give wavelengths which are accurate to 0.01 Angstrom. The prism wavelengths in the visible region are accurate to about 0.1 Å and in the infra red to better than 1 Å. In the vacuum region, it is estimated that the wavelengths are accurate to only about 0.03 Å, the reason being the scarcity of good standard lines. As described earlier the accuracy in the case of large grating measurements is supported by the Fabry Perot interferograms.

Selenium I and II

The neutral atom contains six electrons outside the closed shell, and has a $4s^24p^4\ {}^3P_2$ ground state. Ruedy and Gibbs (42a,b) in the analysis of Se I have observed 510 lines and classified 391 lines between 300 Å and 11000 Å. Meissner et al (29,30) have published a list of selenium I lines between 3588 Å and 9665 Å. As mentioned in the 'Atomic Energy Levels' Vol. II compiled by Mrs. Sitterly (33), these two lists are discordant with regard to wavelengths of a number of lines common to both. Ruedy and Gibbs quote the ionization potential for Se I as 78658.22 cm^{-1} which corresponds to 9.75 ev. As mentioned earlier (page 2) Shenstone's recent analysis of Se I supports that of Ruedy and Gibbs. We made no attempt to analyse this spectrum. In Se II the ground state is $4s^2 4p^3\ {}^4S^{\circ}_{3/2}$. No attempt has been made to extend the analysis of Se II presented by Martin (24), and most of his measurements are in good agreement with our values. For full details of the assignment of the lines and the structure of the spectrum reference should be made to his paper. He has classified 192 lines in the range between 694 and 9816 Å. The ionization potential for Se II quoted by him is 173557 cm^{-1} which corresponds to 21.5 ev. Some 40 lines on our plates, apparently not observed by him, could be classified as transitions between levels established by him. These lines are marked II** in our wavelength tables 2.

Selenium III

The ground state of Se II is $4s^2 4p^2\ {}^3P_o$ and the chief series are due to the successive excitation of one of the 4p electrons. The only attempts made in analysing this spectrum are by Badami and Rao (4) and by Rao and Murti (39) and they have classified 218 lines in the region λλ 517 Å - 6613 Å . Since some of their wavelenths were of doubtful accuracy, we have found it necessary to revise the values of most of the levels reported by them although the names assigned to these levels are correct. Many lines due to the transitions $4s^24p4d$ - $4s^24p5p$ are situated above λ 6700 and some of these calculated values are identified in our investigation which support their classification. In addition to this many lines apparently not observed by Rao have been classed as transitions between levels established by him.

$^5S_2^\circ$ Term in Se III

The terms associated with the configuration $4s4p^3$ are $^5S^\circ$, $^3S^\circ$, $^3P^\circ$, $^3D^\circ$, $^1P^\circ$, $^1D^\circ$, the $^5S_2^\circ$ member of which lies quite low. The discovery of two new germanium lines by Andrew and Meissner (1) led to the recognition of the $^5S_2^\circ$ term in Ge I. The recognition of the $^5S_2^\circ$ term in As II was established in this laboratory a few years ago (6). Using these values and the irregular doublet law the position of the $^5S_2^\circ$ term in Se III was calculated. By sweeping the wavelength list in the expected region for a difference of 2196 cm^{-1} ($4s^24p^2\ ^3P_2$ - $4s^24p^2\ ^3P_1$) we arrived at 2 possibilities and all the four lines were unobserved by earlier workers. However, an examination of the plate together with a comparison of intensities for the same transitions in Ge I and As II led us to choose 65200 cm^{-1} and 67400 cm^{-1} instead of 64566 and 66760.

Irregular doublet law applied to Ge I, As II, Se III

	Ge I		As II		Se III
$4s^24p^2\ ^3P_2$-$4s4p^3\ ^5S_2^\circ$	40512		52275		64275
		11763		12000	observed = 65,200 cm^{-1}

The establishment of the $4s4p^3$ $^5S_2^\circ$ term has been gratifying since this is one of the basic terms in Se III. As can be seen from the table above its position is reasonably close to that predicted by the irregular doublet law.

<u>$4s^2$4pns configurations</u>

The theory for the intervals between the levels belonging to this configuration is known for any type of coupling and is helpful in identifying the levels of higher members of this configuration. We applied Houston's theory for intermediate coupling to 4p5s and 4p6s and found it quite good (see page 54). We have established the 4p7s in this series.

The missing level 4p5d $^3P_o^\circ$ is also established and it is interesting to note that the three transitions 4p5d $^3P_{0,1,2}$ to the ground level $4p^2$ $^3P_1$ lie as a strong group on our plates. We have also established $4p^2$ ^1S_o in Se III by its combination with 4p5s $^3P_1$ and $^1P_1$ levels. A thorough but unsuccessful attempt has been made in locating the terms arising from the 4p4f configuration, using the theory of intermediate coupling in the pair coupling approximation. We had expected to add several new terms to this spectrum, but have been disappointed.

<u>Ionization Potential for Se III</u>

Badami and Rao (4) give the limit 274924 cm^{-1}. Mrs. Sitterly (33) has recalculated the limit and the value

Houston's Theory (16) applied to np·n's configuration in Se III

Config.	$^3P_0$	$^3P_1$	$^3P_1-{}^3P_0$	$^3P_2$	$^3P_2-{}^3P_0$	$^1P_1$ Calc.	$^1P_1$ Obs.
4p.5s	126275	126779	504	130388.6	4113.6	133855.7	131653.6
4p.6s	187168.7	187426.5	275.8	191523.0	4354.3	193519.8	192161.8
4p.7s	209235	209391	156	213628	4393	215402.9	214017

given is 258000 cm^{-1}. Calculations of n* for the members of the np.n's series showed that even Mrs. Sitterly's limit was high. Hence we calculated the limit from the $^3P_2$ levels of np6s and np7s series and the value is 253027 cm^{-1}. Using the $^3P_0$ levels the lower limit was calculated to be 248583 cm^{-1}. For n* values (Table 3) we have used the value 250,000 cm^{-1}.

We have added another 55 classified lines to this spectrum.

Selenium IV

The ground state of Se IV is $4s^2 4p\ ^2P_{\frac{1}{2}}$. This spectrum is isoelectronic with Ga I, Ge II, As III. Rao and Badami (37) have analysed this spectrum and classified 35 lines between 635 Å and 3059 Å.

a) Location of the term ^4P in Se IV

The terms arising from the configuration $4s4p^2$ are ^4P, ^2P, ^2D, ^2S of which the ^4P member lies quite low. In As III this term was established by Bedford (6). Hence we could use the irregular doublet law to predict the location of this term in Se IV. The following tables show the use of this law and give the calculations for the interaction constant for 4p electron in ^4P.

Irregular doublet law applied to ^4P in Se IV

	GaI		GeII		AsIII		SeIV	
c.g. ^4P	38565		52709		67228		82628 (pred)	82015 (obs)
		14144		14719		15400		
$4p\ ^3P_{3/2} - 4p^2\ ^4P_{\frac{1}{2}}$	37146		49809		62469		75124 (pred)	75022 (obs)
		12663		12660		12655		

Interaction constant for 4p electron in ^4P in Se IV

	GaI	GeII	AsIII	SeIV
$\Delta\ ^4P$	941	1791	2868	4200 4187 (obs)
$A\ ^4P$	235	448	717	1050 1047 (obs)
γ_p	705	1344	2151	3100 3141 (obs)

A = Landé interval factor for ^4P

γ_p = Interaction constant of 4p electron

b) $4s^2ng$ and nh series

A search was made to locate the members of the ng and nh series and we were successful in extending the ng series up to n = 9 and the nh series up to n = 8. The level $6g\,^2G$ is fixed by its combination with $7h\,^2H$ and $8h\,^2H$. But we do not find proper combinations for $6g\,^2G$ with $4s^25f_{5/2,7/2}$ levels. However, the levels $4s^2\,5f\,^2F_{5/2}$, $^2F_{7/2}$ depend only on their combinations with $4s^25d\,^2D_{3/2}$, $^2D_{5/2}$ and hence should be taken as tentative. In the nh series, using Rydberg series extension, we have established the members 6h, 7h and 8h by their strong combinations with 5g. All the three lines are new and very intense and were already suspected to be of high excitation from excitation data. Further, since these lines do not exhibit any structure, it is concluded that 5g is not split. The level $4s^27s\,^2S_{\frac{1}{2}}$ suggested by Rao (37) is rejected on the basis of n* values and now we have established this level by its combinations with the $4s^24p\,^2P_{\frac{1}{2},\frac{3}{2}}$ and $4s^25p\,^2P_{\frac{1}{2},\frac{3}{2}}$.

	Level	n*
$4s^25s\ ^2S_{\frac{1}{2}}$	157241	3.047
$4s^26s\ ^2S_{\frac{1}{2}}$	240751	4.077
$4s^27s\ ^2S_{\frac{1}{2}}$	288146 (Rao)	5.491
	280145 (Present work)	5.149

In addition the levels $4s^26p\,^2P_{\frac{1}{2}}$, $^2P_{3/2}$, $4s^27p\,^2P_{\frac{1}{2}}$, $^2P_{3/2}$ and $4p^3\,^4S_{3/2}$ are also established. It is seen that the ns $^2S_{\frac{1}{2}}$ levels combine strongly with the np $^2P_{\frac{1}{2}}$, $^2P_{3/2}$ levels. Out of the two levels $4s^2 6d$ $^2D_{3/2}$, $^2D_{5/2}$, $^2D_{3/2}$ is well supported by its combinations with 5p and 6p but $^2D_{5/2}$ is tentative because of large separation from $^2D_{3/2}$.

Ionization Potential

Using the $4s^2nh$ series a new ionization potential was calculated

$$I.P. = 346360 \text{ cm}^{-1}$$

Using the formula given by Edlén and Risberg (11a) the correction ΔT to be added was also calculated

$$\Delta T = 15.5 \text{ cm}^{-1}$$

Ionization potential = 346,375 $\pm$ 100 cm^{-1} which corresponds to 42.94 $\pm$ 0.01 ev.

We have added another 52 classified lines to this spectrum.

Selenium V

The ground state of Se V is $4s^2\ ^1S_0$. This spectrum consists of a singlet and triplet system, similar to Zn I. Sawyer and Humphreys (44) have classified 16 lines between λλ 839 - 506 Å, mainly by the application of the irregular and regular doublet laws to the isoelectronic spectra Zn I, Ga II, Ge III, As IV and Se V. These chief triplet terms found by them due to the configurations 4s4p, 4s4d, 4s5s and $4p^2$ are further confirmed by Rao and Badami (38) by identifying a few singlets and intercombinations arising from the above configurations. All these lines appear very strongly on our plates and we support their classifications.

However, a comparison of the n* values with those of As IV immediately showed a discrepancy regarding the ionization potential. By an extrapolation along the isoelectronic sequence we estimate the ionization potential to be 551600 cm^{-1}. We have established the 4s5p $^3P_{0,1,2}$ $^1P_1$ and the 4s4f $^3F_{2,3,4}$ $^3F_3$ levels by their combinations with the 4s4d $^3D_{1,2,3}$. The term 4s5s $^1S_0$ is also found. One of the lines supporting this is doubly classified in the same spectrum. The levels 4s5d $^3D_{1,2,3}$ should be taken as tentative, even though the interval ratios for

4s5d $^3D_{1,2,3}$ compared to 4s4d look good (Table 5). A peculiarity of this spectrum is the appearance of the singlets deeper than the triplets in the nd series. All members of the isoelectronic sequence exhibit the same effect. We have added another 32 lines to this spectrum.

In our calculations for n* (Table 5) we have taken the value of the ionization potential for Se V as 550976 cm^{-1}, quoted by Finkelnburg and Humbach (52).

Selenium VI and Selenium VII

The ground state of Se VI is $3d^{10}\ 4s\ ^2S_{\frac{1}{2}}$. By extrapolation along the isoelectronic sequence Sawyer and Humphreys (44) have classified seven lines between 452 Å and 886 Å and the limit is given as 658994 cm^{-1}. All these lines appeared on our plates too. However, we did not try to extend the analysis of this spectrum, mainly because we did not expect our source to excite more Se VI lines strongly.

Se VII

The ground state of Se VII is $3d^{10}\ {}^1S_0$. Rao and Murti (39) attribute some 42 lines in the region λλ 860 - 560 Å to Se VII. They have also given tentative classifications for four of them. Out of these, 28 lines have appeared on our plates including two of their classified lines. Even though we agree with them that these lines are highly enhanced, we still feel that these lines should belong to Se V or at the most to Se VI. We feel our source was not capable of exciting lines in Se VII. With the exception of the resonance lines, even the Se VI lines were not strong on our plates.

TABLE 2

Catalogue and Classification of Selenium Lines

M.I.T.: Intensity given in M.I.T. wavelength tables (51)
E_DP : Intensity on prism spectrograph (electrodeless discharge)
R : Intensity observed by Rao (4,37,38,39)
S_{HE} : Intensity on prism spectrograph (Spark in Helium)
E_DG : Intensity on 21 foot grating (electrodeless discharge)
K : Intensity given by Kayser (19)
Ky : Intensity given by Kelly (20)
V_G : Intensity on vacuum grating (electrodeless discharge)
* : Interferometric measurement
d : Diffuse line
δ : Double line c: Carbon line

Lines marked I are classified in Se I by Ruedy and Gibbs (42a)

Lines marked II are classified in Se II by Martin (24)

Lines marked II** are now classified in Se II using the levels in (24)

Lines marked III are classified in Se III by Rao (4,39)

Note: All intensities are on a visual scale of 0 - 300 on E_DP
0 - 2000 on E_DG
0 - 100 on V_G
0 - 10 on S_{HE}

The intensity estimates are consistent only within restricted wavelength ranges since the lines were recorded on emulsions of different sensitization and no attempt was made to correct for this difference.

Intensity						Wave-length	Wave-number	Classification
M_{I_T}	E_DP	R	S_{He}	E_DG	K	λ(Å)	(cm^{-1})	
	10d					10457	9560.2	
	8d					10320	9687.3	
	10d					10106	9892.4	
	2					9968.2	10029.2	I
	2					9941.0	10056.6	

Intensity						Wave-length	Wave-number	Classification
M_{I_T}	E_DP	R	S_{He}	E_DG	K	λ(Å)	(cm^{-1})	
	1					9904.6	10093.6	
	1					9850.3	10149.2	
	6					9799.9	10201.4	
	4					9780.6	10221.5	
	10					9769.6	10233.0	
	6					9755.1	10248.2	I
	3					9726.0	10278.9	
	10					9674.8	10335.4	
	30					9654.2	10355.4	
	10					9618.6	10393.7	
	20					9598.5	10415.5	
	8					9549.8	10468.5	I
	25					9536.1	10483.6	I
	10d					9471.4	10555.2	
	8					9417.9	10615.1	II**
	30					9392.8	10643.5	
	10					9387.9	10649.1	
	10					9350.9	10691.2	
	10d					9276.2	10777.4	
	10d					9246.9	10811.5	III $4p4d\,^3P_2-4p5p\,^3D_2$
	2					9220.2	10842.8	
	100					9219.5	10843.6	
	40					9189.7	10878.8	
	8					9179.9	10890.6	
	200					9119.9	10962.0	
	20d					9104.0	10981.2	
	8d					9094.3	10992.9	
	10d					9079.1	11011.3	
	20d					9065.6	11027.7	
	30d					9033.8	11066.5	
	10d					9014.7	11089.9	II**
	40d					8998.6	11109.8	
	5d					8993.0	11116.7	
	25d					8984.0	11127.8	
	10d					8968.2	11147.4	I
	200					8916.1	11212.6	I
	20					8903.5	11228.5	
	6d					8826.7	11326.2	
	10d					8801.1	11359.1	
	1					8782.0	11383.8	

Intensity						Wave-length	Wave-number	Classification
M_{I_T}	E_DP	R	S_{He}	E_DG	K	λ(Å)	(cm^{-1})	
	40d					8770.5	11398.7	
	20d					8760.3	11412.0	
	1					8742.1	11435.8	I
	1					8708.9	11479.3	
	1					8700.4	11490.6	
	8					8685.9	11509.7	III $4p4d\,^3D_3-4p5p\,^3D_2$
	15					8678.8	11519.1	II
	20d					8665.6	11536.7	I
	1					8647.5	11560.8	
	5					8636.5	11575.5	
	5d					8630.4	11583.7	IV $6d\,^2D_{5/2}-7p\,^2P_{3/2}$
	3					8627.1	11588.2	
	1d					8591.7	11635.9	
	20d					8570.9	11664.1	
	1d					8567.1	11669.3	I
	3					8548.2	11695.1	
	0					8536.7	11710.8	
	1					8527.7	11723.2	
	80d					8519.5	11734.6	
	5					8477.3	11793.0	
	1					8451.4	11829.1	I
	5					8444.4	11838.9	
	200					8422.5	11869.7	
	100					8405.5	11893.7	
	4					8393.2	11911.1	
	2					8383.8	11924.5	
	1					8371.8	11941.6	
	1					8346.5	11977.8	
	1					8336.8	11991.7	
	6					8307.2	12034.4	
	1					8291.0	12057.9	
	1					8283.4	12069.0	
	0					8272.0	12085.6	I
	100					8261.5	12101.0	
	10					8260.2	12102.9	
	4					8254.2	12111.7	
	1					8240.9	12131.2	
	0					8221.1	12160.4	
	10d					8214.0	12170.9	
	1					8198.2	12194.4	II**

Intensity						Wave-length	Wave-number	Classification
M_{I_T}	E_DP	R	S_{He}	E_DG	K	λ(Å)	(cm^{-1})	
	6d					8186.6	12211.7	
	80		5			8169.3	12237.7	
	8		3			8149.4	12267.5	I
	30					8113.5	12321.8	
	100					8112.2	12323.8	
	8d					8102.9	12337.9	
	80					8101.1	12340.7	
	100					8098.8	12344.2	I
	40					8091.6	12355.1	
	20					8075.2	12380.2	
	2					8053.0	12414.3	
	0					8036.0	12440.6	I
	10					8013.7	12475.2	
	100			100		8012.2	12477.5	
	100					8005.3	12488.3	
	60			30		8003.1	12491.7	III $4p4d\,^1F_3-4p5p\,^1D_2$
	50					7989.1	12513.6	
	0					7963.2	12554.3	I
	4					7947.5	12579.1	
	100			100		7944.7	12583.5	
	0					7933.0	12602.1	II**
	1					7885.9	12677.3	
	0					7868.8	12704.9	
	60					7838.6	12753.8	II
	15d					7798.1	12820.2	
	60d					7772.9	12861.7	II
	3					7735.3	12924.2	I
	10					7724.3	12942.6	II
	100			100		7721.7	12947.0	IV $6h\,^2H-7g\,^2G$
	4					7705.1	12974.9	
	3					7675.1	13025.6	II
	1					7669.1	13035.8	
	50					7662.6	13046.8	IV $6g\,^2G-7h\,^2H$
	0					7642.7	13080.8	II**
	20					7635.4	13093.3	
	150			150		7632.1	13098.9	
	4					7618.0	13123.2	
	3					7597.8	13158.1	
	5					7589.9	13171.8	
	100			100		7587.1	13176.6	I

Intensity MI_T	E_DP	R	S_{He}	E_DG	K	Wave-length λ(Å)	Wave-number (cm^{-1})	Classification
	1					7560.7	13222.6	
	4					7515.4	13302.3	
	30			[illegible]		7512.8	13306.9	
	15					7504.8	13321.1	
	60			[illegible]		7501.6	13326.8	
	8					7492.4	13343.1	
	4					7469.0	13384.9	
	20					7460.8	13399.6	
	2					7443.2	13431.3	
	0					7424.4	13465.5	I
	10					7392.9	13522.8	II
	10d					7384.4	13538.4	
	60			[illegible]		7382.7	13541.5	
	3d			40		7378.8	13548.7	
	0					7350.6	13600.6	III $4p4d\,^3P_1-4p5p\,^3P_1$
	8			[illegible]		7346.8	13607.7	
	1					7322.3	13653.0	III $4p4d\,^3P_2-4p5p\,^3P_1$
	3					7271.7	13748.2	
	3					7270.3	13750.8	
	4					7265.7	13759.3	
	1					7258.5	13773.2	
	25					7244.5	13779.8	
	8			[illegible]		7232.2	13823.2	
	0					7216.4	13853.5	
	2					7172.9	13937.5	
	4					7160.5	13961.6	
	6					7148.0	13986.0	III $4p4d\,^3P_2-4p5p\,^3D_3$
	2					7139.5	14002.7	II
	8			[illegible]		7112.3	14056.2	
	8					7085.5	14109.3	III $4p4d\,^3D_2-4p5p\,^3D_2$
	5					7068.5	14143.3	III $4p4d\,^3D_1-4p5p\,^3P_0$
	20					7064.2	14151.9	II**
	10d					7061.1	14158.1	
	0					7048.4	14183.8	
	1					7021.2	14238.7	
	1					6965.4	14352.8	
	8d			[illegible]		6964.2	14355.2	
	2					6955.4	14373.4	
	3					6947.8	14389.1	II**
	0					6925.6	14435.2	II

Intensity						Wave-length	Wave-number	Classification
M_{I_T}	E_DP	R	S_{He}	E_DG	K	λ(Å)	(cm^{-1})	
	0					6914.7	14458.0	
30	0					6895.9	14497.4	
	6d			[illegible]		6885.3	14519.7	
	6d					6884.4	14521.6	
	0					6862.5	14567.9	
	4d					6861.9	14571.3	
15	2			4d		6830.6	14635.9	I
	15					6810.5	14679.1	III $4p4d\,^3D_3 - 4p5p\,^3D_3$
	1					6799.3	14703.3	
	1					6792.6	14717.8	
	2					6782.8	14739.0	
15	1					6777.6	14750.4	
	2			[illegible]		6755.3	14799.3	I
30	1					6751.6	14807.4	
	3					6697.1	14927.6	
	6					6684.0	14957.1	
	50		8	[illegible]		6683.0	14959.3	II**
	1					6659.2	15012.7	II**
	20					6642.2	15051.1	
	8					6637.5	15061.8	
	10					6629.69	15079.5	
	20					6614.29	15114.6	III
	1					6603.44	15139.5	
	2					6598.91	15149.84	
8	50	3				6591.58	15166.68	III
	0		0			6582.3	15188.1	
	1		2			6578.4	15197.1	
	50		10			6563.41	15231.78	
4	25	2				6545.48	15273.49	
300	60					6534.94	15298.12	II
	8					6524.34	15322.99	IV $6s\,^2S_{\frac{1}{2}} - 6p\,^2P_{\frac{1}{2}}$
3	15					6517.19	15339.80	
	4d					6512.69	15350.40	I
	6d					6505.51	15367.33	
500	100			40		6490.54	15402.79	II
200	40					6483.11	15420.44	II
	15	1				6448.99	15502.03	
100	40			75		6444.29	15513.33	II
	2					6432.67	15541.34	
	4					6429.03	15550.14	

Intensity M_{I_T}	E_DP	R	S_{He}	E_DG	K	Wave-length λ(Å)	Wave-number (cm^{-1})	Classification
125	35			40		6422.93	15564.90	
6	40	3		8d		6416.99	15579.33	II
	2d					6411.61	15592.40	
	4d					6397.05	15627.88	
	10d					6382.72	15662.98	
30	6					6370.91	15692.01	II
5	20	1				6359.24	15720.80	III
	15d					6349.45	15745.03	
	15d					6343.80	15759.08	
15	4d					6338.12	15773.19	II
	4d					6332.61	15786.91	
	10d					6326.04	15803.31	II
	5d					6322.46	15812.25	I
	8d					6308.86	15846.35	
				5d		6305.09	15855.83	
1000	100	8		40		6303.40	15860.08	III
3	5					6296.71	15876.92	
	6	0				6290.75	15891.96	
300	2					6284.59	15907.53	I
30	8					6281.74	15914.75	
	2					6272.42	15938.39	
	2					6265.91	15954.97	
5	8d					6261.06	15967.32	
30	10d					6244.65	16009.27	
	120	2				6238.79	16024.33	IV $6s^2S_{\frac{1}{2}}-6p^2P_{\frac{3}{2}}$
5	8					6220.81	16070.63	I
10	2					6206.36	16108.04	II
	2					6200.95	16122.09	
	8					6197.83	16130.20	
	4					6191.16	16147.60	
15	3					6183.74	16166.97	II
	6					6177.37	16183.64	
	6d					6171.48	16199.08	
30	8					6164.51	16217.39	
	8d					6149.88	16255.99	
15	10d					6144.35	16270.61	
	2d					6142.31	16276.02	
	3d					6138.00	16287.44	II**
70	8					6135.04	16295.30	II
	1					6131.51	16304.68	II

Intensity						Wave-length	Wave-number	Classification	
M_{I_T}	E_DP	R	S_{He}	E_DG	K	λ(Å)	(cm^{-1})		
4	8d	2				6125.58	16320.48		
60	15					6123.38	16326.34	II	
4	15	1				6115.89	16346.33		
	1					6110.16	16361.66		
	10	1				6105.80	16373.34		
	40					6101.27	16385.49	II	
50	10					6096.18	16399.17	II	
	10d					6084.53	16430.59		
80	15					6065.73	16481.50	II	
3	8d					6060.56	16495.55		
1000	80		2	70		6055.84	16508.41	II	
	6d					6054.12	16513.09		
	60	5		5		6042.56	16544.70	III	
	8d			0		6038.48	16555.88		
30	10d			0		6029.94	16579.32	II	
	60	6		10		6023.61	16596.74	III	
	6d					6020.27	16605.94		
	2d					6009.09	16636.86	II	
35	15					5990.73	16687.83	II	
8	20					5984.82	16704.31		
5	8d					5962.78	16766.06	II	
5	12	0				5959.53	16775.20		
	6d					5948.10	16807.43		
	5d					5936.95	16838.99	V	$4s4f\,^3F_4-4s5d\,^3D_3$
30	4d					5925.04	16872.85	I	
	4d					5910.23	16915.12		
	60	5		50	5	5898.09	16949.96	III	
	80	2		0	3	5885.21	16987.04	III	
	2d					5879.24	17004.29		
75	60			40	6	5866.19	17042.10	II	
	1					5860.21	17059.52		
	5d					5849.55	17090.60	II	
60	30			5	6	5842.57	17111.01	II	
	6d					5831.40	17143.78	II	
	20	1			5	5826.97	17156.81	III	
	8d	1			3	5824.47	17164.20		
	4d					5812.73	17198.86		
	1					5808.72	17210.73		
	40d				2	5800.34	17235.58	III	$4p4d\,^3D_1-4p5d\,^3P_2$
	20					5794.61	17252.62		

Intensity						Wave-length	Wave-number	Classification
M_{I_T}	E_DP	R	S_{He}	E_DG	K	λ(Å)	(cm^{-1})	
15	20				5	5789.93	17266.56	II
15	20	2			5	5784.73	17282.11	III,II
	2d					5775.39	17310.05	
15	20				5	5768.93	17329.43	II
	5d					5762.45	17348.91	
25	1					5753.38	17376.26	I
50	40		0		7	5747.51	17394.03	II
	5d					5739.65	17417.84	
20	20				5	5732.99	17438.07	II
15	20				5	5730.75	17444.88	II
10	20				5	5725.60	17460.57	
	2d					5716.36	17488.79	III $4p4d\,^1D_2-4p5p\,^3D_3$
	6d					5705.50	17522.10	
45	60		0	0	8	5697.84	17545.64	II
	4d		0			5679.01	17603.81	
	5d				3	5672.37	17624.44	II
	0					5666.95	17641.29	I
				0		5662.12	17656.33	
8	5d				2	5655.41	17677.28	II
				0		5652.62	17686.00	
8	8d				5	5652.36	17686.81	II
	2d				1	5649.98	17694.26	
	2d					5646.66	17704.66	
	3d					5644.43	17711.65	
300	60		2	25	9	5623.12	17778.79	II
15				75d		5618.05	17794.83	
	2d					5616.38	17800.43	II
15	20				5	5611.55	17815.12	
500	60		0	25	8	5591.15	17880.45	II
8	30				4	5586.34	17895.84	II
	4					5577.31	17924.81	
500	60		2	1000	9	5567.03	17957.90	II
8	20				4	5560.51	17978.98	II
	2d				1	5535.74	18059.41	
	2d			0		5528.64	18082.59	
750	80		0	5	8	5522.44	18102.92	II
	6d				4	5511.51	18138.81	
	2d					5507.46	18152.15	
	6d				5	5505.54	18158.48	
	2d					5502.13	18169.73	

Intensity						Wave-length	Wave-number	Classification
M_{I_T}	E_DP	R	S_{He}	E_DG	K	λ(Å)	(cm^{-1})	
				0	1	5497.06	18186.48	
	8d					5489.98	18209.93	
20	25				6	5484.12	18229.41	II
	6d					5481.56	18237.92	
10	20				6	5474.05	18262.94	
15	50			100	7	5455.82	18323.95	II
50	80			5	6	5444.99	18360.41	II
	12					5437.84	18384.55	
	2d					5434.13	18397.10	V $4s4f\,^3F_3-4s5d\,^3D_3$
	4d				2	5429.79	18411.80	III $4p4d\,^3P_1^3-4p5p\,^1D_2^3$
	3d					5427.41	18419.87	
15	8				5	5417.14	18454.78	
	5				2	5414.56	18463.57	III $4p4d\,^3P_2-4p5p\,^1D_2$
75	40d				4	5401.51	18508.20	II
35	40				6	5382.87	18572.27	
20	30			0	6	5380.17	18581.59	II
	4d				3	5375.87	18596.49	
150	4d				1	5374.27	18602.02	I
	8d				2	5370.02	18616.74	
	4					5358.79	18655.7	
	6				2	5354.65	18670.2	III $4p4d\,^1D_2-4p5p\,^3P_2$
	8				3	5328.54	18761.6	II**
	5			5	2	5322.85	18781.7	II**
15	30				5	5315.57	18807.4	
	20				3	5310.67	18824.8	
500	20		6	300	9	5305.347*	18843.75	II
18	40			5	5	5300.97	18859.24	II
	2d				2	5297.77	18870.6	
	8d				2	5287.77	18906.3	
	6d				2	5280.36	18932.8	V $4s4f\,^3F_2-4s5d\,^3D_1$
150	80		6	500	8	5271.179*	18965.72	II
100			6	300	7	5253.67	19029.02	II
50				250	6	5253.10	19031.09	II
35	50		0	50	6	5245.19	19059.78	II
	15d					5241.91	19071.7	
5	20				4	5237.60	19087.4	II
5	30				4	5235.23	19096.03	
	40	5		100	5	5232.78	19104.97	III
	30			50	3	5231.69	19108.99	
600	150		9	800	9	5227.533*	19124.23	II

Intensity						Wave-length	Wave-number	Classification
M_{I_T}	E_DP	R	S_{He}	E_DG	K	λ(Å)	(cm⁻¹)	
8	25			10	5	5223.85	19137.66	
	10				3	5218.05	19158.92	
	2					5202.40	19216.54	II**
18	50			20	5	5187.66	19271.16	II
15	25				5	5183.05	19288.30	II
600	150		9	750	9	5175.925*	19314.83	II
18	40			0	5	5171.49	19331.40	II
	20	0		0d	4	5150.02	19412.01	II
500	100		8	300	8	5142.124*	19441.79	II
35	50		2	0	7	5134.30	19471.43	II
25	40		0	20	6	5117.64	19534.38	II**
15				10	7	5109.62	19565.49	II
15			0	100	7	5109.16	19567.25	II
				50		5109.10	19567.48	
350	120		8	750	8	5096.532*	19615.73	II**
				25		5095.94	19618.00	
50	100		3	250	7	5093.225*	19628.43	II
	12d			100	3	5084.04	19663.94	
	8d			0	2	5081.75	19672.76	
	3d					5078.74	19684.42	
250	120		10	500	8	5068.630*	19723.71	II
	15d				3	5063.39	19744.1	II
				100	3	5062.05	19749.34	
	40d			50d		5061.61	19751.06	II
				750d	3	5060.47	19755.51	
	20d					5039.78	19836.59	
40	80		0	150	8	5031.15	19870.64	II
	50			50	5	5025.63	19892.46	
25	60			100	6	5019.36	19917.34	IV $6p\,^2P_{3/2}-6d\,^2D_{3/2}$
	5d			50		5017.15	19926.07	
	8d			100		5009.32	19957.21	
	2d		0			5006.63	19967.93	II**
	3d		0			5001.45	19988.61	
	5d					4997.04	20006.3	
300			10	500	8	4992.831*	20023.11	II
12				300	5	4992.10	20026.1	II
	0					4989.05	20038.31	
300	80		8	400	8	4975.735*	20091.90	II
	10d	2			2	4974.04	20098.77	III
	15d					4972.41	20105.35	

Intensity M_{I_T}	E_DP	R	S_{He}	E_DG	K	Wave-length λ(Å)	Wave-number (cm^{-1})	Classification
	3d					4966.88	20127.73	
	1d			100		4965.05	20135.17	
	25			60	4	4962.49	20145.57	
	25					4953.74	20181.15	
	5d					4950.69	20193.58	
	8d				2	4938.17	20244.76	
	2d					4935.23	20256.82	
	2d			100		4933.19	20265.23	
15	80		0	50	6	4920.96	20315.58	
	15d			150	2	4919.03	20323.55	III
8	30			0	4	4917.32	20330.62	
	12d					4911.99	20352.67	
	2d			0		4907.90	20369.63	III $4p5s\,^3P_2-4p5p\,^1P_1$
				75		4904.79	20382.54	
8	20				3	4897.55	20412.66	II
	200			50		4889.05	20448.14	
	200			50		4888.89	20448.81	
	20			2000		4879.844*	20486.72	
	1d					4870.74	20525.03	II**
	20	2		10	3	4860.35	20530.85	III
	1d					4864.91	20549.62	
	20d					4859.74	20571.48	
	2d					4856.86	20583.67	
				0	2	4853.49	20598.00	
	20d			2000		4847.84	20622.00	IV $6p\,^2P_{\frac{1}{2}}-6d\,^2D_{\frac{3}{2}}$
				100		4847.05	20625.57	
				30	2	4847.01	20625.57	II
800	100		10	1500	10	4844.941*	20634.30	II
800	80		8	1000	8	4840.609*	20652.79	II
	1					4837.88	20664.44	
	2					4835.17	20676.02	
12	15				4	4830.79	20694.79	
	5					4829.40	20700.72	
25	40		0	75	6	4819.80	20741.94	
				0		4819.36	20743.85	
	3					4818.28	20748.48	
	6d					4813.56	20768.82	
4	10d					4809.65	20785.74	II
				2000		4806.002*	20801.48	
	4					4801.11	20822.71	II

Intensity						Wave-length	Wave-number	Classification
M_{I_T}	E_DP	R	S_{He}	E_DG	K	λ(Å)	(cm^{-1})	
12	30			0	4	4797.66	20837.67	
	15					4791.89	20862.76	
	6d				2	4783.51	20899.30	
40	40				5	4765.62	20977.77	II
	4					4765.00	20980.50	
800			10		8	4763.646*	20986.23	II
20	30				5	4761.93	20994.03	II
	6				1	4742.59	21079.61	
600	60		6			4741.04	21086.50	II
800	20				1	4739.10	21095.13	I
	2					4737.21	21103.55	
	20					4735.89	21109.47	
8	12				3	4733.69	21119.28	II
1000	40		2		3	4730.86	21131.91	I
	10					4726.81	21150.01	
	30				4	4718.26	21188.33	II
	8				2	4714.37	21205.80	
	5d					4700.01	21270.58	
	6d					4695.94	21289.05	
	1d					4692.41	21305.66	
	8d					4689.79	21316.96	
12	20				5	4685.46	21336.66	II
				50		4682.24	21351.33	IV $6h\ ^2H - 8g\ ^2G$
	2					4680.99	21357.03	
				0		4678.36	21369.04	
	12d					4669.95	21467.50	
	1				4	4665.41	21428.33	
	3					4664.67	21431.72	
	0					4662.00	21444.00	
	5					4659.47	21455.68	II**
	8			500		4657.884*	21462.96	
	40	0		0	2	4651.48	21492.53	
800	120		10	100	8	4648.421*	21506.67	II
	120		2			4644.37	21525.42	
	150	7	6	80	7	4637.869*	21555.49	III $4p5s\ ^1P_1 - 4p5p\ ^3D_1$
150	100			25	6	4636.74	21560.83	
	1					4633.91	21589.79	
12	10d		8	1500	3	4630.54	21589.60	II
25	12				4	4628.12	21600.98	II
8	12d			5	2	4625.09	21615.13	

Intensity						Wave-length	Wave-number	Classification
M_{I_T}	E_DP	R	S_{He}	E_DG	K	λ(Å)	(cm^{-1})	
	2d					4622.76	21626.06	
8	8d			60	2	4621.75	21630.79	
	6d		2	100d		4621.36	21632.57	
100	18		8	300	8	4618.763*	21644.74	II
	1					4616.75	21654.21	
	25			1000		4609.543*	21687.98	IV $5g^2G-6h^2H$
	10		2		1	4607.70	21696.73	
300			10	300	9	4604.311*	21712.56	II
	20d					4602.65	21720.53	
70	300		2	40	5	4599.94	21733.32	II
25	50			10	3	4597.93	21742.82	II
8	5d					4596.60	21749.11	II
8	10			100	3	4592.38	21769.09	
	12					4589.874*	21781.04	
	1d					4587.08	21796.23	
	2d					4583.89	21809.44	
	10d					4581.63	21820.20	
	20d					4579.62	21829.77	
	1d					4578.27	21836.21	
	50	3		50	6	4572.25	21865.00	III
10	20d				3	4567.18	21889.21	II
200	100		8		9	4563.93	21904.85	II
20	25d				2	4561.65	21915.74	II
40	60				7	4559.30	21926.99	
	1					4557.74	21934.54	
	80	3		80	5	4553.96	21952.74	
	50	3			5	4551.05	21966.77	III
	20				2	4548.25	21980.34	
	8d					4547.06	21986.09	II**
	10d			750		4545.03	21995.88	
25	40			30d		4541.31	22013.92	II
8	15d					4534.00	22049.40	
	6d					4531.31	22062.40	
	3					4527.88	22079.20	
	6d	8		75d	5	4523.53	22100.42	
70	40		8	2000	8	4516.30	22135.79	II
	6				1	4512.14	22156.20	II**
20	25				3	4507.61	22178.51	
	10					4504.75	22192.58	
25	40				2	4503.03	22201.06	

Intensity						Wave-length	Wave-number	Classification
M_{I_T}	E_DP	R	S_{He}	E_DG	K	λ(Å)	(cm^{-1})	
	10					4501.76	22207.32	
10	10				2	4500.67	22212.70	II**
	25d					4494.48	22243.3	
	12				2	4488.50	22272.9	
	4			30	2	4485.55	22287.55	
	4				2	4483.67	22296.9	II
	6					4481.93	22305.5	
10	12			50	3	4476.86	22330.8	II
12	15				4	4475.17	22339.2	
300	50		8	200	9	4467.58	22377.22	II
	10d					4460.67	22411.9	
50	30		0	10	6	4454.87	22441.05	
300	50		2	75	8	4449.14	22469.94	II
200	80			200	8	4445.97	22485.96	II
	10d					4443.97	22493.5	
				1500		4442.50	22503.5	
	10d					4437.19	22530.4	II
40	20					4435.20	22540.6	II
25	20			150	3	4433.85	22547.46	II
60	40			75	6	4432.28	22555.44	II
	30					4430.39	22565.1	
20	30			100	4	4425.98	22587.5	II
20	20			0	5	4421.62	22609.8	
	8d	0				4421.00	22613.0	
10	15d			40	2	4415.71	22640.1	II
20	10				3	4413.46	22651.6	II
	6d			0	3	4409.13	22673.8	
70	50			60	7	4406.56	22687.1	
100	80			1000	9	4401.00	22715.7	II
12				500	1	4400.10	22720.35	II
15				20	4	4399.04	22725.8	II
	30			50		4383.60	22805.9	
800	30			400	10	4382.85	22809.8	II
	15					4379.91	22825.1	
40	40			10	5	4374.22	22854.8	
40	25					4373.59	22858.1	
	5					4371.76	22867.6	II**
	8					4371.35	22869.8	
	3			750	3	4370.74	22873.0	
	82				1	4368.24	22886.1	

Intensity						Wave-length	Wave-number	Classification	
M_{I_T}	E_DP	R	S_{He}	E_DG	K	λ(Å)	(cm^{-1})		
	6d					4362.81	22914.5		
	100			5	2	4357.31	22943.5		
40	120			25	6	4355.11	22955.10	II	
	8			750		4352.18	22970.6	III	
8	50			2000		4348.06	22992.3	II	
25	30				4	4345.66	23005.0	II	
	15d					4344.50	23011.1		
	2d					4342.40	23022.3		
	4d				5	4339.95	23035.3		
40	25			75	1	4337.67	23047.37	II	
25	30			0		4335.54	23058.69		
	4d					4332.32	23075.8		
	15			1000		4331.22	23081.68		
200	4d					4330.50	23085.5	I	
	15d				4	4329.29	23092.0		
40		3		75	5	4322.75	23126.89	III	
60		4		100	5	4322.21	23129.78	III	
100	60			400	9	4320.40	23139.52	II	
8	30d					4319.00	23047.0	II	
40	30			75	6	4316.24	23161.8		
	6d					4314.36	23171.9		
25	30			30	5	4309.11	23200.1	II	
10	15					4308.19	23205.1	II	
	25			4	2	4304.98	23222.4		
10	10d			10d	3	4304.19	23226.65	II	
	8d					4298.78	23255.9		
40	30			60	6	4297.31	23263.82	II	
	5					4291.75	23293.9		
	25			100d	5	4290.50	23300.74		
	15					4290.13	23302.7		
				300		4282.90	23348.6		
100	30			300	7	4282.10	23353.0		
150	50			400	8	4280.35	23356.0	II	
	10d			1000		4277.52	23371.5	IV	$6p\,^2P_{1\frac{1}{2}}-7s\,^2S_{\frac{1}{2}}$
	4d					4275.24	23383.94		
				0		4267.28	23427.54		
	10			500		4266.53	23431.66		
	4d				5	4259.21	23471.9		
	20d				2	4257.72	23480.1		
	4d					4255.38	23493.0		

Intensity						Wave-length	Wave-number	Classification
M_{I_T}	E_DP	R	S_{He}	E_DG	K	λ(Å)	(cm^{-1})	
40	2			20d	2	4251.69	23513.4	
50				0		4248.10	23533.3	
100				300	7	4247.96	23534.1	II
8	15			10d	1	4243.97	23556.24	
	4					4237.42	23592.6	
	6					4236.44	23598.1	
	30	1		5d	3	4234.38	23609.57	
	20d					4231.97	23623.0	
40	30			40	6	4230.04	23633.79	II
	10d			400		4228.13	23644.46	
						4227.36	23648.77	
20	30			25	5	4226.34	23654.47	II
20	30			25	4	4221.59	23681.08	
	15d					4218.56	23698.1	
150	80			400	6	4215.04	23717.87	
200	100			500	7	4212.55	23731.89	II
200	100			500	6	4211.85	23735.83	IV
	50			50	2	4210.37	23744.17	
				20		4210.30	23744.57	
				0		4206.69	23710.99	
10				100	3	4206.57	23765.67	
	8					4201.00	23797.2	
40	30			200	5	4198.01	23814.11	II
20	100			40	3	4196.24	23824.15	II
100				200	5	4195.57	23807.96	
50	100			150	6	4194.54	23833.81	II
20	20			10	2	4193.33	23840.68	
	8					4191.28	23852.3	
	10					4188.90	23865.9	
	20	5			4	4186.53	23879.4	
	30	6			4	4184.89	23888.8	
				200		4182.95	23899.8	
	20					4181.45	23908.4	
800	30			1000	9	4180.90	23911.54	II
	10					4178.96	23922.6	
	30					4176.23	22938.3	
800	20			1000	9	4175.28	23943.7	II
	40			1000	10	4169.06	23979.46	III
12	15d			20	1	4167.21	23990.11	II**
	40d					4166.54	23994.0	

Intensity						Wave-length	Wave-number	Classification	
M_{I_T}	E_DP	R	S_{He}	E_DG	K	$\lambda(\text{Å})$	(cm^{-1})		
	12d			0		4166.02	23997.0		
40		1		100	5	4165.62	23999.29	II	
				10		4165.44	24000.33		
	10					4160.83	24026.9		
70				120	5	4159.70	24033.44	II	
40		4		100	5	4153.90	24066.98	II	
80				500	7	4152.32	24076.14	IV	$6p\,^2P_{\frac{1}{2}}-7s\,^2S_{\frac{1}{2}}$
	10					4150.51	24086.6		
		4		50	3	4148.98	24095.5		
	20					4147.49	24110.97		
	30					4146.97	24113.99		
				100	5	4145.25	24117.20		
	8					4139.22	24152.3		
10	25			5d	1	4138.95	24153.91	II	
	25					4138.25	24158.0		
50				150	4	4137.27	24163.71	II	
100				1000	6	4136.23	24169.78	II	
	15d					4135.70	24172.86		
	30					4134.77	24178.3		
	8d			20		4134.04	24182.62		
200				500	7	4132.69	24190.51		
	25	4		500		4131.71	24196.23		
200	50			1000	7	4129.11	24211.49		
	12					4128.85	24213.0		
		9		200		4127.00	24223.87	III	
150	15			250	7	4126.52	24226.68	II	
	8d					4122.19	24252.1		
	20					4115.72	24290.2		
40				10	5	4114.31	24298.56	II	
	4					4113.19	24305.2	III	
	20	3		100	4	4112.48	24309.37		
800				500	8	4108.77	24331.31		
	12					4107.60	24338.2		
	50					4107.10	24341.2		
				25	2	4104.15	24358.70		
				500		4103.89	24360.26		
	30					4101.92	24371.9		
	100			0	3	4101.17	24376.39		
	30					4099.51	24386.26		
60		6		300	7	4097.91	24395.83	II	

Intensity						Wave-length	Wave-number	Classification
M_{I_T}	E_DP	R	S_{He}	E_DG	K	λ(Å)	(cm^{-1})	
				50		4097.77	24396.67	
	10					4096.24	24405.72	
				500	7	4095.33	24411.15	
	4d					4093.53	24421.9	
70	2d			300	7	4091.86	24431.85	II
	1d					4089.95	24443.3	
	50					4088.08	24454.5	
	10d					4087.27	24459.3	
		7		500	8	4083.16	24483.9	III
	4d					4082.07	24490.47	
	12d					4081.23	24495.5	
				100		4079.54	24505.66	
	6d					4078.68	24510.82	
	20					4077.74	24516.47	
	6d			200		4076.60	24523.33	
	20					4075.87	24527.72	
				100		4072.36	24548.85	
				400	4	4071.99	24551.08	
500	1			500	7	4070.08	24562.64	II
	1					4069.58	24565.62	
	10					4068.38	24572.9	
	20					4066.41	24584.8	
	4d					4064.91	24593.8	
	4d					4063.73	24601.0	
70				150	6	4061.97	24611.64	II
		5		100	5	4059.79	24624.88	
20				50	5	4058.17	24634.69	II
	80					4054.28	24658.29	
	2					4052.46	24675.67	
				75		4052.90	24666.7	
	8d					4051.43	24675.64	
	6					4050.86	24679.2	
	50					4049.34	24688.4	
		9		1000	10	4046.72	24764.4	III
	20d					4043.60	24723.47	
8				0	3	4041.77	24734.63	
				25d		4041.29	24737.60	
	15					4039.00	24751.61	
40				65	5	4038.24	24755.05	II
				10		4035.44	24773.5	III

Intensity						Wave-length	Wave-number	Classification
M_{I_T}	E_DP	R	S_{He}	E_DG	K	λ(Å)	(cm^{-1})	
				75		4033.79	24783.58	
10				0	4	4032.84	24789.54	
150				300	7	4029.99	24806.94	
	6				2	4028.37	24816.91	
	60					4024.60	24840.15	
10	50			40	2	4019.45	24871.97	II
	5					4019.22	24873.4	
70				200	6	4018.47	24878.08	II
70	4					4014.89	24900.21	I
	5	8		100		4013.95	24906.1	
				500		4013.83	24889.92	
	100	10		300		4008.21	24941.71	
150	20			250		4007.84	24944.06	II
	1			30		4007.63	24944.13	
				20		4007.26	24947.86	
60				100	5	4003.02	24974.65	II
60				100	7	4001.99	24980.50	
				1000		3994.99	25024.26	
				5d		3994.56	25026.97	
		8		400	5	3993.66	25032.60	
		1		25	2	3981.26	25110.57	
				200		3968.35	25192.29	II**
		1		5	4	3963.90	25220.55	
	40	0		500	4	3957.24	25263.02	
5	3				2	3952.60	25292.70	
25	20			50	5	3951.76	25298.01	
20	10			100	7	3948.77	25317.21	II
20	6d			1	5	3941.38	25364.64	
6	80	10		40	6	3935.73	25401.08	
60				25		3935.31	25403.79	
5		10		250	6	3931.57	25427.95	
	10			1000		3928.62	25447.04	
2	10			0	2	3924.01	25476.91	II
8				25	5	3923.36	25481.12	
				1	5	3920.61	25499.02	
				60	5	3917.04	25522.25	II
8				5	5	3916.46	25526.06	II
8				30	5	3913.78	25543.53	II
25		8		300	7	3904.85	25601.90	II**
		5		100	3	3903.95	25607.80	

Intensity						Wave-length	Wave-number	Classification
M_{I_T}	E_DP	R	S_{He}	E_DG	K	λ(Å)	(cm^{-1})	
				500		3901.59	25623.22	
5		10		750		3901.52	25623.81	
				0	6	3897.25	25651.87	II**
		1		100	5	3883.33	25743.80	
				30		3883.28	25744.15	
				50	6	3880.51	25762.53	
50	4			120	8	3877.23	25784.3	II
	4					3875.37	25796.6	
				0	2	3870.81	25827.1	
	10					3868.52	25842.3	
		5		80	3	3858.08	25912.3	
	80	9		150	6	3857.25	25917.8	
8				5	3	3855.21	25931.5	
4	30	8		75	6	3853.26	25944.7	
				1000		3850.59	25962.7	
	100	5		75	8	3849.60	25969.3	III
20	6d			5	6	3841.95	26021.1	
	12					3838.25	26046.1	
20	8d			100	7	3836.23	26059.72	II
	6					3829.73	26104.1	II**
	2	1			7	3827.67	26118.2	
	4					3826.68	26124.9	
5	5d			75	6	3818.68	26179.6	II
	2	2			2	3813.03	26218.4	III
4	20	7		1000	6	3812.12	26224.7	
4				5		3811.54	26228.6	II
2	6			400		3809.42	26243.1	
		1		0	3	3807.49	26256.6	III
	200	10	0	1000	10	3800.94	26301.8	III
	7d			0	3	3795.90	26336.8	
25	8d		4	500	7	3793.61	26352.7	II
5			4	50	5	3789.66	26380.1	
12	8			500	7	3786.57	26401.6	
				10	2	3783.25	26424.8	
	4	2		200	5	3782.49	26430.1	III
	12		1	750		3780.82	26441.8	
5				50	4	3779.12	26453.7	
	4		1	75		3776.81	26469.9	
8	4			100	2	3770.51	26514.07	II**
	15		0			3765.18	26551.6	

Intensity						Wave-length	Wave-number	Classification
M_{I_T}	E_DP	R	S_{He}	E_DG	K	λ(Å)	(cm^{-1})	
20	6			30	7	3763.22	26565.46	II
20	8d			400	7	3754.32	26628.40	II
	10d		2	150	5	3749.59	26662.02	
	5	3		30	3	3743.99	26701.86	
	30	8		100	8	3742.95	26709.32	III
	200	10	4	2000	10	3738.73	26739.4	III
				100		3737.88	26745.5	
20				1	2	3733.22	26778.92	I
	40			1000	3	3729.31	26806.99	
20			0	100	6	3728.23	26814.75	
	3			4		3727.41	26820.65	
				15		3727.32	26821.30	
	2			5		3726.91	26824.25	
	0			5		3724.51	26841.57	
	3		4	20	1	3720.42	26871.04	
	6			0	2	3718.75	26883.08	
				50		3718.19	26887.13	
	2			1	2	3716.44	26899.80	
	100	9	1	2000	10	3711.68	26934.29	III
						3693.5	27068	
						3688.23	27105	
				100	7	3686.18	27120.64	IV $6h^2H-9g^2G$
				25	2	3683.45	27140.7	
		1		0	2	3667.58	27258.2	III
3	8	3		150	6	3654.88	27352.90	
25	2			10	6	3653.03	27368.7	
12	12					3639.40	27469.24	II
				15	3	3639.15	27468.37	
			2	1000		3637.88	27480.68	
	200	10		750	10	3637.53	27483.33	III
				10		3635.92	27495.04	II**
				0		3634.31	27507.67	
25	15			500	7	3631.35	27530.08	
	3			40	3	3622.03	27600.90	
35	6		5	150	6	3618.72	27626.14	II
	15	3		500	6	3615.99	27646.99	III
35	5		4	200	6	3610.49	27689.25	II
	3			100		3605.88	27724.48	
	4					3593.64	27818.89	
	50			2000	3	3588.44	27859.30	

Intensity						Wave-length	Wave-number	Classification
M_{I_T}	E_DP	R	S_{He}	E_DG	K	λ(Å)	(cm^{-1})	
				5		3588.15	27861.57	II
				10	2	3583.39	27898.57	
	50			1000		3582.35	27906.71	
				500		3581.60	27912.51	
				500	6	3578.87	27933.82	
	20			200		3576.60	27951.54	
	20	8		800	9	3570.19	28001.71	III
	10d					3563.66	28053.01	
	10			100	5	3561.02	28073.82	II**
	12			150		3559.49	28085.89	
		1	5	0	2	3554.67	28123.98	III
	15d	0				3548.69	28171.32	
				5		3546.68	28187.98	
	15					3545.68	28195.07	
	80	9		500	10	3543.44	28211.51	III
	2d					3538.23	28254.49	
	6d			0	2	3535.74	28274.57	II
	2d					3532.60	28299.51	
		2		10	5	3516.93	28425.76	
				50	7	3515.64	28436.19	
			3	1000		3514.39	28446.3	
	40			2000		3514.20	28447.9	
	30			2000		3511.15	28472.6	
				100		3509.79	28483.6	
	6			75		3509.35	28487.2	
	12			1000		3503.71	28532.3	
	2			75d		3502.69	28542.64	
	6			750		3499.66	28566.0	
	2					3498.26	28577.55	
		0	4	5	3	3493.85	28613.61	
	40			2000		3491.53	28632.55	
				1000		3491.24	28634.92	
20				5	6	3489.03	28653.05	
	8	2	1	50	5	3485.89	28678.87	
	15			2000		3480.45	28723.75	
	10		0	5		3476.73	28754.44	
				5	2	3471.58	28797.07	
				5	3	3468.42	28823.35	
		1		10	4	3465.16	28850.44	III
				75		3458.38	28906.95	

M_{I_T}	E_DP	R	S_{He}	E_DG	K	Wave-length λ(Å)	Wave-number (cm^{-1})	Classification
	100	10	5	2000	9	3457.79	28911.96	III
8	8			200	3	3454.07	28943.06	
	6					3452.24	28958.40	
35	10		2	100	7	3444.27	29025.39	II
	60		1	25		3437.13	29085.72	
	80	8	2	1000	9	3428.39	29159.84	III
	6			5d	3	3425.57	29183.86	
	2					3419.61	29234.81	
				40		3414.38	29279.48	
			5	75		3414.19	29281.1	
	200	10		2000	10	3413.92	29883.43	III
				5		3407.85	29335.75	
				0		3393.88	29456.43	
				0		3393.69	29458.12	
				2		3393.25	29461.17	
		6		75d		3392.64	29467.06	
	20			300	8	3392.39	29469.32	III
				5		3390.24	29488.0	
	100	10	4	2000	10	3387.24	29514.11	III
			2	5	2	3385.90	29525.8	
25	4			200	3	3384.95	29534.10	II
				5		3384.21	29540.6	
	2	1		15	3	3382.84	29552.5	III
			1			3380.50	29572.9	
	40	8		1000	8	3379.82	29578.89	III
	20	4		300	7	3376.24	29610.3	
	4					3374.79	29622.9	
			5			3371.31	29653.5	
	25d			100		3370.69	29659.16	
			0	40	5	3369.28	29671.4	III
	6					3367.16	29688.9	
				60	5	3364.36	29714.9	
			1	40	3	3362.74	29729.2	
				40	2	3360.32	29750.5	
	15			100		3358.22	29769.2	
	15d			100	3	3353.64	29809.78	II
	4					3350.59	29837.03	
				200	5	3346.59	29872.62	
	50		1	2000		3344.74	29889.11	
	4d	1			3	3342.41	29909.91	

Intensity						Wave-length	Wave-number	Classification
M_{I_T}	E_DP	R	S_{He}	E_DG	K	λ(Å)	(cm^{-1})	
				25d	2	3339.46	29936.36	
				3000		3336.17	29965.84	
8	50					3335.84	29968.8	
	6					3331.03	30012.1	
	4					3329.81	30023.1	
	8					3328.57	30034.33	
	4		1	75	3	3325.76	30059.53	
	4			25	5	3324.86	30067.81	
	20	5		150	8	3323.16	30083.16	III
				1500		3319.50	30116.35	
	5	1		50	3	3317.98	30130.12	
	50			2000		3311.24	30191.50	
	60			2000		3301.84	30277.41	
	3	2		60d	5	3293.60	30353.21	III
	3	0		200	5	3292.56	30362.78	
	50			2000		3285.82	30425.04	
	10			300	7	3282.86	30452.43	
				1000		3278.49	30493.10	
	6d					3267.45	30596.1	
	4			10	2	3265.32	30616.02	
	4					3263.74	30630.9	
8	2			10	2	3260.69	30659.89	
	2			5	2	3258.75	30677.81	
	2					3257.59	30688.7	
20	5			10d	3	3251.67	30744.6	
	5					3249.81	30762.1	
	10	4		200	7	3248.01	30779.18	III
				50		3243.70	30820.1	
10		5		120		3242.75	30829.1	
25	8			65	4	3242.15	30834.83	II
15				50	4	3238.40	30870.51	II
		1		25	3	3236.48	30888.85	
8				10d	3	3228.14	30968.70	II
	30	5	1	200	8	3225.77	30991.51	III
	4	2		10d	5	3218.00	31066.23	III
	40	5	0	500	8	3215.24	31092.88	III
	10			40	3	3210.69	31136.99	
	6		0	50	5	3204.50	31197.06	II
	25	5		150	9	3185.47	31383.47	III

Intensity						Wave-length	Wave-number	Classification
M_{I_T}	E_DP	R	S_{He}	E_DG	K	λ(Å)	(cm^{-1})	
	3					3180.97	31427.86	
12	15	6		20	7	3178.16	31455.68	
	2					3174.89	31488.03	
	10					3169.19	31544.65	
	50d					3158.31	31653.28	
8				0	2	3150.19	31734.95	III $4p5p\,^3D_3-4p5d\,^3F_2$
				0	7	3141.11	31826.66	II
	8					3138.64	31851.70	
	50d			40	5	3134.46	31894.18	II
	0					3125.50	31985.57	
	10d					3115.81	32085.12	
	8	4		100	6	3110.98	32134.89	III
				5d		3109.98	32145.25	
		2		5d		3109.90	32146.05	III
15	2			50	4	3108.51	32160.42	II
	0				3	3106.27	32183.63	
	50				4	3105.14	32195.34	II
	6	5	1	140	7	3102.71	32220.60	III
	12	4	0	75	8	3094.23	32308.81	III
	6			50		3093.39	32317.59	
	6			10	2	3088.21	32371.78	
8	6			10	3	3085.73	32397.79	
20				100	3	3084.37	32412.17	
	4			100		3077.86	32480.76	
	10	4		400	8	3073.99	32521.56	III
	30			500	6	3072.67	32535.53	
				0	2	3070.71	32557.38	
	25	5		400	8	3069.89	32565.06	III
	3					3064.63	32620.89	
	2	4		50	4	3063.75	32630.31	
	4	3		50d	5	3062.48	32643.84	III
	200	5		2000	10	3059.85	32671.92	IV $5s\,^2S_{\frac{1}{2}}-5p\,^2P_{\frac{1}{2}}$
	20			200d	3	3054.76	32726.30	III
	4	1		40	4	3051.07	32765.92	III
	1					3048.51	32793.55	
35	4			80	5	3046.16	32818.72	II
		0		5	2	3042.44	32858.80	III
60	2		5	200	8	3041.27	32871.43	II
20				60	2	3039.50	32890.6	

Intensity						Wave-length	Wave-number	Classification
M_{I_T}	E_DP	R	S_{He}	E_DG	K	λ(Å)	(cm^{-1})	
	20			500	8	3038.63	32900.0	II
	4	1	5	50	3	3033.50	32955.63	III
	2					3031.87	32973.37	
	2	0		0	3	3031.44	32978.08	
	2					3028.92	33005.48	
	4	2		50	4	3027.05	33025.82	III
	20			500		3023.96	33059.60	
	6	1			6	3020.29	33099.78	
	3			40d	3	3009.95	33213.47	
	2					3008.14	33233.41	
	6					3006.87	33247.44	
	30			1000		3002.63	33294.41	
		2		50	4	2999.63	33327.78	III
	15	2		55	6	2987.48	33461.07	
				0	2	2983.98	33502.52	
	6	2		100	4	2979.04	33558.06	III
10	5			500	6	2972.53	33631.49	
10	5			100	7	2971.42	33644.05	
	10	6	6	550	7	2970.97	33649.20	III
	4	4		50	5	2970.00	33660.17	III
				100	2	2967.17	33692.27	
	10		4	75	7	2963.91	33729.36	II
		2			3	2955.72	33822.81	III
12				0	3	2952.40	33860.83	II
	150	6		2000	10	2951.68	33869.11	IV 5s $^2S_{1/2}$ - 5p $^2P_{1/2}$
	8	6	0	75	7	2948.46	33906.05	III
	6	2			3	2947.83	33913.35	
4	2					2947.06	33922.2	II
	9	4				2944.02	33957.24	III
	10					2942.83	33971.0	
15	6		2	20	7	2941.50	33986.32	
	2d	0			2	2940.29	34000.3	III
	25			200	5	2933.31	34081.27	IV 5d $^2D_{2\frac{1}{2}}$ - 5f $^2F_{7/2}$
	10			100	2	2931.47	34102.59	IV 5d $^2D_{2\frac{1}{2}}$ - 5f $^2F_{5/2}$
	0				2	2929.79	34122.1	
	1					2928.73	34134.5	
	2				2	2927.67	34146.8	
	6					2926.14	34164.7	
	0				2	2924.65	34182.1	
	0					2923.73	34192.8	

Intensity						Wave-length	Wave-number	Classification
M_{I_T}	E_DP	R	S_{He}	E_DG	K	λ(Å)	(cm^{-1})	
	1	2			3	2921.80	34215.4	III
10				5	4	2919.22	34245.7	
				200		2918.97	34248.7	
				75		2918.54	34253.7	IV $5d\,^2D_{3/2}-5f\,^2F_{5/2}$
	10		2	100	2	2917.82	34262.2	
10	4			40	3	2916.09	34282.4	
				10		2915.54	34287.0	III
	20		6	300	9	2914.88	34296.7	
	10			100		2912.92	34319.7	
5	2				3	2911.11	34341.1	
	1			100	3	2908.24	34375.05	
	8	3	0	10	6	2907.06	34388.91	III
5	1					2905.87	34403.0	
7	2			10	4	2905.10	34412.12	II
	3d	1		0	4	2899.29	34481.09	III
	8		4	100	6	2895.89	34521.64	II
	3				3	2894.41	34539.3	
10	4		1	1	5	2892.73	34559.29	
	3					2891.61	34572.6	
	60			500		2884.21	34661.37	IV $5g\,^2G-7h\,^2H$
				1	4	2881.45	34694.57	
25	12		6	100	8	2880.33	34708.01	
	12			40		2878.76	34727.05	
	1				2	2874.20	34782.1	
5	1		0		3	2873.30	34793.0	
	1				2	2872.12	34807.3	II
	30	6		150	8	2870.20	34830.58	III
10	10		4	1000	6	2865.87	34883.19	
	20	6	4	100	6	2864.44	34900.55	III
	10	6		100	6	2863.86	34907.63	III
	3					2856.20	35001.3	
5	20			200		2855.30	35012.3	
	8					2853.28	35037.1	
	6					2849.57	35082.7	
	4					2846.70	35118.0	
	10d	1		100	4	2842.96	35164.30	III
				30		2839.79	35203.57	
	15	5		5	6	2838.71	35216.97	III
35	15		6	100d	8	2837.23	35235.35	
	2d			100d		2836.69	35241.97	

Intensity						Wave-length	Wave-number	Classification	
M_{I_T}	E_DP	R	S_{He}	E_DG	K	λ(Å)	(cm^{-1})		
	2					2830.14	35323.6		
	1				2	2827.12	35361.3		
	4					2824.56	35393.3		
	2					2823.60	35405.4		
	15	5		100	6	2822.08	35424.44	III	
		4		25		2821.60	35430.46	III	
20	8			30	4	2821.48	35431.94	II	
15	8		2	50	6	2820.07	35449.68		
				2		2817.65	35480.1		
	8		6	100d	9	2816.98	35488.55		
	8			25		2809.44	35583.77		
	2			0		2806.95	35615.3	IV	$5d\,^2D_{5/2}-4p^3\,^4S_{3/2}$
	20	3		40	7	2804.38	35648.01	III	
	30	8	2	75	9	2802.25	35675.04	III	
				5		2798.41	35724.11		
			3	40		2796.63	35746.8		
	8	3		40	6	2793.15	35791.31	III	$4p5p\,^3S_1-4p5d\,^3P_0$
	10	3		50	6	2792.36	35801.41	III	
	8			75		2788.89	35846.02		
	5	1		5	3	2787.75	35860.60	III	
	8			10	3	2785.59	35888.47		
	2			50		2785.20	35893.52		
	5			100		2784.40	35904.6		
	2					2783.55	35914.8		
	1					2782.17	35932.6		
	100	8	2	1000	9	2777.52	35992.75		
	1			5		2777.03	35999.1		
	2			10		2776.20	36009.82		
	4					2775.01	36025.26		
	30	7	0	150	7	2773.81	36040.93	III	
	15	5		50	6	2772.46	36058.48	III	
	80	8	1	400	10	2767.20	36126.95	III	
	2					2765.00	36155.64		
	4			100d	3	2764.60	36160.87		
10	20		3	75d	5	2762.16	36192.81		
	6d				3	2760.45	36215.22		
	10d			5	3	2759.26	36230.85		
	8			20		2757.89	36248.92		
	4			20	3	2756.89	36262.08		
5	30			1000		2753.92	36301.17		

Intensity						Wave-length	Wave-number	Classification
MI_T	E_DP	R	S_{He}	E_DG	K	λ(Å)	(cm^{-1})	
15	12		6	25	8	2749.85	36354.85	
	6	2	0	10	5	2745.88	36407.50	III
	4	2		10	5	2738.95	36499.49	III
10	4		2	50	5	2738.15	36510.25	II
	2d			10	4	2733.58	36571.24	
5				5		2738.37	36574.04	
				5		2738.22	36576.06	
				0		2731.21	36602.95	
			0	5		2729.18	36630.20	
5	2				3	2729.13	36630.87	
	20	2		100	7	2726.52	36665.99	III
	5d			60d	8	2724.78	36689.40	
	400	8		1000		2724.22	36696.94	IV $4d^2D_{3/2}-5p^2P_{1/2}$
	2			5	2	2722.58	36719.00	
				5		2719.95	36754.49	
35	10		8	100	6	2719.52	36760.30	
	40	5		200	8	2715.92	36809.03	III
	2			5		2714.48	36828.6	
	3					2713.47	36842.26	
	20	4		100	6	2712.69	36852.92	III
	3					2709.88	36891.1	
5	5		2	15	4	2706.98	36930.62	
	20	4		200	6	2705.96	36944.54	III
5	8d			25	2	2705.41	36952.05	
				15		2705.21	36954.79	
10	10		3	75	5	2702.68	36989.39	
	12	3		30	5	2696.32	37076.59	III
	1					2695.37	37089.6	
	1					2694.60	37100.2	
	2					2693.89	37110.0	
	2	0		30		2693.27	37118.63	III
10	10		4	60	6	2692.03	37135.63	
	4	2		1000	3	2689.08	37176.38	
	10		4	60	7	2688.33	37186.73	
				100		2686.00	37218.97	
	120	6	4	75	8	2685.74	37222.61	III
	2					2682.56	37266.71	
	0			5	2	2681.37	37283.16	
	10			3	3	2679.99	37302.44	
	10	2		10	4	2678.68	37320.69	III

Intensity						Wave-length	Wave-number	Classification	
M_{IT}	E_DP	R	S_{He}	E_DG	K	λ(Å)	(cm^{-1})		
	10					2678.41	37324.4		
	1					2677.82	37332.7		
	1				4	2675.89	37359.6		
	1	1				2674.51	37378.89	III	
	4				2	2673.95	37386.8		
	150	9		1500	8	2665.48	37505.48	IV	$4d^2D_{5/2}-5p^2P_{3/2}$
	10		4	75	6	2662.05	37553.83		
	6	0			3	2659.41	37591.16		
	6d	1		1	2	2656.66	37630.07	III	
		1		10	2	2654.91	37654.91		
	60	6	1	500	7	2654.02	37667.51	III	
10	6		2	10	4	2651.41	37703.20		
	4d					2650.16	37722.3		
50	25		4	300		2649.41	37733.02		
	4d			5		2649.35	37733.87		
	6					2644.51	37802.9		
10	8		2	100	5	2643.44	37818.24		
	6					2640.19	37864.7		
5	3		1	40	4	2639.20	37878.99		
	50	3		500	6	2638.15	37894.06	IV	$4d^2D_{3/2}-5p^2P_{3/2}$
5	6		2	30	5	2633.22	37965.06		
	0					2632.27	37978.8		
	2					2631.79	37985.69		
35	40		5	500	8	2630.87	37998.93	II	
	5	2			4	2628.41	38034.47	III	
5	1		0		3	2626.77	38058.22		
	6					2624.76	38087.4		
	1					2624.37	38093.1		
	4			0	3	2623.31	38108.45		
	5					2621.19	38139.3		
	1					2619.73	38160.51		
	100	6		600	9	2617.32	38195.61	III	
	2					2615.54	38221.63		
	4					2615.00	38229.52		
				5	2	2612.69	38263.26		
				5	2	2610.38	38297.17		
10	4			10	4	2609.35	38312.22	III	
	2					2607.96	38332.68		
15			2	100	7	2602.59	38411.81		

Intensity						Wave-length	Wave-number	Classification	
M_{I_T}	E_DP	R	S_{He}	E_DG	K	λ(Å)	(cm^{-1})		
5	60d			10	3	2600.46	38443.31		
	80d			250		2599.23	38461.4	IV	$4p^3\,{}^4S_{3/2}-6s\,{}^2S_{1/2}$
	30				3	2596.00	38509.23		
	60					2592.34	38563.73		
30	80		6	400	10	2591.42	38577.42		
		0		0		2587.16	38640.92	III	
15	25			50	4	2586.40	38652.27		
15	100			80	6	2585.23	38669.76		
	50			0		2584.87	38675.16		
	10		2	30	5	2582.73	38707.18		
	15	1			4	2580.94	38734.02	III	$4p5p\,{}^3P_1-4p5d\,{}^3P_0$
	100			0		2579.01	38762.99		
	100	5	0	100	8	2571.31	38879.04		
	305					2567.96	38929.7		
	15d					2567.08	38943.1	V	$4s5s\,{}^3S_1-4s5p\,{}^3P_0$
	40d	2			5	2566.60	38950.38	III	
	6d	0			2	2565.24	38971.02	III	
	6d					2564.4	38983.8		
	40					2563.2	39002.0		
25	100		5	200	8	2561.72	39024.60		
15	40			25	5	2560.87	39037.49		
	6d					2560.12	39048.9		
	15d					2559.07	39064.9		
	20d			5	2	2558.23	39077.81		
10	30		5	100	7	2554.60	39133.40		
	6					2553.44	39151.00		
	8				2	2552.81	39160.75		
				5		2552.61	39163.87		
						2549.83	39206.62		
						2549.79	39207.23		
50	100			250		2549.16	39216.84		
60			6		2	2547.97	39235.17	I	
	30	2		50	6	2546.39	39259.46	III	
	400	0		2	2	2544.58	39287.41		
	300			15		2541.91	39328.73		
	12					2536.14	39418.2		
	2					2535.39	39429.8		
	30					2534.83	39438.6		
	15					2534.02	39451.2		
	6					2531.11	39496.5	V	$4s5s\,{}^3S_1-4s5p\,{}^3P_1$

Intensity						Wave-length	Wave-number	Classification	
MI_T	E_DP	R	S_{He}	E_DG	K	λ(Å)	(cm^{-1})		
3	8					2530.28	39509.5		
	20d					2528.64	39535.1		
25	15d		0		4	2527.91	39546.48		
	60					2525.74	39580.4		
	40					2522.36	39633.5		
	25					2520.88	39656.7		
15	100		0	100	4	2518.68	39691.36		
	30					2517.32	39712.8		
15	60		0		4	2516.53	39725.26		
	30					2516.21	39730.3		
	15					2515.72	39738.0		
	200	2	5	100d		2512.82	39783.99	III	
	30			100		2512.05	39796.08		
	90		4	100d		2509.11	39842.7		
	50					2506.76	39880.0		
	30					2504.45	39917.0		
	80					2496.56	40043.12		
100	200		5	100	7	2496.05	40051.27		
	40					2494.90	40069.7		
	80	6			6	2494.23	40080.40	III	
	50	3		100	4	2493.43	40093.31	III	
	30d			50		2492.97	40100.7		
6	30d				2	2492.57	40107.10		
35	80		0	50	5	2490.84	40135.01		
	2d					2490.29	40143.9		
	3d					2489.75	40152.6	III	$4p5p\,^3D_3-4p5d\,^1F_3$
	100					2488.87	40166.8	III	$4p5p\,^3P_0-4p5d\,^3P_1$
	20					2485.60	40219.6		
	25					2484.84	40231.9		
	60					2484.12	40243.6		
5	10					2482.17	40275.2		
	15					2481.50	40286.0		
	20					2480.87	40296.3		
	2					2480.45	40303.1		
	20					2479.71	40315.1		
			8	80		2478.56	40333.90		
	60					2476.53	40366.85		
	80					2476.06	40374.5		
	8d			30		2475.19	40388.72		
	15d					2473.96	40408.78	V	$4s5s\,^3S_1-4s5p\,^3P_2$

Intensity						Wave-length	Wave-number	Classification
M_{I_T}	E_DP	R	S_{He}	E_DG	K	λ(Å)	(cm^{-1})	
	200		2	50		2472.95	40426.47	
35				10	6	2472.88	40426.75	
	40					2471.89	40442.77	
	3d					2471.00	40457.2	
5	6d					2469.69	40478.6	
10	100		0	10	2	2468.68	40495.3	
	40d					2468.30	40501.6	
	100			50	3	2467.61	40512.8	
	80d					2467.12	40520.8	
	3d					2466.09	40537.7	
	2d					2465.23	40551.8	
	100	0		100		2464.45	40564.7	
10	2					2463.95	40572.9	
	25					2463.03	40588.2	
	20					2461.27	40617.2	
	100	6	1	500	7	2459.52	40646.11	III
	30d					2458.70	40659.7	
	20					2457.99	40671.4	
	15d					2455.08	40719.6	
	100			0		2454.57	40728.09	
	10					2453.05	40753.3	
	15	0		5		2452.50	40762.42	III
5	10					2450.49	40795.8	
	2					2449.47	40812.8	
	30			5		2448.60	40827.37	V $4s5s\,^3S_1-4s5p\,^1P_1$
5	60		0	50		2447.46	40846.39	
	10					2447.02	40853.7	
	15					2445.55	40878.2	
	20					2444.41	40897.3	
10	40		0			2443.66	40909.8	
	3					2442.88	40922.9	
15	2					2441.82	40940.7	
	100	3	0	50	5	2440.93	40955.51	III
5	50					2439.96	40971.9	
5	200d			200d		2438.74	40992.3	
	20					2437.84	41007.5	
	80			50		2436.78	41025.3	
	6	1				2435.60	41045.2	
	4					2435.21	41051.7	
10	10		0		2	2434.04	41071.46	

Intensity						Wave-length	Wave-number	Classification
M_{I_T}	E_DP	R	S_{He}	E_DG	K	λ(Å)	(cm^{-1})	
	15					2433.72	41076.9	III
	200			100d		2432.73	41093.6	
	50			100d		2431.60	41112.7	
	10					2430.06	41138.7	
	100d			100		2437.42	41183.4	
	25					2426.76	41194.6	
	30		0	50	3	2426.01	41207.4	III $4p5p\,^3D_2-4p5d\,^3P_2$
15	50			100		2425.52	41215.7	
5	300			100d		2424.28	41236.8	
				1000		2423.97	41242.22	
	100			500		2423.51	41249.87	
5				70		2423.27	41253.95	
				60		2423.16	41255.83	
	50d					2422.73	41263.15	
	80d					2421.78	41281.03	
		5		75	6	2420.27	41305.16	
				10		2419.91	41311.29	
	200			600d		2418.84	41329.56	
	20					2416.52	41369.32	
				25d		2416.00	41378.23	
				300d		2415.86	41380.62	
	400			400d		2415.65	41384.39	
	30	2		10		2414.15	41409.91	III
125			8	300	5	2413.50	41421.02	I
	200			200		2413.01	41429.47	III $4p5p\,^3D_2-4p5d\,^3P_1$
	60			20		2412.50	41438.23	
10				5		2411.74	41451.29	
	300			100d		2411.00	41464.01	
				100d		2410.86	41466.42	
	60			25		2410.38	41474.64	
10	20		0		2	2409.35	41492.33	
	2d					2408.08	41514.3	
	2d					2407.93	41516.9	III $4p5p\,^3D_1-4p5d\,^3P_2$
	20					2407.22	41529.10	
15	25		0	20	3	2406.59	41539.97	
	300			10		2405.46	41559.48	
	200			12		2404.98	41567.77	
	3d					2403.62	41591.3	
	5d					2403.25	41597.7	

Intensity						Wave-length λ(Å)	Wave-number (cm^{-1})	Classification
M_{I_T}	E_DP	R	S_{He}	E_DG	K			
25	20		1	75	4	2402.25	41615.06	
	1			0		2401.96	41620.0	
	3d					2401.56	41626.9	
	30	3				2400.12	41651.22	
	100			200		2399.19	41668.06	
	8					2398.40	41681.8	
	1					2397.59	41695.9	
	100					2395.64	41729.8	
	2					2394.73	41745.6	
	1					2393.53	41766.6	
	4					2393.39	41769.0	
5	1					2393.19	41772.5	
	10	0				2392.03	41792.7	
	3					2391.00	41810.7	
	80	4	1	50	6	2390.07	41827.04	
10	15					2389.37	41839.3	
	1					2388.24	41859.0	
	2					2387.93	41864.5	
	1					2386.86	41883.2	III $4p5p\,^3D_1-4p5d\,^3P_0$
	12					2385.63	41904.8	
	8					2384.97	41916.4	
	1					2384.01	41933.3	
	8					2383.48	41944.4	
	50					2382.40	41961.6	
	4					2381.43	41978.7	
5	5					2380.56	41994.0	
	6					2380.24	41999.7	
	1					2379.85	42006.6	
	2					2379.30	42016.3	
	10d					2378.69	42027.0	
	80					2377.76	42043.5	
	3					2373.76	42114.5	
25	50		4	1	5	2372.75	42132.30	
	2d					2371.72	42150.7	
	100	6		0	6	2371.07	42162.11	
	2					2370.46	42173.1	
	4					2369.34	42193.0	
	4					2369.03	42198.5	
	6					2367.82	42220.1	
	4			150		2367.65	42223.1	

Intensity						Wave-length	Wave-number	Classification
M_{I_T}	E_DP	R	S_{He}	E_DG	K	λ(Å)	(cm^{-1})	
	10			500		2366.57	42242.4	
	15					2364.98	42270.4	
	12			50		2364.31	42282.8	
5	10		0			2363.53	42297.2	
	25					2360.26	42354.5	
	4					2360.05	42358.1	
	4					2359.61	42367.1	
	10					2357.60	42403.0	II
	20					2357.20	42410.2	
	5					2356.17	42428.8	
25	100		2	200	5	2354.32	42462.14	
	10	2				2353.78	42471.86	
	25					2352.37	42497.31	
	12					2351.72	42509.1	
	20d					2350.47	42531.7	
	30	3		0	3	2349.79	42543.92	III
5	10		0			2349.24	42553.9	
	30					2347.62	42583.3	
	100			100		2345.20	42627.2	
	50			0		2344.25	42644.5	
	10d		0			2343.65	42655.4	
	6d					2342.93	42668.5	
	6					2342.10	42683.6	
	6					2340.83	42706.8	
10	20		1	0	3	2340.13	42719.67	
	4					2339.87	42724.3	
	4					2339.29	42734.9	
	20					2338.23	42754.2	
	25					2337.86	42761.0	
	50					2335.36	42806.8	
	20					2334.49	42822.7	
30	10					2332.43	42860.7	
	100			10		2331.47	42878.2	
	2					2330.93	42888.1	
	100					2329.95	42906.3	
	15					2327.59	42949.8	
	6					2327.17	42957.5	
	3					2326.41	42971.6	
5	8					2325.37	42990.8	
	8					2324.76	43002.1	

Intensity M_{I_T}	E_DP	R	S_{He}	E_DG	K	Wave-length λ(Å)	Wave-number (cm^{-1})	Classification
	1					2324.48	43007.2	
	2					2324.08	43014.6	
	3					2323.27	43029.6	
	100			500d		2321.54	43061.7	IV $5g^2G-8h^2H$
	6d					2320.70	43077.3	
	15					2320.36	43083.6	
	6					2319.93	43091.6	
	500					2319.14	43106.2	
				20		2318.82	43112.2	
				100		2318.62	43116.0	
5	300			1000		2317.84	43130.41	
	300					2317.47	43137.29	
	200					2316.93	43147.34	
	100					2316.41	43157.02	
	10					2315.33	43177.15	
	30					2315.04	43182.55	
	50					2313.77	43206.25	
	20					2312.16	43236.33	
	2					2311.12	43255.77	
10	4					2310.25	43272.06	
	30					2309.19	43291.92	
	2					2308.16	43311.23	
	3					2307.79	43318.17	
	5	0				2307.46	43324.37	III $4p5p\,^3D_2-4p5d\,^1F_3$
	1			100d		2306.92	43334.50	
	12					2305.61	43359.22	
	20					2302.85	43411.07	
	80					2302.07	43425.77	
						2301.39	43438.60	
	40			400d		2300.79	43449.92	
	15					2300.16	43464.8	
	5					2299.68	43470.5	
	25					2299.04	43483.8	
	5			25		2297.57	43510.8	
	300		8	500d		2296.90	43523.49	
	4					2296.13	43538.07	II**
	5					2295.78	43544.4	
	6					2295.29	43553.8	
	15					2294.84	43563.3	
	8					2293.97	43580.4	

	Intensity					Wave-length	Wave-number	Classification
M_{I_T}	E_DP	R	S_{He}	E_DG	K	λ(Å)	(cm^{-1})	
	200					2292.90	43599.4	
10	150			20d		2292.01	43616.3	
	80		2	1000		2291.43	43627.3	
	60					2290.65	43642.2	
	40			1000		2289.68	43660.8	
	3					2289.24	43669.9	
	15					2288.70	43679.4	
	3					2288.36	43685.2	
	6d			50		2286.94	43713.8	
	10					2286.61	43819.3	
	8					2285.73	43736.1	
	50					2283.93	43770.8	
	40					2283.15	43786.02	
	100	4	1	5d		2282.61	43796.07	III
	40			40		2282.20	43803.7	
	40			50		2281.08	43825.3	
	30					2280.77	43831.4	
	20					2280.29	43840.6	
						2279.57	43854.5	
10			0			2279.24	43860.8	
						2279.01	43865.2	
						2278.88	43867.7	
	20					2278.36	43877.7	
	20					2276.94	43905.1	
	2					2275.26	43937.5	
	6					2274.81	43946.2	
	8					2273.63	43969.0	III $4p5p\,^1P_1-4p5d\,^3P_2$
10	12					2272.27	43995.3	
	1					2270.71	44025.5	
	200			100		2269.85	44042.2	
	3					2268.54	44067.6	
	5d					2267.06	44096.4	
5	15		0	1		2265.61	44124.6	
	60		0			2265.13	44133.9	
	3d					2264.51	44146.0	
	2d					2263.40	44167.7	
5	15	0		100		2263.11	44173.3	III
	10					2261.00	44214.5	
	100	2	0	100d		2259.79	44238.2	III
	4d					2256.56	44301.5	

Intensity						Wave-length	Wave-number	Classification
M_{I_T}	E_DP	R	S_{He}	E_DG	K	λ(Å)	(cm^{-1})	
	8d					2255.37	44324.9	
10	60		0			2254.89	44334.3	III $4p5p\,^1P_1-4p5d\,^3P_0$
	15					2254.23	44347.3	
	10					2253.81	44355.5	
	60					2252.76	44376.2	
	10					2252.22	44386.8	
	2					2251.33	44404.4	
	2					2251.01	44410.7	
	2					2249.32	44444.0	
	100					2248.81	44454.1	
	100					2247.88	44472.5	
	30					2246.42	44501.4	
	4					2245.97	44510.3	
	40					2245.52	44519.2	
	2d					2244.38	44541.8	
	15					2243.65	44556.3	
	20					2242.29	44583.3	
	60					2241.71	44594.9	
5	30		2			2241.06	44607.8	
	5					2239.66	44635.7	
				2000		2239.02	44648.4	
	100					2238.54	44658.0	
	2d					2238.01	44668.8	
	2d					2237.75	44674.0	
	2					2236.51	44698.7	
	10d			10		2235.92	44710.5	
	8d					2235.25	44723.9	
	100			500		2234.71	44728.8	II**
	4					2233.48	44759.4	
	10					2233.03	44768.4	
	40	0				2231.43	44800.5	
	4		0			2230.29	44823.4	
	60					2229.63	44836.6	
	15					2229.21	44845.1	
	2					2228.66	44856.1	
	25					2227.29	44883.7	
	40					2225.67	44916.4	
	30					2225.21	44925.6	
	4					2224.45	44941.0	
	2					2223.88	44952.5	

Intensity M_{I_T}	E_DP	R	S_{He}	E_DG	K	Wave-length λ(Å)	Wave-number (cm^{-1})	Classification
	8					2223.43	44961.6	
	4d					2222.63	44977.8	
	6d					2222.11	44988.3	
	2d					2221.32	45004.3	
	6d					2220.50	45020.9	
	80		0	25		2220.06	45029.83	
	2					2219.13	45048.7	IV $5s\,^2S_{\frac{1}{2}}-4p^3\,^4S_{3/2}$
	6					2218.82	45055.0	
	6					2216.62	45099.7	
	6					2216.18	45108.6	
	10					2215.57	45121.06	
	6d					2213.78	45157.5	
	3d		0			2213.34	45166.5	
	50					2212.47	45184.3	
	4d					2210.91	45216.1	
	6d			400		2210.45	45225.9	
	6					2209.27	45249.7	
	20		0	40		2207.86	45278.70	
	8			10		2206.04	45315.92	III $4s4p^3\,^1D_2-4p5p\,^3P_2$
	5			10		2205.42	45328.70	
	8		1	100		2204.83	45340.82	
	25	1	0	10		2201.69	45405.45	
	2					2199.24	45456.0	
	2			0		2198.81	45464.9	
	2d			10d		2197.79	45486.0	
	4d		0			2196.85	45505.4	
	2					2196.26	45517.6	
	10			300		2195.76	45528.0	
	1					2195.17	45540.2	
	10d					2193.33	45578.4	
				100		2192.53	45595.23	
	15			5		2192.00	45606.1	
	1					2191.60	45614.4	
	10					2191.23	45622.3	
	10					2190.43	45639.0	
	10					2189.82	45651.7	
	10			300		2187.98	45690.1	
	10			100d		2187.39	45702.38	
	10			25		2186.63	45718.18	
	5					2185.37	45744.57	

Intensity						Wave-length	Wave-number	Classification	
M_{I_T}	E_DP	R	S_{He}	E_DG	K	λ(Å)	(cm^{-1})		
	10			100		2183.91	45775.06		
	30					2181.23	45831.41		
	75					2177.23	45915.79		
	100			5		2175.62	45949.45		
	5			5		2174.58	45971.58		
	75		1	50		2174.12	45982.51		
	30d					2171.39	46039.0		
	1d					2170.57	46054.3		
	40d					2170.24	46063.4		
	20d		1			2169.97	46069.2		
	2d					2168.30	46104.6		
	100	6		30		2166.63	46140.15	IV	$4f\,^2F_{5/2}-5g\,^2G$
	15					2166.17	46149.9		
	15					2165.83	46157.2		
	150	6		30		2165.25	46169.76	IV	$4f\,^2F_{7/2}-5g\,^2G$
	150		8	50		2164.20	46192.15	I	
	10		1			2161.88	46241.5		
	2		0			2159.50	46307.0		
	2					2157.88	46327.2		
						λvac			
	5			0d		2154.88	46406.30		
	25		1	15		2154.26	46419.65		
	10					2151.74	46474.0		
	1	1		10		2145.02	46619.61	III	$4s4p^3\,^3P_1-4p5p\,^3D_1$
	30	3		20		2144.29	46635.48	IV	$5p\,^2P_{3/2}-5d\,^2D_{3/2}$
	40	4	1	20		2141.59	46694.28	III	$4s4p^3\,^3P_2-4p5p\,^3D_1$
	20	2	1	15		2139.60	46737.71	III	
	200	8	1	50		2137.32	46787.57	IV	$5p\,^2P_{3/2}-5d\,^2D_{5/2}$
	2			15		2136.46	46806.4		
	5					2134.55	46848.3		
	5					2141.13	46923.5	III	$4s4p^3\,^3P_1-4p5p\,^3D_2$
	5	2		10		2127.52	47003.08	III	
	2			10		2126.11	47034.26	IV	$6s\,^2S_{1/2}-7p\,^2P_{1/2}$
	1					2124.18	47076.99		
	200	7	1	50		2111.80	47352.92		
	1					2108.05	47437.21		
	5	4		20		2106.30	47476.62	IV	$6s\,^2S_{1/2}-7p\,^2P_{3/2}$
	2			10		2104.40	47519.48		
	2	1		20		2101.15	47592.98		
	1			10		2095.39	47723.81		

Intensity						Wave-length	Wave-number	Classification	
M_{I_T}	E_DP	R	S_{He}	E_DG	K	λ vac	(cm^{-1})		
	25	7		50		2090.61	47832.91	IV	$5p\,^2P_{\frac{1}{2}}-5d\,^2D_{\frac{3}{2}}$
				10		2084.70	47968.53		
100	50		8	60		2075.45	48182.28	I	
800	5		8	40		2063.45	48462.60	I	
	5		1	40		2062.02	48496.25		
	10	8	1	50		2057.39	48605.32	III	
				2		2048.26	48821.93		
				15		2045.39	48890.43		
1000			10	40		2040.51	49007.5	I	
				10		2031.92	49214.7		
		5		20		2014.52	49639.62	IV	$5p\,^2P_{\frac{3}{2}}-6s\,^2S_{\frac{1}{2}}$
		6		15		2006.35	49841.75	III	

R	K_y	V_G	S_{He}	λ vac	(cm^{-1})	Classification	
	15	8	8	1995.12	50122.3	I	
2	2	3		1993.03	50174.7	III	
		10		1977.04	50580.7		
	4	8		67.04	50837.8	IV	$4s^25p\,^2P_{\frac{1}{2}}-4s^26s\,^2S_{\frac{1}{2}}$
		100		65.05	50889.3		
	50	100		60.91	50996.7	I	
		15		56.96	51099.7		
5	5	15		50.15	51278.1	III	
5	5	25		47.20	51355.8	III	
		3		42.29	51485.6		
		2		41.12	51516.7	III	$4p5p\,^3P_2-4p7s\,^3P_1$
		2		40.28	51538.9		
		2		39.80	51551.7		
		2		39.54	51558.6	IV	$4s4p^2\,^2P_{\frac{3}{2}}-4s^25p\,^2P_{\frac{1}{2}}$
		2		37.94	51601.2		
		3		35.99	51653.2		
		5		32.05	51758.5		
		4		28.92	51842.5		
		1		28.32	51858.6		
		1		22.72	52009.7		
		10		22.47	52016.4	V	$4s5p\,^1P_1-4s5d\,^3D_1$
		1		21.75	52035.9		
		4		21.50	52042.7		
6	6	60		20.36	52073.6		
		100		19.30	52102.3	V	$4s5p\,^1P_1-4s5d\,^3D_2$

Intensity				Wave-length	Wave-number	Classification	
R	K_y	V_G	S_{He}	λ vac	(cm^{-1})		
	30	100	10	19.22	52104.5	I	
	35	5	8	13.84	52251.0	I	
		3		03.90	52523.8		
		8		03.59	52532.3	V	$4s5p\,^3P_2-4s5d\,^3D_2$
	4	35		1901.42	52592.3		
	40	3		1898.56	52671.5	I	
4	8	12		97.30	52706.5	III	
	4	12		94.56	52782.7	III	
	5	25		93.18	52821.2	III	
		6		92.24	52847.4	III	$4p5p\,^1D_2-4p7s\,^1P_1$
6	6	6		91.22	52875.9	III	$4p5p\,^3P_1-4p7s\,^3P_0$
2	2	2		87.66	52975.6		
2	2			85.30	53042.0	III	$4p5p\,^3P_1-4p7s\,^3P_1$
		8		76.62	53287.3		
		2		74.20	53356.1	V	$4s5p\,^3P_1-4s5d\,^3D_1$
		10		70.84	53451.9	V	$4s5p\,^3P_1-4s5d\,^3D_2$
		3		69.50	53490.2		
		6		64.85	53623.6		
	25	8	6	1858.88	53795.8	I	
	30	50	10	55.29	53899.9	I	
		6		54.35	53927.3		
		10		52.87	53970.3		
		6		51.12	54021.4		
	4	12		49.51	54068.4	I	
		8		49.12	54079.8		
		8		43.32	54249.9		
		3		42.61	54270.8		
		12		41.30	54309.5		
		30		39.24	54370.3		
	4	8		38.38	54395.7		
		4		38.08	54404.6		
		2		36.20	54460.3		
		3		32.65	54565.8		
		6		31.03	54614.1	III	$4p5p\,^3P_0-4p7s\,^3P_1$
		2		21.70	54893.8		
		20		19.90	54948.1		
		4		15.90	55069.1		
		4		13.68	55136.5		
		10		1809.35	55268.5		

R	Intensity K_y	V_G	S_{He}	Wave-length λ vac	Wave-number (cm^{-1})	Classification
		30		08.70	55288.3	
		16		08.41	55297.2	
		10		07.76	55317.1	
		4		05.69	55380.5	
		8		03.36	55452.0	
		4		01.97	55494.8	
		3		00.02	55554.9	
		8		1799.09	55583.7	
		3		96.95	55649.9	
		3		95.75	55687.0	
	30	10	2	95.28	55701.6	I
		30		94.14	55737.0	
		15		93.59	55754.1	III $4p5p\,^3P_2-4p7s\,^3P_2$
		4		90.16	55860.9	III $4p5p\,^3D_2-4p7s\,^3P_1$
	3	16		89.43	55883.7	
		20		89.22	55890.3	
		3		85.40	56009.9	
		2		84.66	56033.1	III $4p5p\,^3D_1-4p7s\,^3P_0$
	3			83.06	56083.4	
		15		82.89	56088.7	
		10		81.84	56121.8	
		5		81.45	56134.1	III $4p5p\,^3P_2-4p7s\,^1P_1$
		2		77.24	56267.0	
		2		75.93	56308.5	
		3		1775.00	56338.0	
		6		72.00	56433.4	
		0		71.36	56453.8	
		1		70.00	56497.2	
		3d		65.70	56634.8	
		5		60.93	56788.2	
		10		60.58	56799.5	
	6	5		52.89	57048.7	I
		2		51.70	57087.4	
		0		48.78	57182.7	
		2		46.20	57267.2	III $4p5p\,^3P_1-4p7s\,^3P_2$
		0		43.77	57347.0	
		2		40.18	57465.3	
		0		39.85	57476.2	
		6		36.98	57571.2	
		3		36.04	57602.4	

	Intensity			Wave-length	Wave-number	Classification
R	K_y	V_G	S_{He}	λ vac	(cm^{-1})	
		2		34.30	57660.2	III $4p5p\,^3P_1-4p7s\,^1P_1$
		4		32.00	57736.7	
		3		30.09	57800.5	
		4		21.85	58077.1	
		8		19.75	58148.0	
		2		16.25	58266.6	
		0		14.30	58332.9	
		5		10.73	58454.6	
		2		06.52	58598.8	
		3		05.30	58640.7	III $4p5p\,^1P_1-4p7s\,^3P_1$
		2d		1699.74	58832.5	
	25	4		90.70	59147.1	I
		2		82.78	59425.5	
		1		75.88	59670.1	III
	25	6		75.30	59690.8	I
		3		73.74	59746.4	
		3		72.84	59778.6	
	25	6		71.17	59838.3	I
	2	6		67.24	59979.4	II
		6		65.62	60037.7	
		6		64.70	60070.9	
		16		56.23	60378.1	
		20		53.32	60484.4	III
		5d		52.04	60531.2	
1	1	10		44.90	60794.0	III
		15		41.63	60915.1	
		5		32.10	61270.8	III
	12	2		26.25	61491.2	I
	10	1		22.70	61625.7	I
	15	5		21.16	61684.2	II
		3		1620.68	61702.5	
		2		20.40	61713.2	
		0		15.40	61904.2	
		6		14.80	61927.2	
		5		14.05	61956.0	
		5		13.30	61984.8	
	10	0		10.73	62083.7	I
		30		08.43	62172.4	
		30		07.50	62208.4	
	25	15		06.46	62248.7	I

	Intensity			Wave-length	Wave-number		Classification
R	K_y	V_G	S_{He}	λ vac	(cm^{-1})		
		8		05.95	62268.4		
		2		02.90	62386.9		
		8		00.40	62484.4		
		8		1599.42	62522.7		
		2		98.80	62546.9	II	
		16		96.15	62650.8		
		12		93.20	62766.8	I	
		4		87.87	62977.5		
		8		87.42	62995.3	I	
		3d		82.48	63192.0		
		4		80.34	63277.5		
	20	8		80.04	63289.5	I	
	15	4		79.49	63311.6	I	
		30		77.16	63405.1		
	15	6		75.26	63481.6	I	
	3	50		71.50	63633.5	III	
		12		68.69	63747.5		
		2		64.23	63929.2		
	2	3		63.35	63965.2	III	
		5		58.56	64161.8		
		75		48.80	64566.1	III	
	12	4		47.10	64637.1	I	
		5		46.00	64683.0		
		3		36.60	65078.8		
	2	6		34.90	65150.8	III	
		60		1533.75	65199.7	III	$4s^2p^2\,{}^3P_2 - 4s4p^3\,{}^5S_2$
		6		32.08	65270.7	III	
		8		30.60	65333.9		
		2		29.25	65391.5		
		3		25.15	65567.3		
		4		1524.40	65599.6		
		4		23.00	65659.9		
		30		1516.50	65941.3		
		25		09.50	66247.1		
		50		08.06	66310.4		
		4		1505.30	66431.9		
	15	3		1500.90	66626.7	I	
		16		1499.68	66680.9		
		60		97.90	66760.1	III	
		60		92.74	66990.9		

Intensity R	K_y	V_G	S_{He}	Wave-length λ vac	Wave-number (cm^{-1})	Classification
		100		83.68	67400.0	III $4s^24p^2\,^3P_1-4s4p^3\,^5S_2$
		4		76.60	67723.1	
		12		75.58	67770.0	
		16		74.60	67815.0	
		2		73.40	67870.2	
		2		54.20	68766.3	
	2	10		53.95	68778.2	
		6		52.90	68827.9	V $4s4d\,^3D_1-4s5p\,^3P_0$
		6		51.72	68883.8	
		4		49.27	69000.3	
		20		48.60	69032.2	
	10	2		47.00	69108.5	
		25		45.46	69182.1	V $4s4d\,^3D_2-4s5p\,^3P_1$
		2		41.97	69349.6	
		8		41.38	69378.0	V $4s4d\,^3D_1-4s5p\,^3P_1$
		6		1440.08	69440.6	
		6		37.72	69554.6	
		20		37.13	69583.1	
		20		33.40	69764.2	V $4s4d\,^3D_3-4s5p\,^3P_2$
		25		31.63	69850.5	
		6		26.90	70082.0	V $4s4d\,^3D_2-4s5p\,^3P_2$
		8		13.70	70736.4	V $4s4d\,^3D_1-4s5p\,^1P_1$
		6		10.30	70906.9	
		8		07.80	71032.8	
				05.72	71137.9	
		3		1404.07	71189.6	
		30		02.80	71286.0	
		2		00.60	71398.0	
		2		1399.13	71473.0	
		2		95.70	71648.6	
		45		93.80	71746.3	
		3		90.07	71938.8	
	2	4		84.60	72223.0	I
		4		78.81	72526.3	
		4		70.15	72984.7	
		2		69.10	73040.7	
				61.05	73472.7	
				57.68	73655.1	
		2		39.39	74660.9	
		2		37.57	74762.4	

R	Intensity K_y	V_G	S_{He}	Wave-length λ vac	Wave-number (cm^{-1})	Classification	
		60		1332.92	75022.	IV	$4s^24p\,^2P_{3/2}-4s4p^2\,^4P_{1/2}$
		4		31.12	75124.7		
		2		30.20	75176.7		
		12		29.88	75194.8		
		8		29.35	75224.7		
		3		29.10	75238.9		
		30		24.00	75528.7		
		2		20.07	75753.6		
		60		18.40	75849.5		
	8	50		14.40	76080.3	IV	$4s^24d\,^2D_{5/2}-4s^24f\,^2F_{7/2}$
		5		14.14	76095.3	IV	$4s^24d\,^2D_{5/2}-4s^24f\,^2F_{5/2}$
		2		10.68	76296.3		
		3		10.40	76312.6		
		8		09.04	76391.9		
		8		08.70	76411.7		
		20		07.53	76480.1	IV	$4s^24d\,^2D_{3/2}-4s^24f\,^2F_{5/2}$
		6		06.20	76558.0		
		25		05.49	76612.	IV	$4s^24p\,^2P_{3/2}-4s4p^2\,^4P_{3/2}$
		12		05.06	76624.8		
		2		03.43	76720.7		
		45		02.62	76768.4	III	
		30		02.22	76791.9		
		2		1301.20	76852.1		
		8		1299.08	76977.6		
		8		96.95	77104.0		
	2	12		91.62	77422.2		
	8	20		90.95	77462.3	II	
		4		88.52	77608.4		
		6		86.60	77724.2		
		4		86.04	77758.1		
		16		85.53	77788.9		
		5		84.85	77830.1		
		4		77.64	78269.3		
	2	8		76.86	78317.1	II	
	5	30		62.45	79210.	IV	$4s^24p\,^2P_{3/2}-4s4p^2\,^4P_{5/2}$
	4			61.54	79268.2		
	4	30		59.55	79393.4	IV	$4s^24p\,^2P_{1/2}-4s4p^2\,^4P_{1/2}$
	2	6		56.65	79576.7		
		6		47.40	80166.7		
	4	25		46.00	80256.8		

R	Intensity K_y	V_G	S_{He}	Wave-length λ vac	Wave-number (cm^{-1})		Classification
	0	3		37.60	80801.6	II	
	7	10		34.85	80981.	IV	$4s^2 4p\, ^2P_{\frac{1}{2}} - 4s4p^2\, ^4P_{3/2}$
		2		34.25	81020.9		
		5		32.59	81130.0		
	1	3		31.00	81234.8		
		4		1228.74	81384		
		16		27.56	81462	V	$4s4p\, ^1P_1 - 4s4d\, ^1D_2$
	3	8		24.60	81659	II	
		6		22.02	81832	II	
		3		18.49	82069		
	2	4		18.04	82099	II	
	0	2		08.72	82732		
	1	10		06.54	82882		
	7	5		05.70	82939	II	
	2	5		05.25	82970	II	
		10		02.56	83156		
		2		1200.23	83317		
		6		1199.36	83378		
		2		98.46	83440		
		3		98.17	83460		
	1	3		96.50	83577		
	0			93.68	83775		
	10	30		92.24	83872	II	
	0			88.21	84160		
	2	6		83.98	84461	II	
	2	8		82.69	84553	II	
	2	8		77.99	84890	II	
	1	5		77.31	84940	II	
	1	5		70.78	85414	II	
	8	16		68.50	85578	II	
4	2	12		66.83	85705	IV	$4s4p^2\, ^2D_{3/2} - 4s^2 5p\, ^2P_{\frac{1}{2}}$
	5	20		66.51	85724	II	
5	2	16		57.34	86406	IV	$4s4p^2\, ^2D_{5/2} - 4s^2 5p\, ^2P_{3/2}$
	8	12		56.93	86437	II	
	7	12		55.95	86509	II	
		6		1152.4	86775	IV	$5p\, ^2P_{1/2} - 6d\, ^2D_{3/2}$
7	7	8		1150.96	86884	V	$4s4p\, ^1P_1 - 4p^2\, ^3P_2$
1	1			1150.76	86900	IV	$4s4p^2\, ^2D_{3/2} - 4s^2 5p\, ^2P_{3/2}$
	9	8		41.97	87570	II	
	0	2		34.02	88180		

Intensity				Wave-length	Wave-number	Classification	
R	K_y	V_G	S_{He}	λ vac	(cm^{-1})		
	0	2		32.46	88303		
	1	1		30.49	88457	II	
	0	2		29.96	88499		
	0			28.45	88617		
		2		27.70	88676		
	5	10		26.28	88788	III	
	0	2		23.76	88987		
	0	1		22.93	89053	IV	$4s^2 5p\,^2P_{3/2}-4s^2 7s\,^2S_{1/2}$
	0			22.54	89084		
	0			1121.62	89157		
	0			19.98	89287		
10	8	16		19.20	89350	III	
	0			17.73	89467		
		3		16.49	89566		
	0	2		14.52	89725		
	0			13.33	89821		
	0	6		10.08	90084		
		4		09.42	90137		
	0	2		08.51	90211		
		1		08.00	90252	IV	$4s^2 5p\,^2P_{1/2}-4s^2 7s\,^2S_{1/2}$
	0	2		06.20	90400		
	0			02.14	90733		
7	5	50		1100.50	90868		
6		50		00.36	90879	III	
	1	6		1100.10	90901		
9	6	40		1099.10	90984	III	
	2			98.98	90993		
6	8	12		97.85	91087	III	
9	3	50		94.685	91350.5	V	$4s^2\,^1S_0-4s4p\,^3P_1$
	1	5		90.48	91703	II	
		3		89.97	91746		
	1	12		87.96	91915		
	1	20		85.97	92084	II	
		12		84.64	92196		
	1	6		84.04	92248		
		10		83.38	92304		
	2	12		81.76	92442		
	0			81.23	92487		
	0			80.54	92546		
8	5	45δ		79.74	92615	III	

R	Intensity K_y	V_G	S_{He}	Wave-length λ vac	Wave-number (cm^{-1})	Classification
		3		79.10	92670	
	0	6		78.75	92700	
		3		78.17	92750	
	1	8		77.51	92807	II
		3		76.91	92858	
		5		76.53	92891	
		2		75.72	92961	
1	1	3		69.72	93482	III
		8		69.05	93541	
1	1			68.83	93560	III
		2		67.11	93711	
		4		66.18	93793	
		2		63.41	94037	
		6		1062.47	94120	
	9	40		57.41	94571	II
	1			57.05	94603	
	0			56.25	94675	
	0	2		53.90	94886	
	0			53.42	94929	
		10		52.87	94978	
	3	30		52.13	95045	II
		4		51.60	95093	
		5		50.55	95188	II
5	5	20		50.40	95202	
	0			50.22	95218	
	5	5		49.65	95270	II
	5	60		49.51	95283	II*
	0	10		48.04	95416	
		6		47.64	95453	II
	0	4		47.11	95501	
4	5	20		45.35	95662	II
	1	2		44.64	95727	
	0	12		44.46	95743	
	0	6		44.10	95776	
		0		43.12	95866	
		2		41.82	95986	
		8		39.00	96246	
		4		38.35	96307	II
		60		36.97	96435	
	2	50		36.18	96508	II

R	Intensity K_y	V_G	S_{He}	Wave-length λ vac	Wave-number (cm^{-1})	Classification
		6		35.06	96613	
	0	3		34.34	96680	
	10	45		33.56	96753	II
	3	20		29.52	97133	II
	3	10		28.58	97221	
		0		26.96	97375	
		4		26.28	97439	
		10		25.70	97494	
	3	10		24.86	97574	
		2		23.80	97675	
		2		23.01	97751	
	3	12		22.10	97838	II
	2	12		21.80	97867	
		4		21.28	97916	
		1		1020.02	98037	
	0	6		19.66	98072	
		3		19.35	98102	
2	0	4		17.98	98234	
		6		16.30	98396	
		0		15.88	98437	
		4		15.31	98492	
		6		14.72	98549	
	9	45		13.99	98620	II
	9	50		13.40	98678	II
	0			13.26	98691	
	3	25		11.87	98827	II
	1	4		11.15	98897	II
	0			10.72	98939	
		16		10.25	98985	
		16		09.94	99016	
		20		08.14	99193	
	2	7		07.97	99209	
	0			07.57	99249	
	0			06.23	99381	
		4		05.89	99414	
	5	100δ		04.72	99530	IV $5s\,^2S_{1/2}-6p\,^2P_{3/2}$
	2	60		03.02	99699	
4	4	100		1001.63	99837	IV $4s^24p\,^2P_{3/2}-4s4p^2\,^2D_{3/2}$
	1			1000.75	99925	
	3	60		1000.40	99960	III $4p^2\,^1S_0-4p5s\,^3P_1$

Intensity				Wave-length	Wave-number	Classification	
R	K_y	V_G	S_{He}	λ vac	(cm^{-1})		
	0	2		999.50	100050		
	0			998.73	100127		
		4		998.04	100196		
	0			997.94	100206		
	0			997.54	100247		
10	6	70		996.69	100332	IV	$4s^24p\,^2P_{3/2}-4s4p^2\,^2D_{3/2}$
	0			996.60	100341		
	0	8		995.44	100458		
		3		992.84	100721		
		16		91.83	100824		
	1	2		91.56	100851		
		10		91.40	100867		
		2		90.67	100942		
		5		90.07	101003		
		2		89.76	101035		
	1	0		89.29	101083		
	1	12		988.72	101141		
		2		86.86	101332		
	0			86.68	101350	II	
	1	0		86.58	101360		
	0	4		85.70	101451		
	6	20		83.94	101632	II	
		6		83.44	101684		
		4		82.83	101747		
	1	4		80.28	102012		
		3		78.80	102166		
		4		76.92	102363		
	7	100		74.85	102580	III	
	5	60		74.11	102658	III	
		4		72.27	102852	IV	$4d\,^2D_{3/2}-6p\,^2P_{1/2}$
		25		71.21	102964		
		2		70.37	103053		
		4		70.22	103069		
		4		68.29	103275	V	$4s4d\,^3D_3-4s4f\,^3F_2$
		3		66.03	103516		
	2	3		65.31	103594	V	$4s4d\,^3D_2-4s4f\,^3F_2$
		2		64.93	103634		
		2		63.31	103809	V	$4s4d\,^3D_1-4s4f\,^3F_2$
		2		63.06	103836		
	1	50		61.78	103974	II	

Intensity				Wave-length	Wave-number	Classification	
R	K_y	V_G	S_{He}	λ vac	(cm^{-1})		
	0	3		61.27	104029	V	$4s4d\,^3D_3-4s4f\,^3F_3$
		50		60.03	104163		
	6	2		59.59	104211	IV	$4s^24p\,^2P_{\frac{1}{2}}-4s4p^2\,^2D_{3/2}$
		40		59.04	104271		
	0	2		58.28	104354	V	$4s4d\,^3D_2-4s4f\,^3F_3$
		10		57.91	104394		
	5	75		54.78	104736	III	
	5	60		54.43	104775	III	
8	4	50		53.92	104831	III	$4p^2\,^1S_0-4p5s\,^1P_1$
		40		53.74	104850	III	
	1	10		51.25	105125	II	
	0	4		50.07	105255	II	
		4		47.07	105589	V	$4s4d\,^3D_3-4s4f\,^3F_4$
	0	8		43.56	105981	II	
		12		41.01	106269	II*	
	0			40.64	106311		
	0	30		38.46	106558		
	5	100		38.18	106589	III	
		3		37.42	106676		
		2		36.42	106790		
	0	6		33.98	107069		
		3		932.31	107260		
		6		30.95	107417		
		2		29.20	107619		
		10		27.46	107821		
	1	6		26.32	107954		
		1		24.69	108144		
		4		23.97	108229		
	1	8		22.92	108352	II	
		2		21.93	108468		
	1	12		21.04	108573		
	1	25		20.51	108635	III	$4p^2\,^3P_2-4p^3\,^1D_2$
	0	4		19.68	108733	V	$4s4d\,^3D_2-4s4f\,^1F_3$
	1	30		18.81	108836	II	
	1	25		17.89	108946	II	
		6		16.49	109112		
		4		15.75	109200	V	$4p^2\,^3P_2-4s5p\,^3P_2$
		25		14.63	109334		
	1	1		13.17	109509		
		1		13.00	109529		

Intensity R	Intensity K_y	Intensity V_G	Intensity S_{He}	Wave-length λ vac	Wave-number (cm^{-1})	Classification	
		40		12.69	109566	II	
	0			11.96	109654	V	$4p^{2\,3}P_2-4s5p\,^1P_1$
		2		09.22	109984		
	1			07.72	110166		
		8		07.54	110188		
	1	1		06.56	110307		
		20		06.36	110331		
	0			06.09	110364		
		1		05.50	110436		
		60		04.10	110607		
		50		03.74	110651		
	0			03.51	110680		
		100		03.37	110697		
	3	50		02.28	110830	III	$4p^{2\,3}P_1-4p^{3\,1}D_2$
	2	20		00.74	111020	III	
	1	3		900.25	111080		
		1		899.17	111214		
		2		898.13	111342		
		3		896.94	111490		
	0	2		894.90	111744	II	
	0			894.07	111848		
	0			93.27	111948		
		12		91.61	112157		
	4	2		91.44	112178		
		20		91.22	112205		
3	5	30		90.68	112274	III	
		1		89.52	112420		
	1	3		88.87	112502		
	2			88.06	112605		
	0	10		87.41	112687	II	
	0	30		86.85	112759	VI	$4s\,^2S_{\frac{1}{2}}-4p\,^2P_{\frac{1}{2}}$
		2		84.90	113007		
		6		83.17	113228		
	3	3		82.64	113296	II	
	5			82.13	113362		
		0		81.34	113464		
7	4	15		79.15	113746	III	
	1			78.19	113871		
	1			77.77	113925		
	1			75.36	114239		

Intensity R	K_y	V_G	S_{He}	Wave-length λ vac	Wave-number (cm^{-1})	Classification	
	1			73.77	114447		
	0	2		72.93	114557		
		5		72.37	114630	II	
	0	6		71.60	114732		
	0	0		70.95	114817		
		3		69.40	115022		
	0	0		68.51	115140	V	$4p^{2\,3}P_0-4s5p\,^3P_1$
	0	4		67.80	115234	II	
	0	4		66.98	115343		
	1	3		65.87	115491	II	
	1	3		64.49	115675	II	
	3			60.62	116195		
		4		60.44	116220		
	0			59.95	116286		
		5		58.58	116471	V	$4p^{2\,3}P_0-4s5p\,^1P_1$
		15		56.50	116754		
	0	2		55.76	116855		
	6	8		54.37	117045	II	
	0	4		852.51	117301		
3	3	16		52.10	117357	III	
		3		51.31	117466		
		5		50.58	117567		
		0		50.25	117612		
	4	4		49.62	117700	II	
		2		49.54	117711	IV	$4p^{2\,2}P_{3/2}-6p\,^2P_{1/2}$
		8		46.20	118175		
		25		45.91	118216		
	0	40		45.75	118238	V	$4s4p\,^3P_2-4s4d\,^1D_2$
	0	3		45.04	118338		
		30		44.15	118462	VI	$4s\,^2S_{1/2}-4p\,^2P_{3/2}$
	0			43.41	118566		
9	5	30		43.02	118621	III	
		0		42.06	118756		
		8		41.25	118871		
	0	2		40.32	119005		
		8		40.15	119026		
	4	30		39.48	119121	V	$4s4p\,^3P_2-4p^{2\,3}P_1$
		0		38.30	119289		
		0		37.47	119407		
	2	6		36.01	119616		

Intensity				Wave-length	Wave-number	Classification
R	K_y	V_G	S_{He}	λ vac	(cm^{-1})	
		20		35.27	119722	
	0			34.86	119781	
		25		34.45	119839	
		12		33.78	119936	
		20		33.28	120008	
		20		32.62	120103	III $4p^{2}\,{}^{3}P_{2}-4p4d\,{}^{3}F_{2}$
		3		31.70	120236	
		0		30.99	120338	
		6		30.60	120395	
	6	2		30.33	120434	V $4s4p\,{}^{3}P_{1}-4p^{2}\,{}^{3}P_{0}$
		25		30.15	120460	
		0		29.29	120585	
	8	8		28.44	120709	II
		6		27.30	120875	II*
	0	8		27.03	120915	
	0	6		25.90	121080	
	0			25.30	121168	
6	6	30		23.89	121375	III
7	0	3		20.70	121847	V $4s4p\,{}^{3}P_{1}-4s4d\,{}^{1}D_{2}$
		20		20.54	121871	
		3		20.05	121944	
	0	4		819.52	122023	
	1			18.95	122108	
	2	4		18.63	122155	
	1			18.60	122159	
		30		18.45	122182	
	1			18.10	122234	
	0			17.91	122263	
4	2	30		17.55	122317	III
1	1	4		16.94	122408	
	0			16.33	122499	
	0			15.79	122581	
	0			15.07	122689	
6		25		14.75	122737	V $4s4p\,{}^{3}P_{1}-4p^{2}\,{}^{3}P_{1}$
		4		14.04	122844	III
	0	4		11.90	123168	
		5		11.20	123274	
		4		09.52	123530	
		40		08.68	123658	V $4s4p\,{}^{3}P_{2}-4p^{2}\,{}^{3}P_{2}$
5	3	20		07.06	123907	III

Intensity R	K_y	V_G	S_{He}	Wave-length λ vac	Wave-number (cm^{-1})		Classification
		4		06.56	123983		
	5	20		04.23	124343	V	$4s4p\,^3P_0-4p^2\,^3P_1$
		30		03.78	124412	IV	$4s^24p\,^2P_{3/2}-4s4p^2\,^2S_{1/2}$
6		4		03.02	124530	III	
		30		02.82	124561		
		0		801.60	124751	II	
		10		801.41	124780		
	0			01.22	124810		
	1			00.49	124923		
5	5	2		00.11	124983	IV	$4s4p^2\,^2D_{5/2}-4s^24f\,^2F_{7/2}$
		20		799.95	125008	IV	$4s4p^2\,^2D_{5/2}-4s^24f\,^2F_{5/2}$
4	1	4		799.76	125038	III	
		20		99.64	125056		
	2			99.41	125092		
		2		98.95	125164		
	0	2		98.79	125189		
		6		98.69	125205		
	0			98.46	125241		
	6			98.30	125266		
		20		98.09	125299		
	1			797.94	125323		
		3		797.60	125376		
	0			97.31	125422		
		20		96.80	125502	IV	$4s4p^2\,^2D_{3/2}-4s^24f\,^2F_{5/2}$
		4		95.15	125762		
	0			94.90	125802	V	$4s4p\,^1P_1-4s4d\,^3D_1$
		2		94.58	125853		
5	4	40		92.56	126173	III	
		8		92.08	126250		
0	0	16		91.26	126381	III	
7	4	30		90.77	126459	III	
	0	4		90.05	126574		
	0			89.34	126688		
	0			88.93	126754		
6		20		88.79	126776	III	
		2		86.40	127162	II*	
	0			86.21	127192		
		50		85.76	127265	V	$4s4p\,^3P_1-4p^2\,^3P_2$
	0			85.63	127286		
	0			85.42	127320		

Intensity				Wave-length	Wave-number		Classification
R	K_y	V_G	S_{He}	λ vac	(cm^{-1})		
	0	2		84.52	127466		
3	3	25		83.67	127605	III	
2	2	4		82.92	127727	III	
		25		82.70	127763		
	0			81.81	127908		
	0			80.75	128082		
	0			79.88	128225		
	0			78.52	128449		
	4	8		78.17	128507		
	0			77.99	128536		
8	4	30		77.32	128647	III	
	5	25δ		76.46	128790	IV	$4s^2 4p\ ^2P_{\frac{1}{2}} - 4s4p^2\ ^2S_{\frac{1}{2}}$
	0			75.77	128904		
0	2	8		75.26	128989	III	
	2			74.40	129132	II	
		8		74.19	129167		
		0		773.16	129339		
	3	30		772.24	129493		
	2	4		771.52	129614		
	3	40		70.88	129722	III	
	2	16		69.76	129911	III	
		2		69.01	130037		
		2		67.16	130351		
		0		66.03	130543	IV	$5s\ ^2S_{\frac{1}{2}} - 7p\ ^2P_{\frac{1}{2}}$
		3		65.67	130605		
	2			65.14	130695		
0	0	0		64.56	130794		
		4		64.40	130822		
		6		63.47	130981	IV	$5s\ ^2S_{\frac{1}{2}} - 7p\ ^2P_{3/2}$
	0			61.98	131237		
	0	0		60.62	131471		
	0			60.20	131544		
	1			59.80	131613		
2	2	35		59.54	131658	III	
		40		59.14	131728	V	$4s^2\ ^1S_0 - 4s4p\ ^1P_1$
8	6	40		58.90	131769	IV	$4s^2 4p\ ^2P_{3/2} - 4s4p^2\ ^2P_{\frac{1}{2}}$
		0		58.15	131900		
	0			57.86	131950		
		6		57.06	132090		
		4		56.32	132219		

Intensity R	Ky	VG	SHe	Wave-length λ vac	Wave-number (cm^{-1})	Classification	
	0	0		55.83	132304		
		4		55.63	132340		
	0			55.16	132422		
	0	2		54.80	132485		
		3		53.78	132665		
	3	35		51.81	133012	III	
	0	10		51.05	133147		
		10		50.55	133236		
		3		49.87	133356		
	0	3		48.65	133574		
	0			47.71	133742		
		16		47.56	133769		
	0			47.35	133806		
	0			46.83	133899		
	5	30		46.38	133980	IV	$4s^2 4p\,^2P_{3/2} - 4s4p^2\,^2P_{3/2}$
		30		46.16	134019		
1	1			45.70	134102		
	0	4		44.62	134297		
	0			43.58	134484		
		3		43.40	134517		
	0	2		742.78	134629	IV	$4d\,^2D_{5/2} - 7p\,^2P_{3/2}$
		125		742.21	134733		
	4	30		41.87	134795	III	
		4		40.66	135015	IV	$4s^2 4d\,^2D_{3/2} - 7p\,^2P_{3/2}$
	2	30		39.62	135204	III	
		5		39.40	135245		
	2	30		39.24	135274	III	
	0			38.52	135406		
	3	40		38.12	135479	III	
	0	30		37.22	135645	III	
		30		37.02	135682		
	0			36.24	135825		
	4	45		34.57	136134	IV	$4s^2 4p\,^2P_{1/2} - 4s4p^2\,^2P_{1/2}$
		40		34.36	136173		
	0	6		33.33	136364		
	0	2		32.48	136523		
	0			32.07	136598		
	2	5		31.52	136702	III	
		35		31.37	136730		
	0	4		30.86	136825		

R	Intensity K_y	V_G	S_{He}	Wave-length λ vac	Wave-number (cm^{-1})		Classification
	2	5		30.25	136939	III	
		30		30.08	136971		
	0			29.46	137087		
	1	16		28.87	137199		
	0	3		28.08	137348		
		2		27.48	137461	III	
	2	10		27.41	137474		
	0	40		26.40	137665	III	
		2		25.16	137901		
		32		24.40	138045		
	4	32		24.28	138068	III	
	5	30		22.79	138352	IV	$4s^2 4p\, ^2P_{\frac{1}{2}} - 4s4p^2\, ^2P_{3/2}$
	0			21.78	138546		
		3		21.41	138617		
		16		20.94	138708		
	2	25		20.68	138758	III	
	2	50		20.36	138819	III	
		50		20.22	138846		
6	2	25		19.95	138899	III	
		4		719.35	139014		
		30		718.63	139154		
		5		18.30	139218		
	0	8		16.69	139530		
	1			14.10	140036		
		10		13.87	140082		
		4		13.27	140199		
		1		12.40	140371		
		2		11.85	140479		
	2	30		11.39	140570	III	
	2	30		11.04	140639	III	
	0	4		10.14	140817		
	7	40		09.41	140962	III	
	4	40		09.17	141010	III	
	1	20		06.75	141493		
		3		06.54	141535		
		3		05.70	141703		
	2			05.28	141788		
		25		04.87	141870		
		16		03.84	142078		
		2		03.53	142140		

R	Intensity K_y	V_G	S_{He}	Wave-length λ vac	Wave-number (cm^{-1})	Classification
	2	30		02.74	142300	II*
		4		02.28	142393	
	0	10		01.39	142574	
		2		700.31	142794	
		2		698.62	143139	
	00			97.65	143338	
		4		97.49	143371	
	00			97.28	143414	
		20		694.93	143899	
	0	8		94.29	144032	
	0	4		93.14	144271	
	2	30		92.21	144465	
	0			91.23	144670	
	0			90.89	144741	
	2	20		90.66	144789	
	2	35		90.48	144827	
	2	10		89.96	144936	
	2	15		88.95	145148	
	3	35		87.67	145419	
		30		87.40	145476	
		12		87.10	145539	
	1	10		86.49	145669	
	1	8		85.87	145800	
		2		685.15	145953	
	2	30		684.60	146071	III
	2	12		84.32	146130	
	0	3		84.07	146184	
		2		83.51	146304	
		2		83.06	146400	
		2		82.34	146555	
		1		81.49	146737	
	3	16		80.50	146951	
		2		79.40	147189	
		10		78.86	147306	
		2		77.78	147541	
		4		77.08	147693	
		6		76.63	147791	
		10		76.12	147903	
	5	50		74.49	148260	
		2		73.82	148408	

Intensity				Wave-length	Wave-number		Classification
R	K_y	V_G	S_{He}	λ vac	(cm^{-1})		
		3		72.92	148606		
	8			71.85	148843	IV	$4s^24p\,^2P_{3/2}-4s^24d\,^2D_{3/2}$
		40		71.60	148898	V	$4s4d\,^1D_2-4s4f\,^3F_3$
	10	100		670.10	149232	IV	$4s^24p\,^2P_{3/2}-4s^24d\,^2D_{5/2}$
	0			65.71	150216		
	1	2		65.43	150279		
	0			61.63	151142		
	0			57.95	151987		
		4		57.68	152050	IV	$4p^2\,^2D_{5/2}-6p\,^2P_{3/2}$
	1	6		55.16	152634		
8	9	25		54.16	152868	IV	$4s^24p\,^2P_{3/2}-4s^25s\,^2S_{1/2}$
9	10	20		52.65	153221	IV	$4s^24p\,^2P_{1/2}-4s^24d\,^2D_{3/2}$
		20		52.43	153273	V	$4s4d\,^1D_2-4s4f\,^1F_3$
	0	3		52.12	153346		
		6		51.23	153556		
		2		50.14	153813		
		1		48.44	154216		
		1		46.12	154770		
4	8	30		44.88	155068	III	
		6		44.16	155241		
	3			43.19	155475		
		25		42.90	155545		
	8	30		42.68	155598		
2	2			42.28	155695	V	$4s4p\,^1P_1-4s5s\,^3S_1$
		2		41.68	155841		
	5			41.12	155977		
	4	30		40.87	156038		
	5	20		640.56	156113		
		1		38.22	156686		
8	10	30		35.94	157248	IV	$4s^24p\,^2P_{1/2}-4s^25s\,^2S_{1/2}$
	4	30		35.80	157282		
	4	20		34.58	157585		
	4	40		31.17	158436	III	
3	4	20		30.74	158544		
4				30.67	158562		
	0			27.63	159330		
		2		26.43	159635		
		2		25.82	159790		
3	3	4		22.56	160627		

Intensity				Wave-length	Wave-number		Classification
R	K_y	V_G	S_{He}	λ vac	(cm^{-1})		
		4		19.06	161535		
		4		18.76	161614		
		10		16.94	162090		
		20		16.28	162264		
		3		15.08	162580	V	$4s4p\,^3P_2 - 4s4d\,^3D_1$
	4	50		14.32	162782	V	$4s4p\,^3P_2 - 4s4d\,^3D_2$
3	3			13.64	162962		
		55		13.12	163100	V	$4s4p\,^3P_2 - 4s4d\,^3D_3$
	8	70		612.98	163137		
	3	35		11.10	163639		
		.1		10.11	163905		
		4		09.59	164045		
	1	16		08.36	164376	VI	$4p\,^2P_{3/2} - 4d\,^2D_{3/2}$
	4	12		07.19	164693		
	4	3		05.92	165038	VI	$4p\,^2P_{3/2} - 4d\,^2D_{5/2}$
		1		05.20	165235		
		1		04.75	165358		
		1		02.91	165862		
		6		601.97	166121		
	4	30		01.75	166182	V	$4s4p\,^3P_1 - 4s4d\,^3D_1$
	5	60		00.95	166403	V	$4s4p\,^3P_1 - 4s4d\,^3D_2$
		5		00.52	166522		
	2	30		599.93	166686		
		25		99.75	166736		
		2		97.90	167252		
	0			97.39	167395		
		50		96.12	167751	V	$4s4p\,^3P_0 - 4s4d\,^3D_1$
		7		94.93	168087		
		1		93.97	168359		
		1		93.50	168492		
	0	20		91.35	169105		
	2	20		88.75	169851		
4		2		88.10	170039	VI	$4p\,^2P_{1/2} - 4d\,^2D_{3/2}$
		1		585.45	170809		
		1		82.15	171777		
		10		81.20	172058		
		5		80.50	172265		
		1		75.90	173641		
		1		74.86	173955		
		8		74.44	174083		

R	Intensity K_y	V_G	S_{He}	Wave-length λ vac	Wave-number (cm^{-1})	Classification
	0	10		73.56	174350	III
	0	12		70.20	175377	
		3		68.11	176022	
0	0	12		66.30	176585	III
0		16		65.10	176960	III
		4		64.73	177076	
	0	12		63.74	177387	
		6		62.45	177794	
	0	8		61.25	178174	
	0			60.35	178459	
		12		60.15	178524	
	1	30		58.30	179115	III
		1		57.49	179375	
	00			55.70	179953	
		16		54.97	180190	
1	00			54.77	180255	III
		25		54.59	180313	
		2		53.91	180535	
		2		53.03	180822	
		3		52.40	181028	
		2		51.91	181189	
		2		51.03	181478	
0	0	10		50.46	181666	III
		3		49.49	181987	
		1		45.76	183231	
1	1			45.04	183473	III
		20		44.81	183550	
2	3			44.07	183800	III
		100		43.82	183884	
	00			42.17	184444	
		6		41.90	184536	
		2		40.37	185058	
		12		39.80	185254	
		25		39.47	185367	
		50		39.13	185484	
		150		38.47	185711	III
		150	C	38.15	185822	
		25		37.65	185995	
		12		537.18	186157	
	00			35.89	186605	

R	Intensity K_y	V_G	S_{He}	Wave-length λ vac	Wave-number (cm^{-1})	Classification	
		4		35.48	186748		
	0	20		33.60	187406		
1	2	60		33.16	187561	III	
		2		32.45	187811		
3	2	60		31.21	188249	III	
0		3		30.42	188530		
0		2		29.98	188686		
1		2		29.26	188943		
	00			29.14	188986		
		8		28.92	189064		
	00			28.33	189276		
		8		28.20	189322		
		3		27.52	189566		
	00			27.21	189678		
		6		27.10	189717		
	00			26.88	189797		
4	2	75		26.39	189973	III	
		30		25.82	190179		
	00			25.47	190306		
		10		25.25	190386		
0				25.13	190429	III	
	00			24.47	190669		
3	4	120		24.08	190811	III	
2				24.01	190836	III	
0	0	20		23.53	191011	III	
		2		22.81	191274		
		1		22.56	191366		
1	2			22.05	191553		
		50		21.89	191611		
	00	4		21.28	191835		
		7		20.77	192023		
		3		20.20	192234		
4	3	75		19.60	192456	V	$4s4p\,^3P_2 - 4s5s\,^3S_1$
	0			18.58	192834		
0		20		18.25	192957	III	
2	0	30		17.59	193203	III	
	0	16		17.20	193349	III	$4p^2\,^3P_1 - 4p5d\,^3P_0$
	00			16.60	193573		
		2		15.49	193990		
		3		14.02	194545		

Intensity R	K_y	V_G	S_{He}	Wave-length λ vac	Wave-number (cm^{-1})	Classification
		1		12.14	195259	
		1		11.44	195526	
		1		10.95	195714	
3	3	60		509.98	196086	V 4s4p$^3P_1$-4s5s$^3S_1$
		60		08.13	196800	
		25		07.55	197025	
		5		07.23	197149	
2	1	15		05.72	197738	
		3		04.86	198075	
		2		01.61	199358	
		1		500.33	199868	
		4		499.65 C	200140	
		2		98.07	200775	
	00	6		96.52	201402	
		2		93.59	202597	
		2		93.39	202679	
		2		92.82	202914	
		2		89.88	204132	
	00			89.34	204357	
	00	6		88.84	204566	
	00			88.09	204880	
		4		87.64	205069	
		3		86.03	205749	
		12		85.65	205910	
		12		85.15	206122	
	00			84.67	206326	
	2	35		84.04	206595	V 4s5p$^3P_1$-4s5s$^1S_0$
		4		83.67	206753	
		1		82.66	207185	
		1		82.05	207447	
		4		81.57	207654	III 4p^2 $^3P_1$-4p7s$^3P_1$
		1		80.48	208125	
		2		79.05	208746	
	00			78.64	208925	
		4		78.10	209161	
	00	2		76.94	209670	
		1		76.61	209815	
		1		76.25	209974	
	00			75.23	210424	
		8		75.04	210509	

R	Intensity K_y	V_G	S_{He}	Wave-length λ vac	Wave-number (cm^{-1})	Classification
	00			74.53	210734	
		3		73.47	211207	
		2		73.15	211349	
	00			71.05	212292	
		10		70.47	212553	
	00			69.51	212988	
		1		69.16	213147	
		6		68.57	213415	
		2		466.76	214243	
		2		66.58	214326	
		10		66.47	214376	
	00			66.24	214482	
	00	12		65.53	214809	
2	00	2		64.80	215146	VI $4p\,^2P_{3/2}-5s\,^2S_{1/2}$
		2		63.76	215629	
		0		63.25	215866	
	00	3		62.06	216422	
		2		60.61	217103	
		3		60.23	217283	
		100		C 459.52	217618	
		2		58.70	218007	
	00			57.45	218603	
		2		57.11	218766	
		3		56.58	219020	
2	2			52.83	220833	VI $4p\,^2P_{1/2}-5s\,^2S_{1/2}$
		0		50.69	221882	
		0		47.62	223404	
		2		45.75	224341	
		4		45.42	224507	
		2		43.39	225535	
		2		42.94	225764	
		3		42.02	226234	
		3		40.45	227041	
	00			39.70	227428	
		2		39.51	227526	
		0		39.13	227723	
		0		38.62	227988	
		2		37.50	228571	
		2		37.19	228734	
		2		34.91	229933	

Intensity R	Ky	VG	SHe	Wave-length λ vac	Wave-number (cm^{-1})	Classification
		2		33.42	230723	
	00			33.16	230861	
		10		29.90	232612	
		4		29.68	232731	
		6		28.52	233361	IV $4s^2 4p\ ^2P_{3/2} - 4s^2 5d\ ^2D_{3/2}$
	3	60		28.22	233524	IV $4s^2 4p\ ^2P_{3/2} - 4s^2 5d\ ^2D_{5/2}$
	1			26.82	234291	
		2		24.96	235316	
	2	20		22.95	236435	
	3			21.99	236972	
	2	35		20.65	237727	IV $4s^2 4p\ ^2P_{1/2} - 4s^2 5d\ ^2D_{3/2}$
	1			19.86	238174	
		0		19.21	238544	
	1			418.93	238703	
	2			16.91	239860	
	2	12		15.38	240743	IV $4s^2 4p\ ^2P_{1/2} - 4s^2 6s\ ^2S_{1/2}$
		2		13.48	241850	
		2		13.23	241996	
		2		413.09	242078	
		0		10.15	243813	
		0		09.24	244355	
		2		06.07	246263	
	00	3		05.30	246731	
	00	4		04.90	246975	
		2		04.70	247097	
		3		03.42	247881	
		2		03.16	248040	
		2		02.82	248250	
		3		02.62	248373	
		2		401.50	249066	
		3		397.43	251617	
		4		95.57	252800	
		4		95.38	252921	
		6		92.18	254985	
		4		91.93	255148	
		3		89.27	256891	
		8	C	86.13	258980	
		2		75.93	266007	
		3		74.48	267037	
		6		74.11	267301	

R	Intensity K_y	V_G	S_{He}		Wave-length λ vac	Wave-number (cm^{-1})	Classification
		2			73.81	267516	
		4		C	71.71	269027	
		3			69.64	270534	
	0	6			66.75	272665	
	0	3			64.35	274461	
	0	2			62.62	275771	IV $4s^24p^2P_{3/2}-4s^27s^2S_{\frac{1}{2}}$
		3			61.06	276962	
	0				60.86	277116	
		2			60.01	277770	
		2			59.23	278373	
	0	2			57.00	280112	IV $4s^24p^2P_{\frac{1}{2}}-4s^27s^2S_{\frac{1}{2}}$
		2			55.09	281619	
		1			53.72	282709	
		1			53.34	283014	
		2			50.95	284941	
		1			49.45	286164	
		1			49.01	286525	
		1			46.65	288475	
		2			345.73	289243	
		2			45.36	289553	
	00				38.60	295334	
	00				32.13	301087	

Table 2a. Supplementary list of Selenium lines

Intensity						Wave-length	Wave-number	Classification
M_{I_T}	E_DP	R	S_{HE}	E_DG	K	λ vac	(cm^{-1})	
				100		4980.90	20070	IV $6d\,^2D_{5/2}-6p\,^2P_{3/2}$
	10d					4721.34	21174.5	
	10d					15.15	21202.3	
	10					12.64	21213.6	
	50					10.73	21222.2	
	50					09.30	21228.6	
	50					08.00	21234.5	
	5d					05.54	21245.6	
	100					03.41	21255.2	
	15d					4699.40	21273.3	
	10d					96.72	21285.5	
	50					94.85	21294.0	
	100					93.04	21302.2	
	2d					90.34	21314.5	
	75					87.60	21326.9	
	10					81.41	21355.1	
	5d					80.01	21361.5	
	10d					76.38	21378.1	
	50					75.11	21383.9	
	10d					73.16	21392.8	
	30					67.51	21418.7	
	50					66.74	21422.2	
	25					61.64	21445.7	IV $6g\,^2G-8h\,^2H$
	50					54.67	21477.8	
	50					50.58	21496.7	
	100					43.26	21530.6	
	10					41.99	21536.5	
	20					40.92	21541.4	
	5					32.50	21580.6	
				10		4126.80	24225.0	
				5		4115.27	24292.9	
				10		4097.53	24398.0	
				100		4063.26	24603.8	
				150		4042.89	24727.8	
				5		4035.64	24772.2	
				15d		4035.24	24774.7	
				400d		4026.43	24828.6	
				600d		4026.07	24831.1	
				3		4001.64	24982.7	
				2		3965.71	25209.0	

Intensity						Wave-length	Wave-number	Classification
M_{I_T}	E_DP	R	S_{HE}	E_DG	K	λ vac	(cm^{-1})	
				6		3548.56	28172.4	
				6		3545.85	28193.9	
				30		3535.33	28277.8	
				0		3488.45	28657.8	
				0		3456.24	28924.8	
				0		3429.52	29150.3	
				5		3428.06	29162.6	
				10		3427.80	29164.8	
				10		3020.00	33102.9	
				120		2815.98	35501.2	
				500		2680.74	37292.0	
				5d		2648.95	37739.6	
				40		2640.92	27854.3	
				40		2640.28	37863.4	
				10		2630.61	38002.6	
						2617.24	38196.8	
				5		2598.12	38477.8	
				0		2582.25	38714.4	
				5		2566.20	38956.4	
				0		2563.84	38992.3	
				80d		2513.28	39776.6	
				5		2419.17	41323.9	
				5d		2418.88	41328.8	
				5		2416.23	41374.3	
				500		2413.21	41426.1	
				50		2412.71	41434.6	
				10		2136.63	46788.0	
				10		2111.16	47352.3	
				5d		2089.94	47833.2	
				0		2074.78	48182.6	
				5		2062.78	48462.8	

TABLE 3

TERMS OF THE SE III SPECTRUM

	Term		J	Level	Interval	n*
EVEN:						
	$4s^2 4p^2$	^3P	0	0.0		-
					1739	
			1	1739		1.9945
					2194	
			2	3933		2.003
		^1D	2	13031		2.0415
		^1S	0	26821		2.104
	4p5p	^1P	1	150760		3.154
		^3D	1	153210		3.194
					309.5	
			2	153519.5		3.199
					3171.5	
			3	156691.0		3.254
		^3P	0	154781		3.221
					1577	
			1	156358		3.247
					1514	
			2	157872		3.274
		^3S	1	159300.5		3.300
		^1D	2	161168		3.334

		Term	J	Level	Interval	n*
ODD:	$4s4p^3$	^5S	2	69136		2.337
		^3D	1	91088		2.493
					1634	
			2	92722		2.506
					3827	
			3	96549		2.537
		^3P	0	106475		2.536
					115	
			1	106590		2.624
					-74	
			2	106516		2.6235
		^1D	2	112565		2.681
	4p4d	^3F	2	124050		2.800
					1258	
			3	125308		2.814
					2100	
			4	127408		2.838
	4p5s	^3P	0	126275		2.825
					504	
			1	126779		2.831
					3609.6	
			2	130388.6		2.873
		^1P	1	131653.6		2.889

	Term	J	Level	Interval	n*
4p4d	^1P	1	136946		2.956
	^1D	2	139203		2.985
	^3D	1	140639		3.005
				-1228.5	
		2	139410.5		2.988
				2607.3	
		3	142013.8		3.025
4p4d	^3P	0	142316		3.0285
				443	
		1	142759		3.0345
				-52	
		2	142707		3.034
	^1F	3	148676.3		3.122
4p6s	^3P	0	187167.4		3.965
				257.6	
		1	187425.0		3.973
				4096.5	
		2	191521.5		4.110

	Term	J	Level	Interval	n*
4p5d	^3F	2	188427.2		4.004
				1219.3	
		3	189646.5		4.045
				1945.0	
		4	191591.5		4.112
	^3D	1	190840		4.086
				-821	
		2	190019.2		4.058
				3894	
		3	193915		4.196
4p6s	^1P	1	192159.7		4.131
4p5d	^1D	2	193303.5		4.174
	$^3P_0$	0	195094		4.241
				-143.3	
		1	194950.7		4.236
				-223	
		2	194727.7		4.227
	^1F	3	196844.2		4.311
4p7s	^3P	0	209235		4.922
				166	
		1	209391		4.932
				4237	
		2	213628		5.211
	^1P	1	214017		5.239

Se IV (^2P) limit 250,000 cm^{-1}

= 30.99 ev

TABLE 4

TERMS OF THE SE IV SPECTRUM

	Term		J	Level	Interval	n*
ODD:						
	$4s^24p$	^2P	½	0.0		
					4372.4	
			1½	4372.4		2.266
	$4s^25p$	^2P	½	189913		3.350
					1198	
			1½	191111		3.363
	$4s^26p$	^2P	½	256074		4.409
					701	
			1½	256775		4.427
	$4s^27p$	^2P	½	287785		5.475
					442	
			1½	288127		5.491
	$4s^2.4f$	^2F	2½	229714		3.880
					-30	
			3½	229684		3.879
	$4s^2.5f$	^2F	2½	272001		4.859
					-21	
			3½	271980		4.859

Term		J	Level	Interval	n*
$4s^2.6h$	^2H	4½, 5½	297542		5.996
$4s^2$ 7h	^2H	4½,5½	310515		6.997
$4s^2$ 8h	^2H	4½,5½	318915		6.997
$4p^3$	^4S	1½	202290		3.482

EVEN:

Term		J	Level	Interval	n*
$4s4p^2$	^4P	½	79393		2.5645
				1588	
		1½	80981		2.572
				2599	
		2½	83582		2.585
	^2D	1½	104211		2.693
				494	
		2½	104705		2.6955
	^2S	½	128787		2.8405
	^2P	½	136140		2.890
				2214	
		1½	138354		2.905
$4s^24d$	^2D	1½	153217		3.015
				389	
		2½	153606		3.018

	Term	J	Level	Interval	n*
$4s^25s$	^2S	½	157241		3.047
$4s^25d$	^2D	1½	237747		4.020
				152	
		2½	237899		4.023
$4s^26d$	^2D	1½	276696		5.020
				153	
		2½	276849		5.026
$4s^26s$	S	½	240751		4.077
$4s^27s$	^2S	½	280145		5.149
$4s^25g$	^2G	3½,4½	275854		4.993
$4s^26g$	^2G	3½,4½	297468		5.991
$4s^27g$	^2G	3½,4½	310489		6.996
$4s^28g$	^2G	3½,4½	318893		6.996
$4s^29g$	^2G	3½,4½	324662		8.992

Se V (^1S_o) Limit = 346,373 cm^{-1}

TABLE 5

TERMS OF THE SE V SPECTRUM

	Term		J	Level	Interval	n*
EVEN:						
	$4s^2$	^1S	0	0.0		
	$4p^2$	^3P	0	211780		2.844
					2306	
			1	214086		2.8535
					4532	
			2	218618		2.8735
	4s4d	^1D	2	213196		2.850
		^3D	1	257536		3.0575
					210	
			2	257746		3.0585
					319	
			3	258065		3.0605
	4s5d	^3D	1	380270		4.009
					91	
			2	380361		4.010
					135	
			3	380496		4.0115
	4s5s	^3S	1	287423		3.226
		^1S	0	297930		3.28

		Term	J	Level	Interval	n*
ODD:						
	4s4p	^3P	0	89761		2.439
					1590	
			1	91351		2.443
					3614	
			2	94965		2.453
		^1P	1	131732		2.558
	4s5p	^3P	0	326365		3.495
					553	
			1	326918		3.499
					912	
			2	327830		3.506
		^1P	1	328249		3.510
	4s4f	^3F	2	361336		3.803
					762	
			3	361998		3.811
					1558	
			4	363656		3.837
		^1F	3	366467		3.856

Se VI ($^2S_{\frac{1}{2}}$) limit = 550,976 cm^{-1}

CHAPTER IV

The Precise Determination of Spectral Wavelengths.

Interference Spectroscopy.

Two specialized types of spectroscopic problems call for instruments of very high resolving power. In the first, of which hyperfine and isotope structure studies are involved, it is desired to separate very close and narrow lines and in the second, it is desired to measure the spectral wavelengths as precisely as possible.

Five principal types of instruments are available to give resolving power larger than 200,000. These are the large diffraction grating, the Michelson echelon, the Lummer-Gehrcke plate, the wedge etalon(40a,b) and the Fabry-Perot etalon. The interferometer of Fabry and Perot is the most important, since it can be used for a) wavelength measurements of highest precision relative to one single standard line, b) resolution of narrow line structures and c) determination of true line width and intensity distribution in spectral lines. The interferometer consists of a plane parallel "air plate" formed by two plane surfaces of two glass or quartz plates which are kept at a constant distance by means of a spacer made of quartz or invar (64 per cent iron, 36 per cent nickel) since both have very small thermal expansion coefficients. The resolving power of this instrument can be varied over a wide range by proper choice of the gap between the plates and the reflecting power of the metal films. The two surfaces forming the "air plate" are coated with a thin but highly reflecting metal film, usually aluminum or silver. The metal film reflects 80% to 90% of the incident light and transmits 2% to 5%. An incident wave is multiply reflected between the interferometer plates and split into many waves which interfere at infinity, i.e. in the focal plane of a projecting lens. The patterns formed are interference fringes of equal inclination and consist of concentric sharp circles. The sharpness is due to the great number of interfering waves formed by successive splitting (division) of amplitude.

Fundamental Relations.

The path difference between consecutive waves is given by the fundamental relation

$$p\lambda = 2t\cos\theta \qquad (4.1)$$

where p is the order number, λ is the wavelength in air, t is the thickness of the plane parallel "air plate", and θ is the angle of incidence of the wave normal (ray). Constructive interference takes place if p is an integer. To each of the concentric circles belongs a certain angle θ and a certain order number p.

Introducing the radius R of an interference ring and the focal length F of a projecting lens we can replace $\cos\theta$ by a series expansion

$$\cos\theta = 1 - \frac{\theta^2}{2} + - - - - - = 1 - \frac{R^2}{2F^2} + - - - -$$

We can neglect higher terms since $R \ll F$. Thus we obtain

$$p\lambda = 2t\ (1 - \frac{R^2}{2F^2})$$

or using the diameter D of the interference rings equation (4.1) can be written as

$$p\lambda = 2t\ (1 - \frac{D^2}{8F^2}) \ . \qquad (4.2)$$

From figure we can see that

$$\cos\Theta i = \frac{F}{(F^2 + Ri^2)^{\frac{1}{2}}} \qquad (4.3)$$

$$\approx (1 - \frac{Ri^2}{2F^2})$$

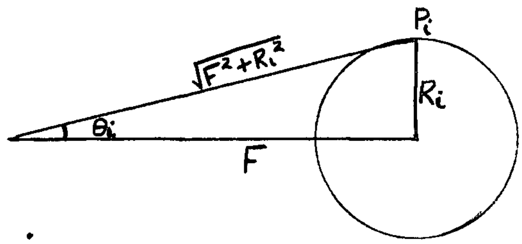

$$\approx (1 - \frac{Di^2}{8F^2}) \ .$$

But $$p = (\frac{2t}{\lambda})\cos\Theta = (\frac{2t}{\lambda})(1 - \frac{R^2}{2F^2})$$

$$= (\frac{2t}{\lambda})(1 - \frac{D^2}{8F^2}) \qquad (4.4)$$

or in terms of wave numbers ν as

$$p = 2t\nu\cos\Theta = 2t\nu\ (1 - \frac{D^2}{8F^2}) \qquad (4.5)$$

Differentiating equation (4.4) we get

$$dp = -(\frac{2t}{\lambda})\sin\Theta d\Theta = -(\frac{2t}{\lambda})(\frac{R}{F^2})dR \qquad (4.6)$$

It can be seen from (4.6) that the order of the fringes decreases with increasing angle of incidence θ or increasing radius R . For dp = -1 we get

$$R = \frac{\lambda F^2}{2tR} \tag{4.7}$$

which means that for larger radii, consecutive circles are closer together.

Let R_o be the radius of the innermost ring, R_1 that of the next ring and so on. Then R_k will be the radius of the $(k+1)^{th}$ ring. We can write

$$P_o = \frac{2t}{\lambda} - \frac{R_o^2 t}{\lambda F^2} \tag{4.8}$$

$$P_i = P_o - i = \frac{2t}{\lambda} - \frac{R_i^2 t}{\lambda F^2} \tag{4.9}$$

$$P_k = P_o - k = \frac{2t}{\lambda} - \frac{R_k^2 t}{\lambda F^2} \tag{4.10}$$

Subtracting (4.10) from (4.9) we get

$$(P_i - P_k) = (k - i) = \frac{(R_k^2 - R_i^2)t}{\lambda F^2} \tag{4.11}$$

or

$$\frac{(R_k^2 - R_i^2)}{(k-i)} - \frac{\lambda F^2}{t} = \Delta R^2 \tag{4.12}$$

Using D

$$\frac{(D_k^2 - D_i^2)}{(k-i)} - \frac{4\lambda F^2}{t} = \Delta D^2 \tag{4.13}$$

Order Number of the Center of the Ring System.

At the center

$$P = \frac{2t}{\lambda} \tag{4.14}$$

where P is the non-integral order.

P can be expressed by the integral order of the first bright fringe P_o and a positive fractional part, ϵ, or by the order of the $(k+1)^{th}$ fringe as

$$P = P_k + k + \epsilon \quad .$$

Using equations (4.4) and (4.14) we have

$$= P - P_k - k = (\frac{t}{\lambda F^2})R_k^{\ 2} - k \tag{4.15}$$

Using equation (4.13)

$$\epsilon = \frac{R_k^{\ 2}}{\frac{(R_k^{\ 2}-R_i^{\ 2})}{(k-i)}} - k \quad .$$

$$= \frac{Ri^2}{\frac{(R_k^{\ 2}-R_i^{\ 2})}{(k-i)}} - i$$

$$= \frac{Di^2}{\frac{(D_k^{\ 2}-D_i^{\ 2})}{(k-i)}} - i$$

$$= \frac{R_i^{\ 2}}{\Delta R^2} - i = \frac{D_i^{\ 2}}{\Delta D^2} - i \tag{4.16}$$

Since for the innermost circle i = o, we have

$$\epsilon = \frac{Ro^2}{\Delta R^2} = \frac{Do^2}{\Delta D^2} \quad . \tag{4.17}$$

Crossing the Interferometer with a Spectrograph.

Two different methods are usually used.

a) External mounting.

The interferometer is set up in front of the slit of the spectrograph in such a way that the interference fringes are projected on the slit by means of an achromatic lens. The light source is focused on the interferometer. This gives a symmetric intensity distribution in the interference fringes. The interferometer is oriented so that the center of the circular fringes coincides with the center of the rather wide slit. The different spectral lines seen in the spectrograph are traversed by fringes symmetrically arranged with respect to the center of the slit.

b) Internal mounting.

Here the interferometer is placed between the collimator lens and the dispersing system.

Adjustment of the Interferometer.

When one looks normally through the etalon at a monochromatic source, say a cool AH-1 mercury lamp, the fringe system will be seen. With the etalon fixed, move the eye across the field of view along a diameter with a spring clip at one end. Theory shows that the fringe of highest order occurs at the center of the pattern. Therefore as the eye is moved so that the line of sight travels along a diameter, widening the fringes (i.e. a new fringe appears in the center of the pattern) means that in this direction the separator spacing must be reduced. Conversely if the fringes collapse the eye is looking through a part of the etalon with a reduced separator thickness. By adjusting the pressure of the spring clips make the separator spacing so equal that the ring diameters stay constant as the eye is moved over the surface of the etalon. Now the etalon is adjusted to be crossed with the spectrograph.

Resolving Power of the Fabry-Perot Interferometer.

By definition the resolving power of a spectrograph is given by the expression

$$R = \frac{\lambda}{\Delta\lambda}$$

where $\Delta\lambda$ is the wavelength difference of two spectral lines which can be seen just separated by the instrument.

$$p\lambda = 2t$$

On differentiation we get

$$p\Delta\lambda + \lambda\Delta p = o\ .$$

Resolving power $$R = \frac{\lambda}{\Delta\lambda} = \frac{p}{\Delta p}\ .$$

This means measuring the shift of one line in terms of the order number of the other line, we have a shift of at least $\Delta p = \frac{p}{R}$ to obtain the limit of resolution.

The resolving power depends on the reflectivity r of the metallic film and the order of interference p .

It is given by the approximate expression (32)

$$R = \frac{3p\sqrt{r}}{1-r} .$$

Intensity Distribution in the Interference Patterns.

In the case of the interferometer which can be compared to a grating consisting of a great number of slits, the striking difference is that the intensities of two consecutive beams are not equal but decrease systematically with the number of reflections.

The following expressions are derived by Meissner (32)

$$I_{max} = \frac{s^2}{(1-r)^2}$$

$$I_{min} = \frac{s^2}{(1+r)^2}$$

where the intensity coefficients s and r are called transmission and reflection powers.

The change in wavelength necessary to shift the ring system by the distance of consecutive orders is called "spectral range" $\langle\Delta\lambda\rangle$

$$p\lambda = 2t$$

$$\nu = \frac{p}{2t} .$$

The change in ν corresponding to a change of one integer in p is

$$\nu_2 - \nu_1 = \frac{p_2}{2t} - \frac{p_1}{2t} = \frac{1}{2t}$$

$$\langle \Delta\nu \rangle = \frac{1}{2t} \text{ cm}^{-1} .$$

Correction for Phase Change at Reflection.

It can be seen that if we determine any wavelength λ with respect to a standard line, using different etalon gaps, λ varies systematically with increasing thickness t. This is so because in deriving the fundamental relation $P = \frac{2t}{\lambda}$, we did not take into account the phase change which waves suffer when reflected at the surface of the metal film of the interferometer plates. If this phase shift is constant for all wavelengths there will be no correction, since the standard line will also be shifted by the same amount. Unfortunately it can be shown that the phase shift is a function of λ. Meissner (32) gives a good account of the derivations and using 2 different spacer gaps t_1 and t_2 he gives the wavelength corrections for the same λ as

$$\Delta\lambda_1 = (\lambda_2 - \lambda_1) \frac{t_2}{t_2 - t_1}$$

$$\Delta\lambda_2 = (\lambda_2 - \lambda_1) \frac{t_1}{t_2 - t_1}$$

where λ_1 and λ_2 are the values obtained for the same λ using t_1 and t_2 respectively. The corrections $\Delta\lambda_1$ and $\Delta\lambda_2$ should be added to the uncorrected wavelengths λ_1 and λ_2. It is possible to explain this phenomenon "dispersion of phase change" by the application of electromagnetic theory of metals as was shown by Juergen Bauer (18). It can be seen that the correction for phase change is only necessary if measurements of wavelengths at a larger distance from the standard line have to be made.

Correction for the Dispersion of Air.

The standard wavelengths are by definition referred to "standard air", viz. dry air containing 0.03 per cent by volume of CO_2 at a pressure of 760 mm Hg at 0°C and a temperature of 15°C. Meggers & Peters give the following correction to be added (28)

$$\Delta = \lambda \ (n_o - n_o') \frac{(\rho - \rho_o)}{\rho_o}$$

where λ is the wavelength of the unknown line, n_o is the index of refraction for this wavelength, n_o' that of the primary standard, both at normal conditions, ρ the density of the air for the conditions (t°C, hcm Hg) at which the measurements are made, and ρ_o the density for standard condition (15°C, 76 cm Hg).

However, Edlén (10) points out that the above formula is no longer sufficiently accurate for precision spectroscopists and he has derived the following dispersion formula,

$$\lambda_2^o - \lambda_2 = (\Delta\lambda_2 - \Delta\lambda_1 \frac{\lambda_2}{\lambda_1}) (\frac{0.0013882p}{1+0.00367t} - 1)$$

where λ_2^o is the unknown wavelength at standard conditions, λ_2 the same as actually measured, λ_1 is the reference wavelength, $\Delta\lambda_2$ and $\Delta\lambda_1$ are the vacuum corrections for λ_2 and λ_1 p and t actual pressure and temperature.

Calculation of the Fractional Part ϵ.

From equation (4.17)

$$\epsilon = \frac{D_o^2}{\Delta D^2} .$$

If only two fringes are available there is only one method possible. Let the diameter of the first ring be D_o, that of the second D_1. In this case

$$D_1^2 - D_o^2 = \Delta D^2$$

$$\epsilon = \frac{D_o^2}{\Delta D^2} .$$

However, in high precision work a better method is highly preferable. Roeser gives a convenient method using the method of least squares.

From equation (4.13)

$$D_k^2 = D_o^2 + k\Delta D^2 \qquad (4.18)$$

Let $D_k = Y$, $D_o^2 = A$, $k = X$ and $\Delta D^2 = B$.

Then (4.18) becomes

$$Y = A + BX \ . \qquad (4.19)$$

Referring to Roeser's paper (43) it is seen

$$B = 6\,\frac{(n-1)(y_n - y_1) + (n-3)(y_{n-1} - y_2) + \ . \ . \ .}{n(n^2 + 1)}$$

$$= \frac{\sum}{\frac{n}{6}(n^2-1)}$$

and

$$A = Y_m - BX_m \ .$$

n being the number of observations, in our case $n = k - 1$.

$$X_m = \text{Average of } X\ (k)$$

$$Y_m = \text{Average of } Y\ (D_k^2)$$

In the present case the method used can be illustrated by an example for the neon line $\lambda = 5852.4878$ Å .

Fringe No.	D^2
7	95.199
6	83.302
5	71.334
4	59.582
3	47.582
2	35.545
1	23.590
0	11.539

$$Y_m = \frac{\Sigma D^2}{8} = 53.459 \text{ (center of gravity)}$$

$$D_o^2 = \text{center of gravity} - \Delta D^2 \times \frac{7}{2}$$

$$= 53.459 - 11.947 \times 3.5 = 11.645.$$

To calculate ΔD^2, the difference between the squares $D_7^2 - D_o^2 = 7\,\Delta D^2$, $D_6^2 - D_1^2 = 5\,\Delta D^2$, $D_5^2 - D_2^2 = 3\,\Delta D^2$, $D_4^2 - D_3^2 = \Delta D^2$ are taken. These differences are multiplied by 7, 5, 3 and 1 and the final average value of ΔD^2 is calculated as below:

		D^2
83.660 x 7 =	585.620	(49)
59.712 x 5 =	298.560	(25)
35.789 x 3 =	107.367	(9)
12.000 x 1 =	12.000	(1)
	1003.547 ÷ 84	

$$\Delta D^2 = 11.947 .$$

$$\epsilon = \frac{D_o^{\,2}}{\Delta D^2}$$

$$= \frac{11.645}{11.947}$$

$$= 0.975 .$$

Accurate Wavelength Measurement.

1) Calculation of 2t using Standard Line (λ).

Approximate value of 2t = 2t'.

$$p\lambda = 2t'$$

$$p = \frac{2t'}{\lambda} .$$

Calculate ϵ for standard line (λ).

$$2t = (p + \epsilon)\lambda .$$

2) To find other Wavelengths when 2t is known.

Step I.

Calculate integral order p

$$p = \frac{2t}{\lambda'}$$

where λ' is the approximate value from literature.

Step II.

Calculate wavelength from

$$\lambda = \frac{2t}{p+\epsilon}$$

where ϵ is calculated for the line (λ').

Sample Calculation.

Approximate value of 2t, $2t' = 1.577887$

Standard line $\lambda_1 = 5400.5617$ Å.
(Neon)

$$p = \frac{1.577887}{5400.5617} = 29217.091$$

ϵ for $\lambda_1 = 0.065$ where P_o is the integral order number.

$$2t = (p_o+\epsilon)\lambda_1 = (29217.065)5400.5617 = \underline{1.577885}$$

$$\lambda' = 5748.29$$

$$\epsilon \text{ for } \lambda' = 0.605$$

Integral order $p = \dfrac{1.577885}{5748.29}$

$$= 27449.641$$

$$\lambda = \frac{1.577885}{27449.605} = \underline{5748.297 \text{ Å}} .$$

To Check the Order Number.

To make sure that the order number we calculated for λ' (standard line) 5400.5617 is the correct one we adopt the following method.

Choose three lines including λ_1

$$\lambda_1 = 5400.5617$$
$$\lambda_2 = 5748.2985$$
$$\lambda_3 = 5764.4180 .$$

According to the fundamental relations

$$(p_1+\epsilon_1)\lambda_1 = (p_2+\epsilon_2)\lambda_2 = (p_3+\epsilon_3)\lambda_3 .$$

Integral order $p_1 = 29217$.

Calculate ϵ_1, ϵ_2 and ϵ_3

$$\epsilon_1 = 0.065$$
$$\epsilon_2 = 0.605$$
$$\epsilon_3 = 0.856$$

$$p_2+\epsilon_2 = (p_1+\epsilon_1)\frac{\lambda_1}{\lambda_2} . \qquad \frac{\lambda_1}{\lambda_2} = 0.93950613$$

$$p_3+\epsilon_3 = (p+\epsilon_1)\frac{\lambda_1}{\lambda_3} . \qquad \frac{\lambda_1}{\lambda_3} = 0.93687891$$

$p_1+\epsilon_1$	$p_2+\epsilon_2$	$p_3+\epsilon_3$
29215.065	27447.733	27370.978
29216.065	27448.672	27371.918
29217.065	27449.611	27372.852
29218.065	27450.551	27373.788
29219.065	27451.490	27374.725

Checking with the calculated values of ϵ_2 and ϵ_3 it is seen that 29217 is the correct order number p_1.

Error Calculation for λ.

Derivation of the Formula used.

$$\epsilon = \frac{D_o^2}{\Delta D^2} = \frac{A}{B}$$

$$\log \epsilon = \log A - \log B$$

$$\left(\frac{d\epsilon}{\epsilon}\right)_{max} = \frac{dA}{A} + \frac{dB}{B}$$

$$d\epsilon = \epsilon \left[\frac{dA}{A} + \frac{dB}{B}\right] \qquad \text{(A)}$$

$$P_x\lambda_x = P_s\lambda_s$$

where the subscript x stands for the unknown line and s stands for the standard line.

$$\lambda_x = \frac{P_s\lambda_s}{P_x}$$

$$\frac{d\lambda_x}{\lambda_x} = \frac{d\epsilon_s}{(P+\epsilon)_s} + \frac{d\lambda_s}{\lambda_s} + \frac{d\epsilon_x}{(P+\epsilon)_x} \quad .$$

Since $\frac{d\lambda_s}{\lambda_s}$ is negligibly small we can write

$$d\lambda_x = \lambda_x \quad \frac{d\epsilon_s}{(P+\epsilon)_s} \quad \frac{d\epsilon_x}{(P+\epsilon)_x} \quad . \qquad \text{(B)}$$

Sample Calculation.

$$\lambda_s = 7601.5444\ \text{Å}$$

$$A = 8.773 \qquad dA = 0.003$$

$$B = 3.969 \qquad dB = 0.014$$

$$\epsilon_s = .452$$

$$d\epsilon_s = 0.452 \left[\frac{0.003}{8.773} + \frac{0.014}{3.969}\right]$$

$$= 0.002$$

$$\lambda_x = 7664.891$$

$$A = 8.837 \qquad dA = .003$$

$$B = 7.963 \qquad dB = .037$$

$$\epsilon_x = 0.901$$

$$d\epsilon_x = 0.901 \left[\frac{0.003}{8.837} + \frac{0.037}{7.963}\right]$$

$$= 0.005$$

$$d\lambda_x = 7664.891 \ \frac{0.002}{20757.452} - \frac{0.005}{20585.901}$$

$$= \pm\, 0.003\ \text{Å}\ .$$

Interferometric Wavelength Measurements in the Arc Spectrum of Potassium (KI).

Using the above method wavelengths have been measured for 38 lines in the arc spectrum of potassium. The purpose of this investigation was to measure interferometrically as many lines as possible and to check the interferometric wavelength measurements of the diffuse series satellites made by Masaki and Kobayakawa (25).

Experimental Details.

Light Source.

An electrodeless discharge tube containing potassium and argon as a carrier gas at a pressure of 0.8 mm of Hg was used. This source was excited by means of a "Raytheon Microtherm" microwave generator operating at a frequency of 2450 megacycles per second.

Spectrographic Equipment.

A big glass prism spectrograph and a Hilger large glass spectrograph were used in this investigation. 2 different spacers were used ($2t \approx 20$ mm; ≈ 12 mm). The green line of Hg^{198} from a water-cooled Meggers tube was used as the standard line. The wavelength of this line is $\lambda_{air} = 5460.7529$ Å.

Spectrogram.

All spectrograms were taken on Eastman spectroscopic plates. Exposure time varied from two minutes to six hours. The exposure time for the standard line was four minutes. All spectrograms were measured on a Zeiss-Abbe comparator. The wavelengths were reduced to standard conditions. Corrections for temperature and pressure are made by means of Edlén's formula. Corrections for phase change were not made since they were estimated to be smaller than the random errors of the measurements. Wavelengths determined are mean values from two or more spectrograms except for the 1st nine lines which were based on only one spectrogram. The error limits are estimated to be 0.003 Å at 6000 Å and 0.002 Å at 4000 Å. In the region above 9500 Å sensitized I - Z(2) plates were used.

Results.

Wavelength Tables.

Table 6.

At present the most accurate and extensive measurements of potassium wavelengths seem to be those of Risberg (41). Most of the wavelengths measured are in excellent agreement with Risberg's values. Table 7 contains a comparison of the present measurements of the diffuse series satellites, with the values of Masaki and Kobayakawa (25). The only possible explanation for the disagreement could be that Masaki and Kobayakawa might have made an error in determining the integral order number (see page 156 for the method).

Table 6 WAVELENGTHS MEASURED IN POTASSIUM.

References to some previous measurements.

D = Datta (8)
E = Edlén (9)
HBB = Hetzler, Borman and Burns (15)
M(1) = Meggers (26)
M(2) = Meggers (27)
R = Risberg (41)
W = Wagman (49)
MK = Masaki and Kobayakawa (25)

Intensity	λ_{air}, Å	Previous Measurements	cm^{-1}	Classification
9	11772.83	2.83R; 3.05M(1); 2.66M(2)	8491.81	$4P_{3/2} - 3D_{5/2}$
8	11769.64	9.62R; 9.41M(1)	8494.12	$4P_{3/2} - 3D_{3/2}$
9	11690.21	0.21R; 0.17M(1); 89.76M(2)	8551.82	$4P_{1/2} - 3D_{3/2}$
8	11022.66	2.67R; 2.3M(1)	9069.73	$3D_{3/2} - 5F_{5/2}$
9	11019.86	9.87R;	9072.04	$3D_{5/2} - 5F_{7/2}$
7	9597.829	7.829R; 7.1M(1) 7.76E	10416.17	$3D_{3/2} - 6F_{5/2}$
8	9595.703	5.704R; 5.60E	10418.47	$3D_{5/2} - 6F_{7/2}$
10	6938.764	8.767R; 9.50D; 8.76E; 8.774HBB	14407.81	$4P_{3/2} - 6S_{1/2}$
9	6911.081	1.084R; 1.80D; 1.08E; 1.087HBB	14465.53	$4P_{1/2} - 6S_{1/2}$
8	5831.886	1.887R; 2.31D; 1.89E	17142.36	$4P_{3/2} - 5D_{5/2}$
6	5831.718	1.593MK	17142.85	$4P_{3/2} - 5D_{3/2}$
7	5812.149	2.148R; 2.71D; 2.15E	17200.57	$4P_{1/2} - 5D_{3/2}$
8	5801.753	1.752R; 2.16D; 1.74E	17231.39	$4P_{3/2} - 7S_{1/2}$
8	5782.387	2.384R; 2.77D; 9.66E	17289.10	$4P_{1/2} - 7S_{1/2}$

Table 6 (Continued)

7	5359.576	9.574R; 9.521D; 9.66E	18653.01	$4P_{3/2} - 6D_{5/2}$
5	5359.498	9.583MK	18653.28	$4P_{3/2} - 6D_{3/2}$
6	5342.970	2.970R; 2.974D; 3.07E	18710.98	$4P_{1/2} - 6D_{3/2}$
7	5339.688	9.688R; 9.670D; 9.79E	18722.48	$4P_{3/2} - 8S_{1/2}$
6	5323.278	3.276R; 3.228D; 3.38E	18780.19	$4P_{1/2} - 8S_{1/2}$
6	5112.256	2.249R; 2.204D	19555.39	$4P_{3/2} - 7D_{5/2}$
4	5112.217	2.129MK	19555.54	$4P_{3/2} - 7D_{3/2}$
6	5099.201	9.200R; 9.180D	19605.45	$4P_{3/2} - 9S_{1/2}$
5	5097.173	7.171R; 7.144D	19613.25	$4P_{1/2} - 7D_{3/2}$
5	5084.236	4.226R; 4.212D	19663.16	$4P_{1/2} - 9S_{1/2}$
5	4965.034	5.031R; 5.038D	20135.23	$4P_{3/2} - 8D_{5/2}$
3	4965.011	4.919MK	20135.36	$4P_{3/2} - 8D_{3/2}$
4	4956.148	6.146R; 6.043D	20171.33	$4P_{3/2} - 10S_{1/2}$
4	4950.823	0.815R; 0.816D	20193.03	$4P_{1/2} - 8D_{3/2}$
4	4942.011	2.015R; 1.964D	20229.03	$4P_{1/2} - 10S_{1/2}$
5	4869.766	9.757R; 9.70D	20529.13	$4P_{3/2} - 9D_{5/2}$
4	4863.482	3.483R; 3.61D	20555.66	$4P_{3/2} - 11S_{1/2}$
4	4856.098	6.090R; 6.03D	20586.92	$4P_{1/2} - 9D_{3/2}$

Table 6 (Continued)

3	4849.868	9.865R; 9.88D	20614.21	$4P_{1/2} - 11S_{1/2}$
4	4804.349	4.348R; 5.19D	20808.66	$4P_{3/2} - 10D_{5/2}$
5	4642.370	2.373R; 2.172D	21534.69	$4S_{1/2} - 3D_{5/2}$
6	4641.872	1.876R; 1.585D	21537.00	$4S_{1/2} - 3D_{3/2}$
8	4047.210	7.206R; 7.201D; 7.214W	24701.40	$4S_{1/2} - 5P_{1/2}$
9	4044.139	4.136R; 4.140D; 4.145W	24720.16	$4S_{1/2} - 5P_{3/2}$

Table 7 WAVELENGTHS OF THE FOUR SATELLITES MEASURED IN DIFFUSE SERIES

λ_{air}, Å	λ_{air}, Å (MK)	λ_{air} Å (C)	Classification
5831.718	5831.593	5831.715	$4P_{3/4} - 5D_{3/2}$
5359.498	5359.583	5359.499	$4P_{3/2} - 6D_{3/2}$
5112.217	5112.129	5112.208	$4P_{3/2} - 7D_{3/2}$
4965.011	4964.919	4965.006	$4P_{3/2} - 8D_{3/2}$

Wavelengths in column 2 (MK) are due to Masaki and Kobayakawa.

Wavelengths in column 3 (C) are calculated using the splittings observed by Masaki and Kobayakawa.

TRACES OF THE SPARK SPECTRA OF SELENIUM FOR λ 1100 Å

The following figures are photoelectric traces made with a Jarrell-Ash console comparator microphotometer.

The source is an electrodeless spark discharge (see Chapter II).

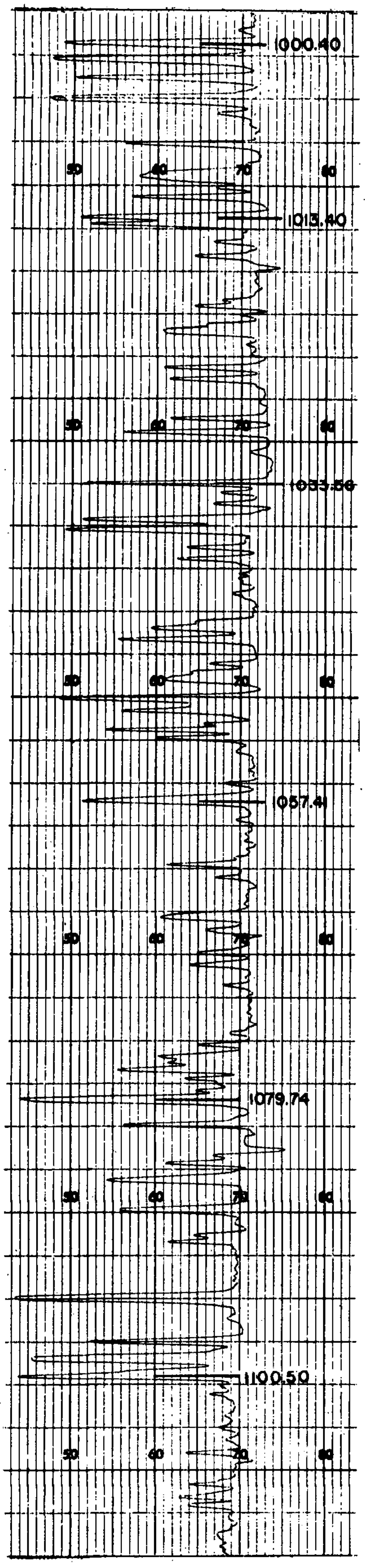
1000.40
1013.40
1033.86
1057.41
1079.74
1100.50
50
60
70
80

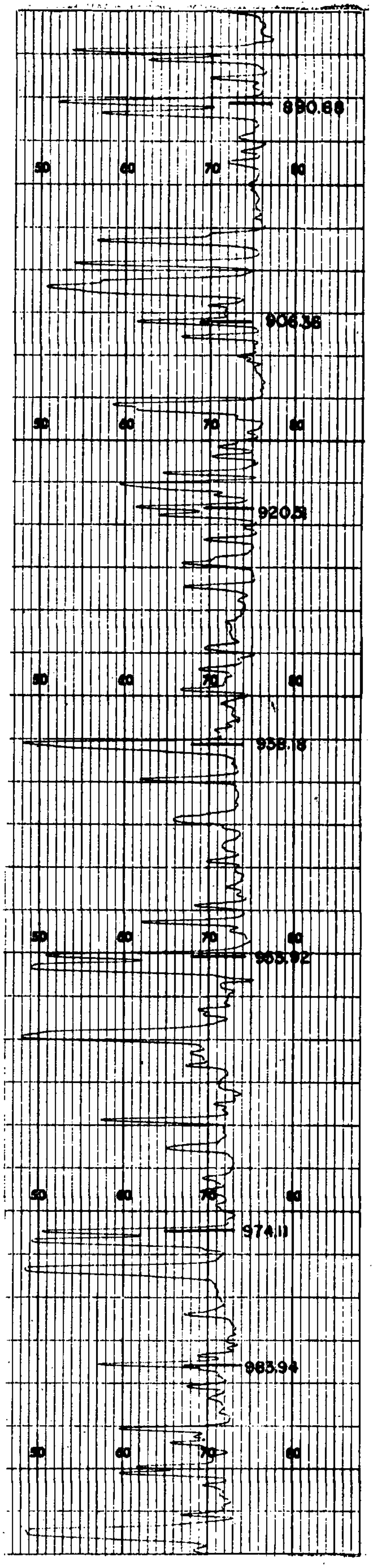
890.68
906.38
920.51
938.18
955.92
974.11
983.94
50
60
70
80

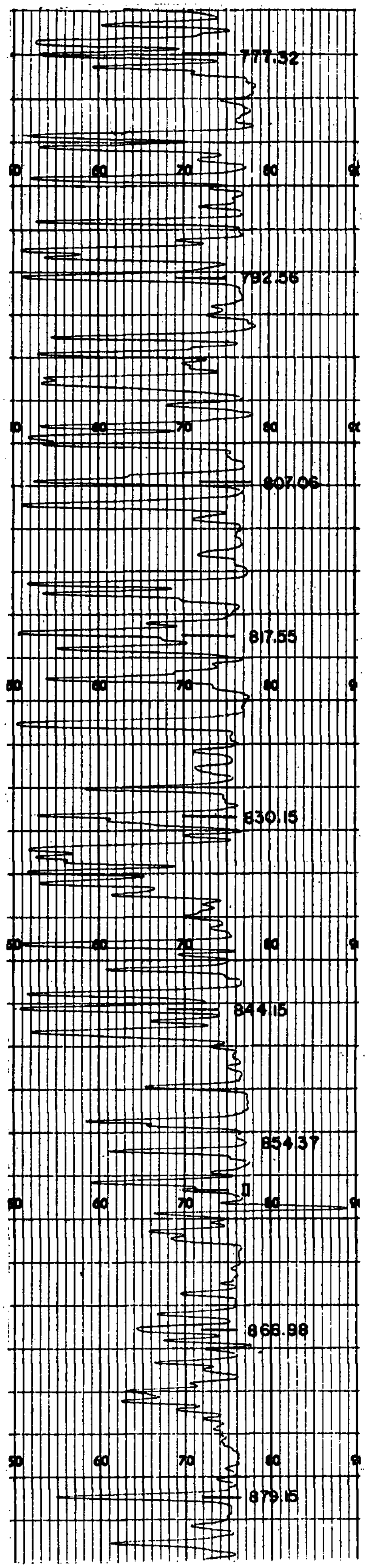
777.32
792.56
807.06
817.55
830.15
844.15
854.37
866.98
879.15
50
60
70
80
90

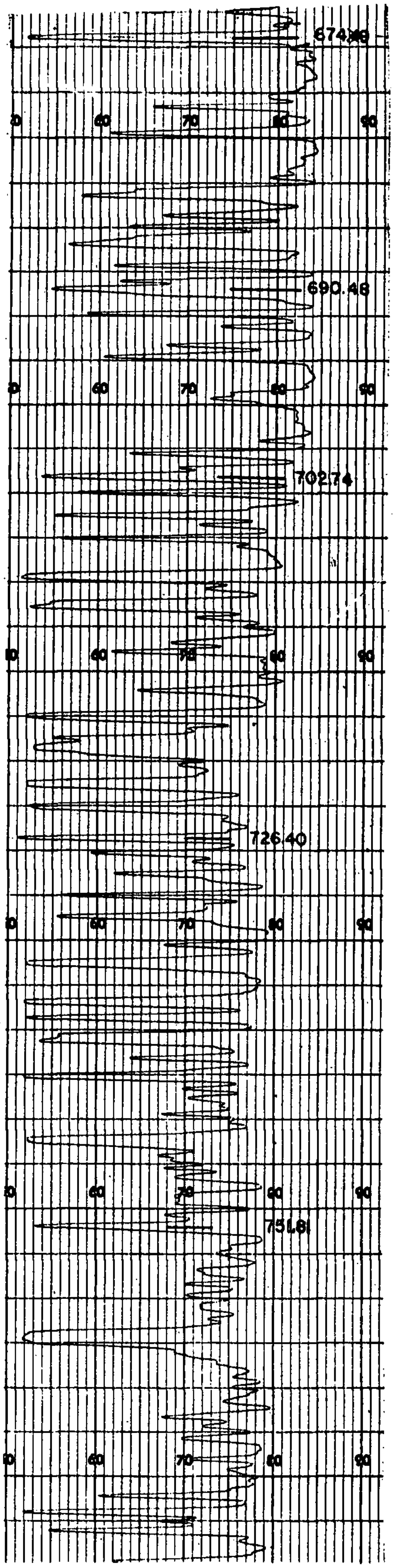
690.48
702.74
726.40
751.81
60
70
80
90

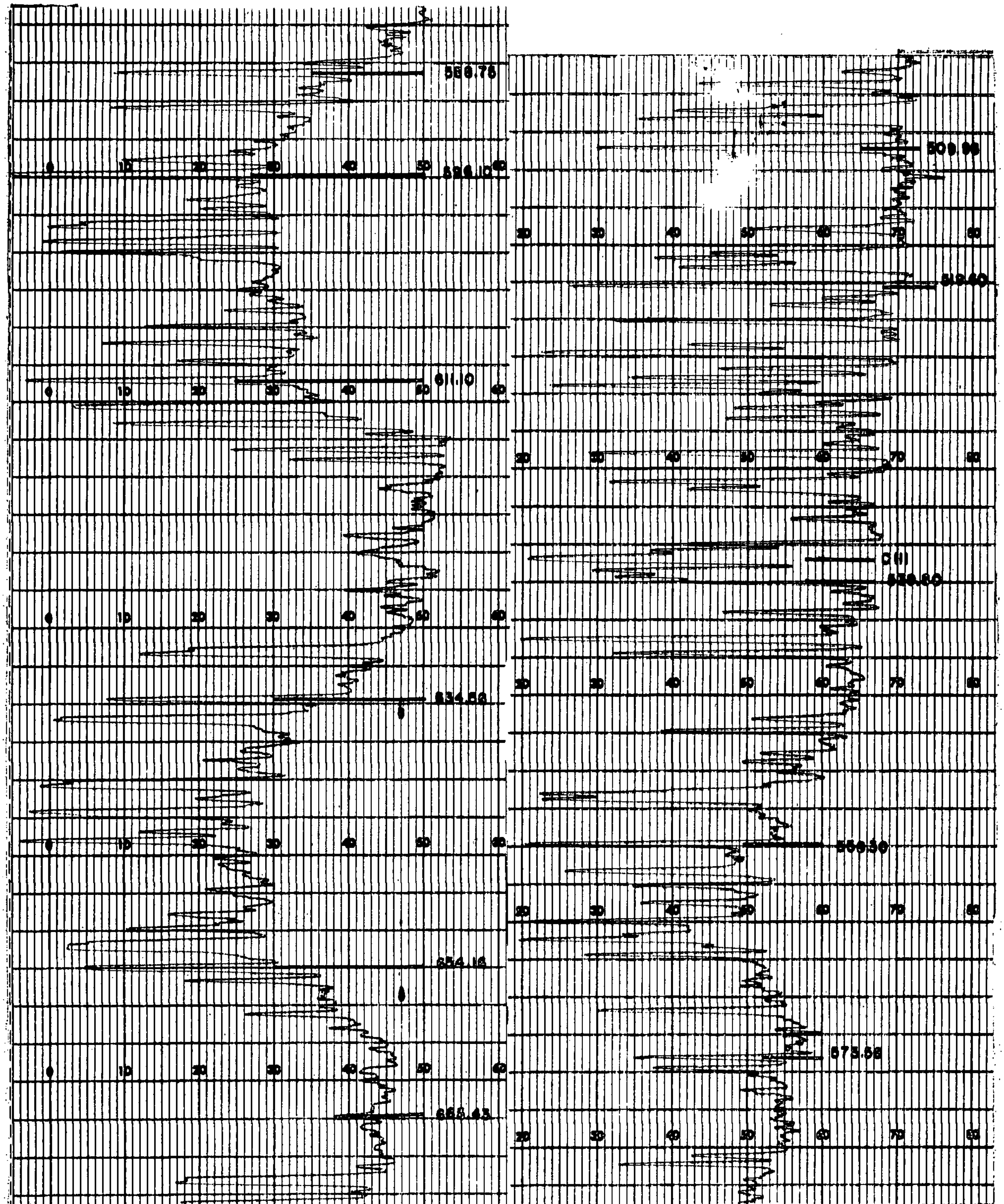

611.10
634.56
654.16
665.43
674.49
509.98
519.40
CHI
536.60
566.30
573.56

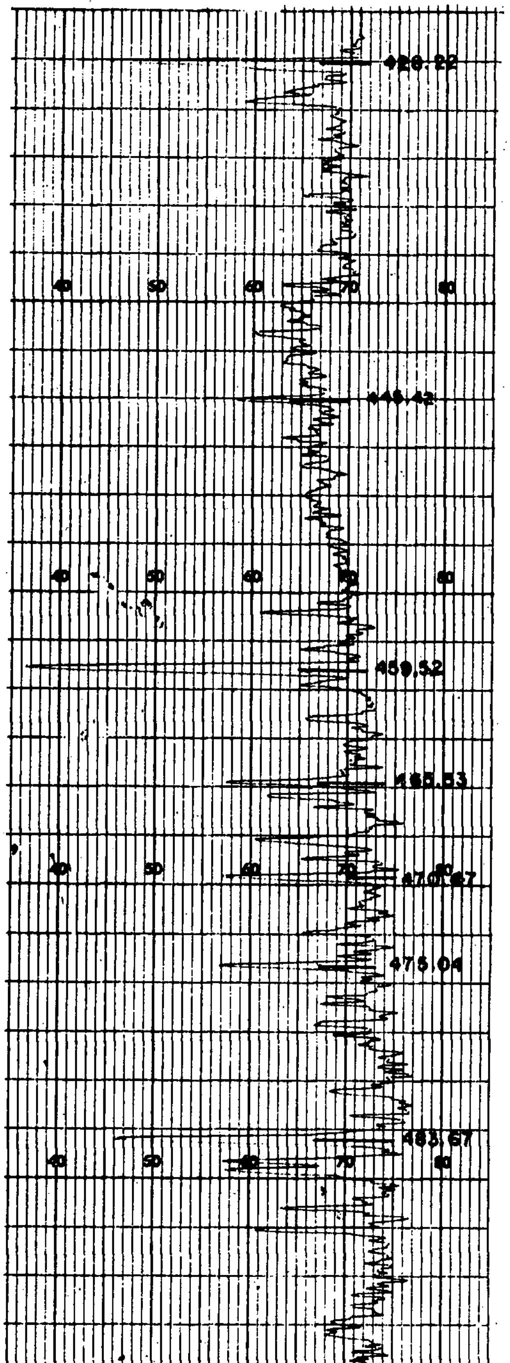
445.42
459.52
465.53
475.04
483.67
496.52

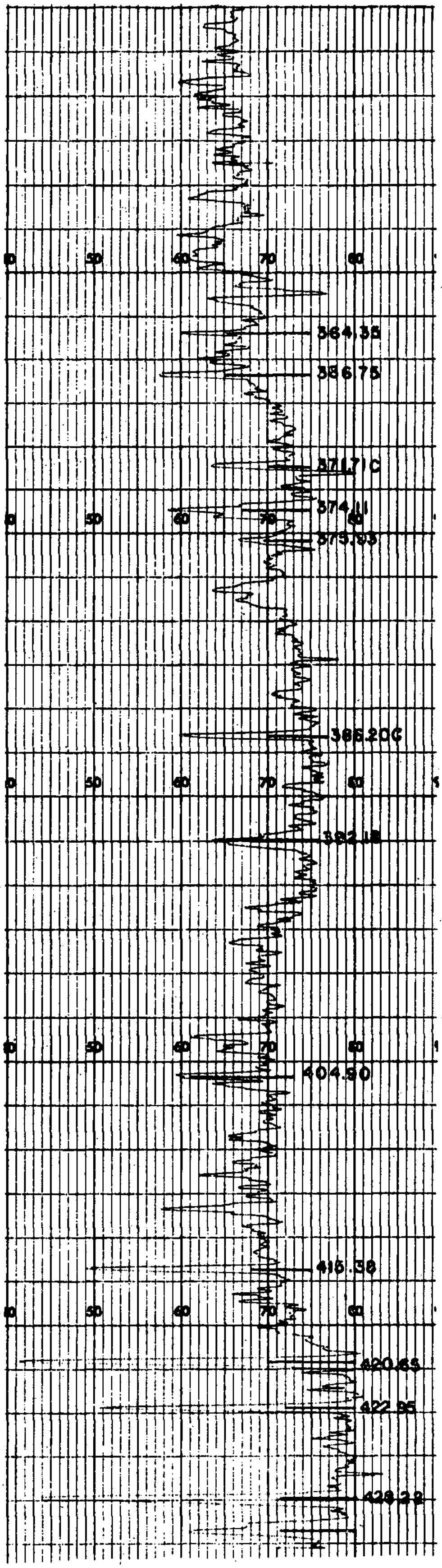
364.35
404.90
415.38
422.95

Summary

We may summarize in a few sentences the main results attained and the conclusions reached in the course of this research. We have confirmed, with the aid of Fabry Perot patterns, that the electrodeless spark discharge is an ideal source for the production of sharp and intense lines at quite high excitation. We have outlined detailed steps for the "method of set-backs", used in the identification of the spectral lines in the vacuum grating region.

We have introduced our observations to make a complete revision of the square arrays of Se II, Se III, Se IV, Se V and Se VI and have revised most of the term values and extended the previous analyses in Se III, Se IV and Se V. The main features of the analysis are the establishment of the deepest excited terms $4s4p^3\ {}^5S_2^\circ$ in Se III and $4s4p^2\ {}^4P$ in Se IV. In addition we have also established some of the basic terms in Se III, Se IV and Se V.

Intermediate coupling theory has been compared with observed levels wherever possible. In most cases the agreement is good. We have noticed that the study of the spark spectra of bromine is far from complete and experimental investigations in these are desirable. The number of unclassified lines is quite large, and we estimate that it involves about 40% of the total light output. Thirty eight lines in the arc spectrum of potassium have been measured interferometrically.

APPENDIX

Grating Ghosts.

Both the 21 foot concave grating and the 2 meter vacuum grating displayed Rowland ghosts. This has been a valuable help in identifying the order of lines from the grating since the ghost spacing at various $n\lambda$ is a function of the order. Rowland ghosts have an intensity $I(n)$ in the n^{th} order $I(n) = I(1)n^2$, where the intensity in the first order $I(1)$ may be approximately 0.2% of the parent line intensity and are positioned according to the equation

$$\Delta(n\lambda) = \frac{m\lambda}{p}$$

where $m = \pm 1, \pm 2$, etc. is the ghost order,

and p = number of rulings involved in the periodic error;

in the 2 m (Bausch and Lomb) grating this $p = 720$

in the 21 foot (Johns Hopkins) grating this $p = 750$.

Since $\Delta\lambda = \vartheta \Delta s$, this gives for the separation of the first order ghost

$$\Delta s = \frac{\lambda}{\vartheta p} .$$

We can, therefore, use the dispersion tables to calculate Δs. For example, using $\lambda = 2040$ Å $\vartheta = 4.339$ Å/mm.

$$\Delta s = \frac{2040}{4.339 \times 720} \text{ mm.} = 0.653 \text{ mm.}$$

Paschen (34) has summarized the properties of Rowland ghosts.

BIBLIOGRAPHY

1. Andrew, K.L., and Meissner, K.W. J.O.S.A. 47, 850, 1957.
2. Bacher, R.F. Phys. Rev. 43, 264, 1933.
3. Bacher, R.F., and Goudsmit, S. Phys. Rev. 46, 948, 1934.
4. Badami, J.S., and Rao, K.R. Proc. Roy. Soc. London (A) 140, 387, 1933.

5a. Bartelt, O. Naturwiss 22, 291, 1934.

b. " " Zeit. Phys. 91, 444, 1934.

6. Bedford, R.E. Ph.D. Thesis, University of British Columbia, 1955.
7. Condon, E.U., and Shortley, G.H. "Theory of Atomic Spectra", Cambridge University Press, 1935.
8. Datta, S. Proc. Roy. Soc. London (A) 99, 69, 1921.
9. Edlen, B. Zeit. Phys. 98, 445, 1936.
10. Edlen, B. J.O.S.A. 43, 339, 1953.

11a. Edlen, B., and Risberg, P. Arkiv för Fysik 10, 553, 1956.

b. Eriksson, K.B.S., Phys. Rev. 102, 102, 1956.

12. Goudet, G. J. Phys. et Rad. 6, 443, 1935.
13. Goudsmit, S.A., and Humphreys, C. Phys. Rev. 31, 960, 1928.
14. Harrison, G.R. Reports on Progress in Physics 8, 212, 1941.
15. Hetzler, C.W., Boreman, R.W., and Burns, K. Phys. Rev. 48, 656, 1935.
16. Houston, W.V. Phys. Rev. 33, 297, 1929.

17a. Johnson, Jr. M.H. Phys. Rev. 38, 1628, 1931.

b. " " " " " 39, 197, 1932.

18. Jeurgen Bauer, Ann. der Physik (5) 20, 481, 1934.

19. Kayser, H. "Handbuch der Spectroscopie" Vol. 6, p. 456.

20. Kelly, R.L. Vacuum Ultraviolet Emission Lines. Stanford Research Institute, Calif.

21. Krishnamurthi, S.G., and Rao, K.R. Proc. Roy. Soc. London (A) 149, 56, 1935.

22a. Kuhn, H.G. Atomic Spectra, Longmans, 1962.

b. Lubzinski, J.F. M.A. Thesis, Dept. of Physics, U.B.C. 1950.

23. Mack, J.E., Stehn, J. and Edlen, B. J.O.S.A. 22, 245, 1932.

24. Martin, D.C. Phys. Rev. 48, 938, 1935.

25. Masaki, O., Kobayakawa, K.J. J. Sci. Hiroshima Univ. (A) 6, 217, 1936.

26. Meggers, W.F. J. Res. Nat. Bur. Stand. 10, 669, 1933.

27. Meggers, W.F. J. " " " " 14, 487, 1935.

28. Meggers, W.F., and Peters, C.G. Bull. Bur. Stand. 14, 697, 1919.

29. Meissner, K.W., Bartelt, O., and Eckstein, L., Zeit. Phys. 91, 427, 1934.

30. Meissner, K.W. Zeit. Phys. 94, 810, 1935.

31. Meissner, K.W. and Luft, K.F. Ann. der Phys. 5, 29, 698, 1937.

32. Meissner, K.W. J.O.S.A. V. 31, 6, 405, 1941.

33. Moore, C.E. "Atomic Energy Levels". National Bureau of Standards, Vol. 2, 1952.

34. Paschen, F. Ann. der Phys. 34, 130, 1939.

35. Pauling, L., and Goudsmit, S. "The Structure of Line Spectra". McGraw Hill, New York, 1930.

36a. Racah, G. Phys. Rev. 61, 186, 1942.

b. " " " " 62, 438, 1942.

c. " " " " 62, 523, 1942.

d. " " " " 61, 537, 1942.

37. Rao, K.R. and Badami, J.S. Proc. Roy. Soc. London (A) 131, 159, 1931.

38. Rao, K.R. and Badami, J.S. Proc. Roy. Soc. London (A) 131, 166, 1931.

39. Rao, K.R. and Murti, S.G.K. Proc. Roy. Soc. London (A) 145, 681, 1934.

40a. Rasmussen, E. Dan. Mat. Fys. Medd. 23, nr 3, 1945.

b. Hermansen, A. Univ. Fysik Lab. Copenhagen, Denmark.

41. Risberg, P. Arkiv för Fysik, Bd. 10, nr 41, 1956.

42a. Ruedy, J.E., and Gibbs, R.C. Phys. Rev. 46, 880, 1934.

b. " " " " " Zeit. Phys. 94, 080, 1935.

43. Roeser, H.M. Sci. Pap. Bur. Stand. 16, 363, 1920.

44. Sawyer, R.A. and Humphreys, C.J. Phys. Rev. 32, 583, 1928.

45. Shenstone, A.G. Reports on Progress in Physics 5, 222, 1938.

46. Shenstone, A.G. and Russell, H.N. Phys. Rev. 39, 415, 1932.

47. Slater, J.C. Phys. Rev. 34, 1293, 1929.

48. Van den Bosch, J.C. Physica 14, No. 4, 249, 1948.

49. Wagman, N.E., Univ. Pittsburgh Bull. 34, 1, 1937.

50. White, H.E. "Introduction to Atomic Spectra". McGraw Hill, New York, 1934.

51. Harrison, G.R. M.I.T. Wavelength Tables, New York, John Wiley & Sons, Inc., 1939.

52. Finkelnburg, W., and Humbach, W. Naturwiss. 42, 35, 1955.